UNIVERSITÀ DEGLI STUDI DI BRESCIA

UNIVERSITÀ
DEGLI STUDI
DI BRESCIA

DOTTORATO DI RICERCA IN INGEGNERIA MECCANICA E INDUSTRIALE

Settore scientifico disciplinare: CHIM/07

CICLO XXXV

Mechanochemistry:
Versatile and Functional Strategy for the Realization and the Recycling
of Multi-Phase Materials

DOTTORANDA

ROBERTA CAPUANO

SUPERVISORE: Roberto Avolio, Istituto per i Polimeri, Compositi e Biomateriali CNR

TUTOR: Prof.ssa Laura Eleonora Depero, Università degli Studi di Brescia

Abstract

The present doctoral thesis deals with the development of “greener” methodologies for the modification, the production and the recycling of organic materials, focusing on two classes of materials:

- polyolefins
- cellulose and ligno-cellulosic biomasses

The aim is to increase the sustainability of processes adhering to the principles of Green Chemistry, through the design of strategies that reduce the use of chemicals and solvents, avoid waste generation by extending recycling, enable the utilization of renewable raw materials, promote biodegradability.

Specifically, in this thesis, mechanochemical processes were developed through the use of a ball-milling apparatus. This kind of treatments relies on the application of intense shear and compressive forces to solid materials through the action of the milling bodies, in order to induce morphological and structural changes and, in some cases, chemical modifications in organic materials. Different approaches were followed, to demonstrate the versatility of mechanochemical treatments for the realization of different materials.

In a first approach (II chapter), an in-depth study on the effect mechanochemical treatments on polypropylene (PP), one of the most diffused commodity polymer, is reported to systematically evaluate the effects of mechanochemical processes on polymers. The aim of this study was to explore the possibility to induce radical reactions in PP and PP based mixtures through solid state mechanochemical processes, to either promote the formation of chain branching and/or to obtain the grafting of different molecules. In this study, a crucial aspect is the characterization of resulting materials in order to investigate the structural and chemical modifications induced by the process, and thus to be able to evaluate the effects of mechanochemical treatments. Treated PP samples were analyzed through various characterization techniques. In particular, chemiluminescence

analysis revealed the formation of reactive species, generated by radical reactions, especially abundant for long BM treatments. Thermo-mechanical and rheological analyses highlighted that molecular weight is decreased for long treatment times. To provide a proof of concept of the exploitability of the produced radicals to chemically modify PP, BM treatments were performed in presence of chemicals susceptible to radical reactions, low MW polybutadiene (BR) and glycidyl methacrylate (GMA). After reaction, and purification, spectroscopic analysis gave evidence of the grafting of a small amount of both GMA and BR onto PP.

In the III chapter, BM was exploited as a tool to valorize and recycle polyolefin rich heterogeneous plastic waste. In particular, the mechanochemical treatments were performed on a small-sized film fraction recovered from household waste collection, to investigate the effects induced by the intense mechanical stresses on morphology and properties. Moreover, the possibility to promote compatibilization by radical reactions was explored by adding a small amount of an organic peroxide during the ball milling treatment. Processed materials were analyzed through morphological and mechanical analyses, assessing processing-structure-properties relationships. As a result of the performed treatments, an improvement of mixture morphology and higher ductility were obtained. The low temperature of the BM process reduced the adverse effects of the peroxide on polymers, granting higher stiffness while retaining a significant elongation at break.

Regarding the valorization of cellulose and biomasses, two main research activities were carried out:

In a first study, in the IV chapter, poly(lactic) acid (PLA)-based composites containing cellulosic materials as an organic filler and an oligomeric ester of lactic acid as a plasticizing agent were realized, in order to improve and modulate thermal and mechanical response of this biodegradable polymer. Ball milling was used in different conditions as a green, flexible process to induce structural and morphological changes in cellulose, before composite realization. The thermo-mechanical properties of the realized ternary systems were measured as a

function of the aging time under controlled conditions; the influence of composition on vapor permeability and on the biodegradability under soil burial conditions were also evaluated.

Finally, in the V chapter, the development of a fully bio-based coating based on coffee silverskin (CS), a coffee roasting process by-products, by mechano-chemical treatment is reported. The BM treatment has been proposed for the deconstruction of the complex structure of CS, in mild conditions and using only water as solvent. After BM, the destructured CS suspension were deposited onto PLA substrates by rod coating, without implementing any separation step, taking advantage of the high protein and cellulose content of CS and of the structural modification obtained by the mechano-chemical treatment. CS coatings were characterized in terms of morphology, optical and oxygen barrier properties. The results shows interesting barrier to UV radiation and oxygen permeation of CS coatings, and the effectiveness of the proposed strategy directed at the realization of bio-based coatings with potential applications in the food-packaging sector.

Sommario

La presente tesi di dottorato è incentrata sullo sviluppo di metodologie sostenibili per la modifica, la produzione ed il riciclo di materiali organici, concentrandosi su due classi di materiali:

• poliolefine

• biomasse cellulosiche e lignocellulosiche

L'obiettivo è aumentare la sostenibilità dei processi aderendo ai principi della Green Chemistry, attraverso la progettazione di strategie che riducano l'uso di sostanze chimiche e solventi, evitino la generazione di rifiuti, consentano l'utilizzo di materie prime rinnovabili, promuovano la biodegradabilità.

Nello specifico, in questa tesi, sono stati sviluppati processi meccanochimici mediante l'utilizzo di un mulino a sfere planetario (ball milling, BM). Questo tipo di trattamenti si basa sull'applicazione di forze di taglio e compressione su materiali solidi attraverso l'azione di sfere orbitanti, al fine di indurre cambiamenti morfologici e strutturali e, in alcuni casi, modifiche chimiche nei materiali organici. Sono stati seguiti diversi approcci, per dimostrare la versatilità dei trattamenti meccanochimici per la realizzazione di diversi materiali.

In un primo approccio (II capitolo), viene riportato uno studio approfondito sull'effetto dei trattamenti meccanochimici sul polipropilene (PP), uno dei polimeri più diffusi, per valutare sistematicamente gli effetti dei processi meccanochimici sul polimero. Lo scopo di questo studio è stato quello di esplorare la possibilità di indurre reazioni radicaliche nel PP e in miscele a base di PP attraverso processi meccanochimici allo stato solido, sia per promuovere la formazione di ramificazioni di catena e/o per ottenere l'innesto di diverse molecole. In questo studio, un aspetto cruciale è la caratterizzazione dei materiali realizzati al fine di indagare le modificazioni strutturali e chimiche indotte dal processo, e poter così valutare gli effetti dei trattamenti meccanochimici. I campioni di PP trattati sono stati analizzati attraverso varie tecniche di caratterizzazione. In particolare,

l'analisi in chemiluminescenza ha rivelato la formazione di specie reattive, generate da reazioni radicaliche, particolarmente numerose per trattamenti di BM lunghi. Le analisi termomeccaniche e reologiche hanno evidenziato che il peso molecolare diminuisce per lunghi tempi di trattamento. Per fornire un proof of concept del potenziale utilizzo dei radicali prodotti per modificare chimicamente il PP, i trattamenti di BM sono stati eseguiti in presenza di sostanze chimiche sensibili alle reazioni radicaliche, polibutadiene a basso peso molecolare (BR) e glicidil metacrilato (GMA). Dopo la reazione e la purificazione, l'analisi spettroscopica ha dato evidenza dell'innesto di una piccola quantità sia di GMA che di BR su PP.

Nel III capitolo, il BM è stato sfruttato come strumento per valorizzare e riciclare rifiuti plastici eterogenei ricchi di poliolefine. In particolare, i trattamenti meccanochimici sono stati eseguiti su una frazione di film di piccole dimensioni recuperata dalla raccolta dei rifiuti domestici, per indagare gli effetti indotti dalle intense sollecitazioni meccaniche sulla morfologia e sulle proprietà dei materiali trattati. Inoltre, è stata esplorata la possibilità di promuovere la compatibilizzazione mediante reazioni radicaliche aggiungendo una piccola quantità di un perossido organico durante il trattamento di macinazione a sfere. I materiali lavorati sono stati analizzati attraverso analisi morfologiche e meccaniche, valutando le relazioni processo-struttura-proprietà. A seguito dei trattamenti eseguiti si è ottenuto un miglioramento della morfologia della miscela e una maggiore duttilità dei materiali. La bassa temperatura del processo di BM ha ridotto gli effetti negativi del perossido sui polimeri, garantendo una maggiore rigidità dei materiali pur mantenendo un significativo allungamento a rottura.

Per quanto riguarda la valorizzazione della cellulosa e delle biomasse, sono state svolte due principali attività di ricerca:

In un primo studio, nel IV capitolo, sono stati realizzati compositi a base di acido poli(lattico) (PLA) contenenti materiali cellulosici come filler organico e un estere oligomerico dell'acido lattico come agente plasticizzante, al fine di migliorare e modulare le caratteristiche meccaniche e termiche di questo polimero biodegradabile. Il processo di BM è stato utilizzato in diverse condizioni come

processo sostenibile e flessibile per indurre cambiamenti strutturali e morfologici nella cellulosa, prima della realizzazione del composito. Le proprietà termomeccaniche dei sistemi ternari realizzati sono state misurate in funzione del tempo di invecchiamento in condizioni controllate; è stata inoltre valutata l'influenza della composizione sulla permeabilità al vapor d'acqua e sulla biodegradabilità nel suolo.

Infine, nel V capitolo, viene riportato lo sviluppo di un coating completamente bio-based a base di coffee silverskin (CS), un sottoprodotto del processo di tostatura del caffè, mediante trattamento meccanochimico. Il trattamento di BM è stato proposto per la destrutturazione della struttura complessa del CS, in condizioni blande ed utilizzando solo acqua come solvente. Dopo il BM, le sospensioni di CS destrutturato sono state depositate su film di PLA mediante rod coating, senza attuare alcuna fase di separazione, sfruttando l'elevato contenuto proteico e cellulosico di CS e la modifica strutturale ottenuta dal trattamento meccanochimico. I coating in CS sono stati caratterizzati in termini di morfologia, proprietà ottiche e di barriera all'ossigeno. I risultati mostrano l'interessante barriera alla radiazione UV e alla permeabilità all'ossigeno dei coating in CS e l'efficacia della strategia proposta volta alla realizzazione di coating bio-based con potenziali applicazioni nel settore dell'imballaggio alimentare.

INDEX

Chapter 1

1 Introduction

1.1 Mechanochemistry: A brief history

Mechanically assisted reactions for the synthesis of solid compounds and molecules have been known for a long time; a classic example of such reactions was given by Faraday, who in 1820 demonstrated the reduction of AgCl to Ag by grinding in a mortar and pestle a mixture of AgCl and Zn [1]. The term mechanochemistry has been first established in 1891 by Wilhelm Ostwald in his General Chemistry textbook [2] as a branch of physical chemistry (such as thermochemistry, electrochemistry or photochemistry). More recently, Gerhard Heinicke presented a broad and widely accepted definition of mechanochemistry as the study of "physical-chemical modifications of the solid produced by the action of mechanical factors" [3]. Mechanical forces can, indeed, modify the energy landscape of chemical reactions and create new synthetic pathways, integrating conventional chemistry to technologies and phenomena traditionally associated with grinding [4]. Applications of mechanochemical activation by ultrasound have also been proposed.[5, 6] Although a strict definition of mechanochemistry may suggest that, to be included in this definition, the formation and breaking of covalent bonds is necessary, [7] following the developments of supramolecular chemistry and the importance of "non-covalent bonds" also changes in molecular arrangement and packing (i.e. crystalline structure) should be considered a mechanochemical event.

Despite the long history of mechanically activated reactions, most developments in this field have been described in last decades. Mechanochamistry has long been held as an efficient process for the synthesis of metallic alloys, but a recent extensive review by James et al.[8] highlighted several of the emergent areas now

being actively pursued with regard to the application of mechanical energy in driving various transformations. These include production of materials for medical use, battery components, non-metallic compounds. Modern mechanochemistry is employed in many applications, such as fabrication of nanoparticles,[9] inorganic/organic synthesis,[10] [11]treatment of waste,[12] and preparation of catalysts.[13] Particularly advantageous in mechanochemical transformations is the avoidance, in most cases, of the large volumes of solvent required in many traditional synthesis and purification processes. Hence, a strong "Green Chemistry" aspect is recognized to mechanochemistry, making it increasingly attractive for the development of sustainable production technologies.[14], [15], [16] Given the variety of materials of interest, ranging from metals and ceramics to small organic molecules and polymers, the specific details of how a process occurs will likely be varied and complex.[17, 18, 19]

1.2 Theorical aspects of mechanochemical processes

As discussed, the term mechanochemistry is frequently used in a broad sense, covering any chemical reaction induced mechanically.[20] This definition is not always accepted, as in most cases, mechanical energy is used to directly rupture strong bonds (for example in polymers, or in single molecules [21]). This generates reactive centers (often radicals) which undergo further reactions. However, this restrictive use would exclude grinding-induced reactions promoted by an increase in the contact surface area between reactants, without direct action on covalent bonds. IUPAC defines a mechano-chemical reaction as a 'Chemical reaction that is induced by the direct absorption of mechanical energy' adding that 'Shearing, stretching, and grinding are typical methods for the mechano-chemical generation of reactive sites, usually macroradicals, in polymer chains that undergo mechano-chemical reactions'.[19][20] Grinding is a general term describing mechanical action by hard surfaces on a material, normally to reduce its particle size. It may refer to either manual methods (mortar and pestle) or non-manual methods such as ball milling, or extrusion etc.

Mechanical activation to promote solid state reactions has been initially applied to metals.[22] The first industrial synthesis exploiting high energy grinding was the production of complex nickel-based alloys reinforced with dispersed oxides for high temperature structural applications. Through the so called mechanical alloying, a fine dispersion of the reinforcing oxides in the metal matrix was obtained while traditional metallurgical methods failed to do so. Moreover, the method allowed the addition of titanium powder to the system and its alloying, showing the occurrence of reactions in the solid state. During grinding, the energy supplied by the balls is dissipated both as heat and in collisions causing fracture, plastic deformation and welding of metal particles. Mechanochemical treatments were then applied to polymeric materials, and they were effective in the fine grinding of different thermoplastics, such as polyamide, polyethylene, polypropylene and acrylonitrile-butadiene-styrene (ABS). The obtained powders could be processed at temperatures below their melting temperature; with this technique, blends of polyamide/polyethylene and polyamide/ABS with peculiar structures and properties were realized.[23]

From the chemical point of view, the high-energy mechanical treatment of solids, can cause mechanical activation, mechanical alloying, and reactive milling of solids. The difference between mechanical activation processes and mechanochemical reactions can be explained imagining an hypothetical reaction: A + B → C. In the case of mechanical activation, the product C is not observed, particles of both reactants A and B just get smaller, resulting in an increase of specific surface area. Instead, in the case of mechanochemical reaction, also a chemical reaction between the solid reactants occurs and product C is obtained. The mechanochemical reaction is often preceded by mechanical activation processes, so both processes might take place in one reaction system.[24] In addition to the particle size reduction, also crystallite size is significantly reduced during milling, in a process called amorphization. [25] Usually a limiting crystal size is obtained: from that point on, further mechanical energy entering the system accumulates in the volume or at the crystals surface.

Mechanistic studies and models for mechanochemical processes have been developed for the most traditional applications, like metal alloying, but a complete picture is still lacking. The most widely referred models are the hot spot theory and the magma-plasma model. Hot spot theory was originally developed for a simplified frictional processes between two sliding surfaces. Impacts between small ridges cause plastic deformations and a localized, strong raise of temperatures. Brittle materials would to crack under strain, [26] however, hot spots can also occur at the tips of propagating cracks. Here the local temperatures are thought to reach several hundreds or thousands of degrees Celsius for very brief periods. The magma-plasma model was developed considering direct impacts rather than sliding motions. It proposes that local temperatures greater than 10^4 °C, can be generated at impact points, associated with transient plasmas and the ejection of energetic species including free electrons.[17]

The most popular devices for mechanochemical processes are vibratory, planetary, and attritor ball mills. In all these devices, the material under processing is periodically moved into zones of ball collisions, where energy is transferred to the powdered particles by the action of the balls. In planetary ball mills, in particular, the grinding vials undergo a double rotation/revolution movement (Figure 1.1). The centrifugal force produced by the vials rotating around their own axes and that produced by the rotating support disk both act on the vial contents, that is, the grinding balls and the material under grinding. Since the vials and the supporting disk rotate in opposite directions, the alternating centrifugal forces causes the grinding balls to both run along the inside wall of the vial (high friction), and to detach from the wall traveling through the jar internal space to collide against the opposing wall (high energy impact).

Figure 1.1 *Planetary ball-mill apparatus and illustration of the planetary movement of grinding jars* [27]

During these movements, the fraction of the treated material that remains trapped between the surfaces of the grinding bodies is then subjected to multiple mechanical stresses: compression, shear (friction), impact as impact (particle-sphere) and impact as collision (particle-particle or particle-jar).

The resulting mechanochemical effects depend on many parameters, such as the milling speed (rpm), milling time, milling atmosphere, the dry or wet (presence of liquids as milling aid or as solvents) conditions, and the ball-to-powder weight ratio (BPR), as well as the type of the mill and the size and material of the grinding balls (Figure 1.2). All these variables are not completely independent and it is necessary to optimize the milling conditions experimentally, because the results generally are not predictable á priori. Unfortunately, in most commercially available ball mills, the thermodynamic variables used to study and control chemical reactions, such as temperature and pressure, are not yet routinely measured or controlled. The energetics of mechanochemical reactions, how

much energy is transferred or available to the reactants due to the combined effects of the temperature and the mechanical treatment applied, how it flows through the chemical system to form products, and "why" particular products are obtained (chemical selectivity); the chemical mechanisms; and overall how mass transfer occurs, remain poorly understood, and only recently have inspired an increasing interest from the chemical community worldwide. Substantial fundamental physicochemical knowledge of mechanochemical processes, and how this relates to thermodynamics and kinetics knowledge, is yet to be discovered and fully demonstrated.[28] Despite several studies, a solid theoretical basis for mechanically activated reactions obtained by ball mill is still largely incomplete, resulting in an incomplete control of operating conditions. Most authors adopted then a purely kinetic approach, trying to establish fundamental relations between the structural changes induced by mechanical activation and milling variables. The obtained results show connection among impact energy, frequency and number of collisions and degree of structural transformation. A quantification of mechanical energy transfers occurring during the grinding process, however, would be needed to achieve a more quantitative understanding of mechanochemical reactions. As a result, milling conditions for each system investigated are usually adjusted experimentally.

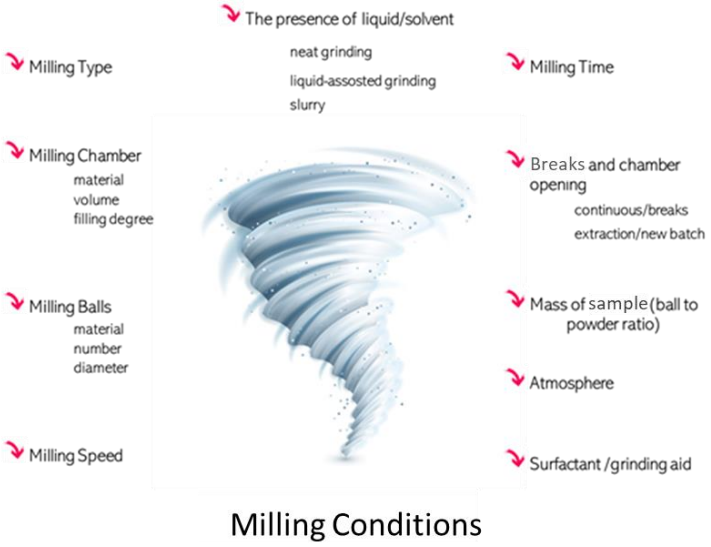

Figure 1.2 *Main milling conditions to be optimized to achieve the best outcome*

1.3 Mechanochemistry of polymers

Polymer mechanochemistry goes back in history, at the very beginning of macromolecular chemistry. Chemical events related to mechanical actions such as grinding, shearing, and stretching of polymer chains have been observed and studied and H. Staudinger, in the '30s, reported on chain scission induced by external stress applied to polymers. Some example of mechanochemistry-induced polymerizations of vinyl monomers have also been reported, in last decades, [29, 30] but only with the recent boost in the research on green and sustainable processes, organic mechanochemistry started to be more widely investigated.

Nevertheless, the mechanism by which the mechanical stress is converted to chemical energy in solid organic materials is complex and up to date not completely identified.[31] Several modes of energy dissipation are involved in the mechanochemical reactions. Intermediate thermal energy conversions as well as plasma formation and electromagnetic processes were suggested in literature.[32 33, 34, 35] Generally, a number of irreversible multi stages characterize these processes. Three fundamental steps can be identified: activation, cracking and condensation. The study of the multistage character of the mechanochemical process showed that the determining step is the cracking, which represents the first step for the mechanical degradation of the macromolecules. On the contrary, the stage of activation takes place at a much lower rate than the other steps and, consequently, it can not be easily distinguished. Irrespective of the stages of the mechanochemical process, a number of free radicals are produced; these might initiate chemical reactions such as grafting, block copolymerization, cross-linking etc. The chemical reactivity of the mechanoradicals is governed by the existence of an unpaired electron at the scission place and by the macromolecular dimension.[36] Thus, a high macroradical length implies a reduced motility, which will determine the subsequent possibilities of conversion. In literature free radicals, ionic species, and other active centers formed by mechanically induced degradation and fracture processes are reported to be able to initiate reactions

of homo- and copolymerization, as well as grafting and block copolymerization.[37] At the molecular level, the mechanochemical transformations progress towards a decrease of molecular weight and the generation of free radicals; however, a reaction with surrounding polymer chains will induce a network formation, i.e., crosslinking. The dynamic competition between chains breaking and chemical cross-linking is related to the polymer chemical nature (chemical bond strength, lateral groups), structure (chain rigidity), its physical state and the presence of a reactive atmosphere or other chemicals.[45] In amorphous polymers above glass transition, the coiled macromolecules tend to orient in the loading direction, so that the stress magnitude must be high in order to locally reach a fully stretched and elastic tensioned state.[38] When the macromolecular chains are organized in a semi-crystalline structure or in a frozen physical network, their movement will be restricted.[39] In this frame, a highly tensioned state can be attained at low level of deformation, as chain movement is concentrated in the ill-ordered zones between crystals. [40] In these zones, under sufficient external forces, the macromolecular chains will be stretched to fracture and chain scissions will occur proportionally to the deformation imposed.[41] Several works addressing the structural changes induced by milling in semi-crystalline polymers and their blends are present in literature.[42], [43], [44], [45], [46]

Mechanochemical treatments of solid polymers have been exploited to different aims, to either modify their network structure, to improve blending, to induce chemical modifications. Many studies involved mechanochemical approaches for the recycling of vulcanized rubber, typically from scrap tyres. ***Rashad at al*** reported on the recycling of rubber as fine aggregate replacement in in cement industry or in composite materials.[47] Waste tire rubber was partially devulcanized, that is, sulphur bridges were cleaved, by ball milling with $CaCO_3$ as processing aid. ***Magini et al*** described the use of high energy ball milling technique on ground rubber in breaking S-S bond and in promoting a more extensive devulcanization process as a mean for rubber recycling.[48] ***Cavalieri et al*** have studied the devulcanization and degradation of the same waste material. The authors presented a scheme showing the formation of radicals, in the absence of antioxidant agents, and a difference between devulcanization and degradation.[49]

Kameda et al studied a treatment on PVC, confirming that both flexible and rigid forms of poly(vinyl chloride) (PVC) were effectively dechlorinated in NaOH/ethylene glycol (EG) solution during ball mill pulverization. This was attributed to enhanced contact between the PVC and dissolved OH as a result of the increased surface area of the PVC exposed during milling.[50]

Ishida studied mechanically milled polyethylene, poly(tetrafluoroethylene), and a 50/50 blend of these two polymers [51], and reported that mechanical milling result in amorphization of crystalline polymers and induce the formation of metastable crystal structures. Investigations performed by ***Castricum*** and co-workers found no chemical changes on milled high-density polyethylene, while in polystyrene they found the appearance of a second glass transition temperature after milling, in contrast to one glass temperature in the original material. They supported Ishida's conclusions and showed that crystalline polyethylene transformed almost completely from the orthorhombic to the monoclinic structure. They concluded that the milling energy was not sufficient to break the C–C bond.[52] Also ***Esterly et al***. achieved a transition from the usual α- phase to the β-phase of PVDF, and the transformation became more pronounced with increased milling times. These β-phase powders maintained their crystal structure during compression molding at 70 °C.[53]

Recently, examples of solvent-free mechanically induced post-polymerization modifications have been reported, overcoming the difficult manipulation of high polymers in the solution state. ***Di Nardo et al.*** reported on the conversion of chitin, a common biopolymer, into chitosan.[54] Ball milling of neat chitin was used to amorphize the polymer, enhancing the mixing of NaOH in a further ball milling step. ***Hirotsu et al.*** demonstrated the grafting of maleic anhydride onto PP, subjecting the two reagents to ball milling in the presence of a peroxide initiator. The resulting grafted polymer showed a lower degradation with respect to PP-g-MA produced by reactive blending in the melt. [55]

As final examples, mechanochemical treatments were exploited to enhance the compatibility of immiscible polymeric phases. These approaches rely on the fact that, the radical species formed during mechanochemical processing of polymers

are highly reactive and their action can either lead to chain scission or to grafting reactions. For most polymers and polymer pairs, at low temperature, grafting is favored over chain scission, favoring the formation of copolymeric species that help stabilize the interface between the polymeric phases during blending.[56] ***Torkelson's*** group worked on this concept through a technique called Solid-state Shear Pulverization, demonstrating the mechanochemical formation of branches in poliolefins [57, 58] and the generation of copolymers at the solid state in different blends.[56, 59] **Cavalieri et al.** performed milling trials under CO_2 atmosphere on PP/PE mixtures followed by melt compouding, evidencing what they call a "self compatibilization", that is, the formation of mixed species (copolymers or grafted polymers) with beneficial effects on blend morphology and properties.[60]

1.4 High energy mechanical treatments of cellulose and biomasses

Cellulose and lignocellulosic biomasses, mainly composed of lignin (15-30%), cellulose (35-50%) and hemicellulose (20-35%), are widely available, natural materials with countless industrial uses. With the rising attention to the environmental impact of materials life cycle, from raw materials extraction to production, use and end-of-life, the use of bio-based materials as alternatives to oil based substances is increasing, in particular in the plastic sector. At the same time, the development of sustainable treatments and processing routes for material production is needed, as a key issue to reduce the overall impact of industrial cycles. In this respect, mechanochemical treatments have been widely investigated for the sustainable manipulation of biobased materials.

1.4.1 Cellulose

Present into the cell walls of almost all plants as a structural component, cellullose is the world's most abundant biopolymer. It is constituted by linear polysaccharide chains, composed of β-(1,4)-D-glucose units linked together by β -1-4-linkages. The structure is stabilised by an intra and inter molecular hydrogen bond network which provide highly ordered three-dimensional crystalline structure. This network makes cellulose a relatively stable polymer, which does not dissolve in aqueous solvents and has no measurable melting point. Natural cellulose does

not occur as an isolated molecule but is arranged in hierarchical structures, where polysaccharide chains are stacked into microfibrils; these are then packed into larger units known as macrofibrils, which are further assembled into the large macroscopic cellulose fibres (Fig. 1.3). An important feature of cellulose is its crystalline nature, which means the cellulose fibrils have a structured order. The component molecules of each individual microfibril are packed so tightly that it prevents penetration by enzymes and even small molecules such as water; however, in the supramolecular structure of the cellulose fibre some amorphous regions are present. The effect of structural heterogeneity is that the macroscopic fibres are at least partially hydrated by water and there is some penetration by larger molecules such as enzymes. [61]

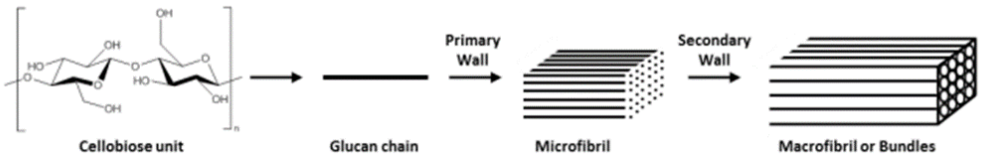

Figure 1.3 *Assembly of native cellulose. Adapted from Delmer and Amor (1995)* [62]

Cellulose is considered to be an almost inexhaustible source of raw material [63] and has found a renewed interest for the production of 'green' composite materials, textiles, drug delivery and personal care products. Cellulosic fiber reinforced polymer composites exhibit many advantages such as low cost, lightweight, good mechanical property, biodegradability and recyclability. Over the last few decades, composites based on biobased/biodegradable polymeric matrices reinforced with cellulosic fibers have been undergoing an extraordinary development and consequently lead to different applications. Cellulosic materials are neither melt formable nor soluble in most common solvents, resulting in limitations of processing techniques. Extrusion is one of the commonly used approach for fiber reinforced plastic composites. However, the hydrophilic and aggregating nature of the cellulose fiber usually leads to poor processability, interfacial incompatibility, and high moisture sensitivity when mixed with hydrophobic plastics. Properties of composites are strongly influenced by the

morphology (aspect ratio, dispersion level) of the cellulosic reinforcement, as well as by interfacial properties. In this respect, mechanochemical treatments have been proposed for the modification of cellulose structure for composite production.

Avolio, R., et al presents a detailed analysis of the partial amorphization induced by a dry ball milling process on cellulose. They showed a progressive decrease of the crystallinity index as a function of the milling time. SEM analysis revealed that the original fibrous structure almost disappeared and fibers were converted into a quasi-circular particles.[64] ***Huang L et al*** analyzed the effect of various ball milling parameters on the pulp fiber grinding performance in order to evaluate the systematic influence of milling conditions and the energy efficiency. Ball mill time, rotational speed, charge ratio, mill ball diameters, and initial moisture content of pulp fiber were studied systematically in a planetary ball mill. The pulverized particle size, particle morphology, crystallinity change, bonding disruption, thermal stability, specific surface area, and energy efficiency were evaluated. Results revealed that cellulose fibers were mainly pulverized during the early milling stage (20 min) and different variables led to changes regarding to the final particle size and shape.[65] ***Mattonai, M. et al*** carried out a combined study of crystallinity index, degree of polymerisation and thermal stability of cellulose for monitoring the effect of ball-milling. They showed that also the degree of polymerization is affected by milling, decreasing by about 20% after 2 hours [66]

Cocca et al. have exploited amorphous cellulose particles, obtained through a solvent-free mechano-chemical process, tested as a potential filler for biodegradable composites based on poly(ε-caprolactone) (PCL). The use of the amorphous cellulose particles combined with the presence of a suitable interfacial agent has allowed to modulate relevant technological properties of the realized composites, such as tensile and thermal properties, water absorption, water vapor transmission rate and biodegradation kinetic.[67] ***Aguiar et al.*** also focused on improving competitiveness and performance of polycaprolactone (PCL) by increasing its mechanical and thermal properties, thus extending its applications in the packaging industry. PCL composites were prepared with

cellulose fibers obtained from different source like lignocellulosic curaua and jute, commercial cellulose samples with different lengths, and amorphized cellulose obtained by ball milling.[68] ***He et al.*** used a solvent-free mechanochemical technology to activate cellulose derived from waste cotton fabrics used as a cost-effective functional additive to enhance the melt-processability and mechanical properties of poly(vinyl alcohol) (PVA).[69]

Within the last 15 years cellolusic micro and nanomaterials have gained significant attention among cellulose derivatives,[70] finding a wide range of applications such as nanocomposites [71] regenerative medicine [72] automotive.[73] Cellulose nanomaterials show, indeed, besides renewability, [74] high aspect ratio (L/d), excellent mechanical properties (high specific strength and modulus) [75] large specific surface area, low coefficient of thermal expansion, and low cost.[76] Furthermore, nanocellulose use implies greener manipulation procedures, such as deposition from water.[77] There are two major classes of micro/nano cellulose; micro (or nano) fibrillated cellulose and cellulose nanowhiskers/nanocrystals, although there are many differing terminologies, which can lead to confusion. Both have at least one dimension in the nano scale (1 to hundreds of nm). Microfibrillated cellulose (MFC) and nanofibrillated cellulose (NFC) can be obtained from cellulose fibrils using a variety of mechanical processes including high pressure homogenisers, grinders/refiners, cryocrushing, high intensity ultrasonic treatments and microfluidisation.[78] These processes generate high shear, which cleaves the cellulose fibrils along their longitudinal axes resulting in long, flexible fibrils with (ideally) nanometric lateral dimension and length in the micrometre scale and consisting of both crystalline and amorphous domains.[79] Cellulose nanowhiskers and nanocrystals are commonly prepared using acid treatments to digest most of the amorphous portions of cellulosic fibers, liberating the highly rigid, elongated crystalline domains.

Piras et al have focused on the applicability of ball milling for the production and the chemical functionalization on cellulose nanofibers and nanocrystals, reviewing recent studies. Mechanical processing must be combined with chemical treatments and ball milling parameters must be carefully optimized to

extract nanocellulose with god properties.[80] ***Baheti et al*** have developed a paper exploring jute fibres as the source to produce nanocellulose by high energy planetary ball milling process and demonstrating its application as filler in biodegradable nanocomposites, for automotive, packaging and agriculture applications.[81] ***Hernandez-Varela et al*** obtained cellulose and cellulose nanoparticles (CNP) from garlic and agave wastes in a high-energy planetary mill, elucidating the structure of the obtained material at different scales using microscopy and spectroscopic techniques.[82] Moreover, ***Souza et al*** compared compositional, thermal, morphological and dimensional properties of cellulose nanostructures obtained through chemical and mechanical isolation processes of paper industry primary waste.[83]

High energy mechanical treatments are an effective complement to chemical treatments, as discussed in some of previous examples, to achieve a partial degradation of cellulosic materials. This is due to the peculiar structure of cellulose, in which strong hydrogen bonding [84] and Van der Waals forces [85] between molecules, especially in crystalline domains, increase resistance towards chemical and enzymatic attacks. Therefore, mechanical treatments able to destructure cellulosic material are crucial when a complete degradation of cellulosic materials is required, as an example for the production of sugars or biofuels. Ball milling techniques have been employed by ***Yamashita et al*** to convert crystalline cellulose to amorphous cellulose in order to facilitate the production of biofuel.[86, 87] ***Millett et al*** studied the effect of ball milling pre-treatments of various duration on the course of enzymatic and dilute acid hydrolysis. The dependence of enzymatic hydrolysis yield on milling was quite dramatic. It appears that, with sufficient milling, the carbohydrates of the three cellulose samples investigated can be made almost totally accessible to enzymatic hydrolysis.[88]

Boissou F et al carried out ball milling of cellulose in the presence of a catalytic amount of H_2SO_4 was found to be a promising pre-treatment process to produce butyl glycosides and xylosides in high yields, important chemicals as they can be

used as hydrotropes but also as intermediates in the production of valuable amphiphilic alkyl glycosides.[89]

1.4.2 Lignocellulosic Biomasses

Lignocellulosic biomass contains three major polymers: cellulose, hemicellulose, and lignin, with small amounts of ash and extractive protein, mineral, and pectin.[90] Hemicellulose is a highly branched heteropolysaccharide formed by glucose polymerized with other monosaccharides such as, mannose, galactose, xylose, arabinose and galacturonic acid. Lignin is the third major component of wood and is a three-dimensional complex polyphenolic network.

The typical lignocellulose contents [91] of some plant materials are given in *Table 1.1.* The physical structure of lignocellulose consists of a network of cellulose fibril bundles, which are well aligned in the secondary cell wall layers and oriented less regularly in the primary cell walls.[92, 93, 94] The cellulose fibril network is embedded in an amorphous matrix of hemicellulose and lignin. Hemicellulose binds to cellulose surfaces by hydrogen bonds, crosslinking the cellulose fibrils, and is also covalently linked to lignin[95, 96, 97]. Lignin fills the remaining spaces, reduces water permeability and acts as a physical barrier towards enzymes.[98, 99] Essentially, lignin provides mechanical stiffness, whereas cellulose provides mechanical strength.[100] Thus, the mechanical response of lignocellulosic biomass is defined by the nature of its cellulose, hemicellulose, and lignin, as well as by the way these components are distributed and bonded.

Table 1.1 *General components in plant biomass*

Typical Lignocellulose Content of Some Plant Materials

	Lignocellulose Content (%)		
plant material	hemicellulose	cellulose	lignin
orchard grass (medium maturity) [a]	40.0	32.0	4.7
rice straw [b]	27.2	34.0	14.2
birchwood	25.7	40.0	15.7

[a] *Data taken from Van Soest [101]*

[b] *Data taken from Solo [102]*

Biomasses of different origin are potential renewable sources of a variety of chemical compounds such as carbohydrates, terpenes, aromatics and fatty esters.[105] However, their complex, strongly connected structure represents a formidable obstacle to the extraction of single compounds. Therefore, the efficient exploitation of lignocellulose biomass remains a challenge from an economic point of view. Industrial lignocellulosic biorefineries face high cost for the energy intensive pre-treatment to break the compact structure and enable hydrolysis of biomass.[106, 107] Mechanochemical treatments of different biomasses and bio-surced materials have been investigated to obtain the desired destructuration.

Tabasso, Silvia, et al. reviewed existing studies and applications of non-conventional energy sources such as microwaves, ultrasound and ball milling searching for convenient, inexpensive strategies for the transformation of bio-waste into useful products. Ball milling pre-treatments are required in many cases to facilitate the application of other technologies.[108] ***Licari et al*** starting from bagasse, an abundant by-product of sugarcane production, tried to overcome the recalcitrant structures of lignocellulose through mechanical pre-treatment before conversion into biofuels. In this study, four mechanical deconstruction methods were compared as new saccharification technologies, all effective without the use of chemical or water, thus minimizing waste generation and treatment.[109]

The destructuration obtained by mechanochemical treatments has been exploited for the extraction of value added materials from lignocellulosic biomasses. **Nagarajan et al** utilized chemical and mechanical processes through ball milling in order to produce Cellulose NanoFibrils (CNFs) from a waste product of Cocos nucifera var-Aurantiaca, belonging to palm family.[45] ***Sofla et al*** have compared the fundamental properties of cellulose nanocrystals (CNC) and cellulose nanofibrils (CNF) extracted from sugarcane bagasse. Conventional hydrolysis was used to extract CNC, while ball milling was used to extract CNF.[39] **Liu et al.** applied a ball-milling process in aqueous mild-alkaline solution to

common reed, without other reagents, producing value-added products like cellulose nanofibers and purified lignin.[110]

Lignocellulosic biomasses, recovered from industrial byproducts or from the harvest of non edible crops, have been also used in combination with bio-sourced, biodegradable polymers for the production of sustainable biocomposites materials. In this respect, ***Da Silva et al*** developed a “green” process for obtaining lignocellulosic nanofibers from ball milled eucalyptus sawdust waste and evaluated the effects of incorporating them into biodegradable poly(butylene adipate-co-terephthalate) (PBAT) nanocomposites. They achieved the isolation of nanostructures by a “green” process and their bio-nanocomposites films showed excellent performance in all the properties in the study.[111] **Pucciariello, R., et al**. realized blends based on lignin powder, obtained from an abundant and low-cost source, straw, with a biodegradable polyester, poly(ε-caprolactone) (PCL), by using high-energy ball milling. Lignin increased the modulus and strongly stabilized PCL against UV radiation.[43]

1.5 Mechanochemistry in the field of polymers: benefits and drawbacks

Among the reasons promoting the increasing study of mechanochemistry, its sustainability features stand out. Mechanochemistry affords versatile chemical processes that do not require the use of reaction solvents, significantly reducing the generation of waste and pollution while simultaneously cutting down the economic and environmental costs related to solvent handling, separation and purification. Usually, the final products of chemical syntheses carried out in solution must be separated and purified, although they may retain undesirable amount of solvent. Remarkable quantities of water in many of these processes are also used, for example for washing steps. In contrast, the workup procedures involved in mechanochemical reactions are generally much simpler, increasing work safety, and requiring minimum purification steps, leading to further cost reductions, overall lower energy consumption, and reduced waste production. Compared to other techniques for material synthesis, mechanochemical

processes often lead to a considerable reduction of reaction times and can improve the yields.

Furthermore, sometimes mechanically driven reactions lead to products not obtainable from solutions or other synthetic methods, in terms of structures, or mixture compositions, for example by making accessible new targets or new synthetic routes which may be hindered or impossible in solution by solvent-based interferences, such as solvation effects, solubility limitations or solvolysis. These observations point to the unique chemical mechanisms involved in mechanochemistry, which sometimes appear to be considerably different from those in the analogous reactions in solution. A large number of inorganic, organic [112], and organo-metallic reactions can be carried out under solvent-free conditions.

Polymers present a particular convenient platform for the study of mechanical effects on molecular chemical bonds: the macroscopic forces applied to a polymer can be transferred along the polymer chain on the molecular level and accumulate to an extent that they are sufficient to break covalent bonds. Current research in polymer compatibilization has progressed into novel processing techniques involving solid-state mechanics and mechanochemistry. Similar to metal alloys, polymer blends can show additive or even synergistic property improvements compared to their neat components, but most polymer blends are fully immiscible, resulting in greatly reduced mechanical properties due to poor component interaction at the interfaces. Mechanochemistry is starting to find applications in polymer blend systems: high-energy mechanical forces cause chain scission and free radical generation in solid-state polymeric systems. These radicals are reported to disproportionate between differing homopolymers when mechanically processed together to form blend-compatibilizing block copolymers.[113]

Usually the performance of immiscible blends is improved through additional processing or the inclusion of additives obtaining blend compatibilization. Compatibilization methods include functionalized monomer inclusion, reactive extrusion, and melt-phase compatibilizing agent mixing, but these all have critical

application limitations. Inclusion of functionalized monomers in the polymer chain can improve secondary interactions between chains, but can only be implemented during the polymerization steps. Melt-mixing of a compatibilizing agents into a blend is often limited by poor dispersion, high compatibilizer cost, and a thermodynamic tendency to migrate over time, reducing blend performance.[114]

Reactive compatibilization is the process that allows generating graft or block copolymers acting as compatibilizers in situ during melt blending [115]. These copolymers are formed directly at the interfaces between suitably functionalized polymers, and they link the immiscible phases by covalent or ionic bonds. reduce the size of the dispersed phase and improve adhesion. In order to achieve efficient compatibilization of polymer blends, the reactions between the functional groups should be selective and fast, and the mixing conditions should minimize the limitation of mass transfer in the course of the reaction. There are several types of reactive compatibilization. If the mixed polymers contain reactive groups, the reaction is straightforward. The polymers without reactive groups have to be functionalized or a miscible polymer containing proper reactive groups is added to the respective component. Therefore, reactive groups such as anhydride, hydroxy, amine, or carboxy are incorporated, into one or both of the polymers to be compatibilized. In any case, melt phase techniques require large amounts of heat to form and maintain the melt state, and can thermally degrade polymeric materials. Moreover, the heated state thermodynamically promotes the coalescence, not dispersal, of the minor phase component and leads to an “uncompatibilized” blend morphology.

Mechanochemistry has attracted much attention also for composites materials [116] [117], combining the potential of a filler in a polymer matrix, realizing composites with exciting functional properties. The remarkable degree of interest in polymer composites and nanocomposites is motivated by the significantly enhanced properties such as modulus and strength, outstanding barrier properties, improved resistance to solvents and heat, and decreased flammability and performances obtained with very small volume fractions of fillers. These improvements can be ascribed to the decreased dimensionality of the fillers,

which increases the degree of intimate contact between the filler and matrix. The manipulation of fillers, particularly nanometric fillers, and polymers for composite production is not easy, due to many limiting factor such as filler agglomeration and low compatibility with the polymer matrix and by the need to control the interface between filler and polymer and the final morphology of the entire composite, as these features would largely influence the final properties. The composites realization method is, then, crucial in determining the physical and chemical properties of polymer composites and nanocomposites. In an ex-situ approach, high-molecular-mass polymers, such as polyethylene, polypropylene, and polystyrene, can be melted at relatively high temperatures to provide a liquid phase that is susceptible to the addition and dispersion of solid fillers; this is the commonly utilized melt compounding approach [118]. In-situ approaches have been also designed in order to obtain more homogeneous and kinetically stable particle dispersions [119]. In this case, suitable precursors are used to synthetize the filler particles directly within the polymer matrix via thermal and chemical treatments [120]. Despite the success of ex-situ and in-situ methods in promoting the effective dispersion of fillers, these methods exhibit many drawbacks. The relatively high temperatures and intense mechanical stirring needed for ex-situ manufacturing can induce undesirable chemical degradation processes that consequently diminish the performance of the resulting composites. This effect is particularly present when polymers with relatively low stability are processed, as many biobased/biodegradable formulations [121]. On the other hand, in-situ methods involve complex procedures, and expensive reactants and processing steps. In addition, neither ex-situ nor in-situ methods effectively prevent the re-aggregation of filler, which makes the dispersion of the filler less uniform than desired, as well as less uniform than what should be possible in principle [122]. Therefore, because of the aforementioned issues, several attempts have been made to identify and develop novel methods for enhancing filler dispersion that have improved environmental and economic sustainability. Different approach can be used to improve the dispersion of a filler into a polymer phase including methods based on non-covalent (surfactant treatments) or covalent filler surface functionalization, usually based on the grafting of low molecular weight

compounds or polymer chains directly on the surface of fillers [123]. However, these methods often require complicated organic treatment processes, in addition, covalent functionalization approaches lead to the filler deterioration.

For these reasons, solid-state mixing via the mechanical processing of powders has attracted considerable interest [124, 125] since the mechanical processing of powder mixtures facilitates the intimate mixing of their components through repetitive plastic deformation. By applying discontinuously high strain rates, ball milling enables the reduction of particle size and characteristic lengths in addition to the effective mutual dispersion of the processed phases.

Several studies have demonstrated the enhanced properties of polymer nanocomposites obtained via ball milling [126], improving the realization of composites based on natural filler, often characterized by narrow thermo-degrading ranges, thus preventing degradation effect of labile components [127, 128, 129].

Ball milling has also been shown to modify the filler morphology [130], which enhances the compatibility of fillers with polymer blends [131], and enables successful grafting reactions [132]. In addition, ball milling has been used to mix filler nanoparticles and the polymer matrix in the solid state prior to melt compounding [133]. The direct modification, or generation, of inorganic nanostructures has also been reported [134].

1.6 Outline of this thesis

In the frame of the literature results illustrated, this thesis project was focused on the development of “green” processing methodologies, based on high energy mechanical treatments, applied to polymers, polymeric waste, cellulose and ligno-cellulosic biomasses. The aim, in all cases, is to modify the properties of the systems investigated, developing materials with enhanced performances.

The treatments investigated involve the application of intense shear and compressive forces to solid materials through the action of a planetary ball mills apparatus, in order to induce morphological and structural changes and, in some

cases, chemical modifications. Mechanochemical effects have been observed in polymers and polymeric blends as a consequence of mechanical milling, and attributed to radical-induced reactions. Such reactions showed interesting beneficial effects on the rheological and thermo-mechanical properties of polymers and polymer blends, of particular interest for recycling applications.

Moreover, mechanochemical treatments applied to cellulose and to biomasses of various nature, have shown a high effectiveness in achieving a destructuration of the compact, hierarchical structure shown by these materials, representing a valuable tool to tune their properties and opening the way for many new applications of these renewable substances.

On these bases, the thesis has been organized in three main sections. First, an introduction on mechanochemistry and its applications on the materials of interest is given (Chapter 1).

In the second section, mechanochemical treatments applied to polymeric systems are reported and discussed, focusing on a neat, virgin polymer and on a complex mixture of waste plastics to be recycled. In Chapter 2, an in-depth study to assess the effect mechanochemical ball milling (BM) treatments on polypropylene (PP) was carried out, to explore the possibility to induce radical reactions in PP and PP based mixtures through solid state processes, promoting the formation of chain branching and/or the grafting of different molecules onto the polymer. The modifications induced on treated PP samples were analyzed through various characterization techniques. In particular, chemiluminescence analysis revealed the formation of reactive species, generated by radical reactions. Thermo-mechanical and rheological analyses highlighted that molecular weight is decreased for long treatment times, while no evidence of long chain branching was observed. BM treatments performed on PP in presence of chemicals susceptible to radical reactions, low MW polybutadiene and glycidyl methacrylate, resulted in the mechanochemical grafting of a small amount of both molecules onto PP. In a second approach, in Chapter 3, a more application-oriented strategy was followed. Mechanochemical treatments were performed on a polyolefin-rich waste fraction derived from household waste collection. To

promote the radically induced generation of copolymeric species, improving blend performances, BM treatments in the presence of a small amount of peroxide initiator were experimented. Processed materials were extruded and analyzed through morphological and mechanical analyses, assessing processing-structure-properties relationships. As a result, an improvement of blend morphology and a strong improvement in ductility were obtained.

Finally, high energy mechanical treatments of bio-sourced materials are illustrated, namely, for pulp cellulose to be used in polymeric composites and for a lignocellulosic industrial byproduct, from which a coating for polymeric films was obtained. In Chapter 4, pure cellulose fibers were subjected to different BM treatments, in both dry and wet conditions, resulting in a range of different morphologies. The cellulose samples were then combined with poly(lactic acid) (PLA) and with an oligomeric plasticizer, producing plasticized composites, to assess the influence of cellulosic fillers with different morphologies on materials properties, in particular the thermo-mechanical response as a function of aging time, water vapor permeability and on biodegradability under soil burial conditions. In a second approach (Chapter 5), a fully bio-based coating has been developed by mechanochemical treatment of coffee silverskin (CS), a coffee roasting process by-products. The treatment led to a strong destructuration of CS, obtaining a stable water suspension of nanometric lignocellulosic particle-like structures. Such suspensions were deposited, without any further purification, onto PLA substrates, forming compact coatings exploiting the film-forming properties of the proteic phase contained in CS. Coatings were characterized in terms of morphology, optical and oxygen transmission, showing remarkable gas barrier properties.

BIBLIOGRAPHY

1. TAKACS, L. The mechanochemical reduction of AgCl with metals: Revisiting an experiment of M. Faraday. Journal of Thermal Analysis and Calorimetry, 2007, 90: 81-84.

2. A. Reis, Zeitschrift für Elektrochemie und Angew. Phys. Chemie 1919, 25, 371–372.

3. G. Heinicke, H.-P. Hennig, E. Linke, U. Steinike, K.-P. Thiessen, K. Meyer, Cryst. Res. Technol. 1984, 19, 1424–1424.

4. BOLDYREVA, Elena. Mechanochemistry of inorganic and organic systems: what is similar, what is different? Chemical Society Reviews, 2013, 42.18: 7719-7738.

5. BOLDYREV, V. V. Mechanochemistry and sonochemistry. Ultrasonics Sonochemistry, 1995, 2.2: S143-S145.

6. CRAVOTTO, Giancarlo; GAUDINO, Emanuela Calcio; CINTAS, Pedro. On the mechanochemical activation by ultrasound. Chemical Society Reviews, 2013, 42.18: 7521-7534.

7. KAUPP, Gerd. Mechanochemistry: the varied applications of mechanical bond-breaking. CrystEngComm, 2009, 11.3: 388-403.

8. JAMES, Stuart L., et al. Mechanochemistry: opportunities for new and cleaner synthesis.Chemical Society Reviews, 2012, 41.1: 413-447.

9. BALÁŽ, Peter, et al. Hallmarks of mechanochemistry: from nanoparticles to technology. Chemical Society Reviews, 2013, 42.18: 7571-7637.

10. JAMES, Stuart L., et al. Mechanochemistry: opportunities for new and cleaner synthesis. Chemical Society Reviews, 2012, 41.1: 413-447.

11 Margeti, Davor Mechanochemistry as a green method in organic chemistry and its applications Sustainable Chemistry Research: Analytical AspectsVolume 3, Pages 171 - 18223 October 2023

12. GUO, Xiuying, et al. A review of mechanochemistry applications in waste management. Waste management, 2010, 30.1: 4-10.

13. RALPHS, Kathryn; HARDACRE, Christopher; JAMES, Stuart L. Application of heterogeneous catalysts prepared by mechanochemical synthesis. Chemical Society Reviews, 2013, 42.18: 7701-7718.

14. CAVE, Gareth WV; RASTON, Colin L.; SCOTT, Janet L. Recent advances in solventless organic reactions: towards benign synthesis with remarkable versatility. Chemical Communications, 2001, 21: 2159-2169.

15. CANNON, Amy S.; WARNER, John C. Noncovalent derivatization: green chemistry applications of crystal engineering. Crystal growth & design, 2002, 2.4: 255-257.

16. RALPHS, Kathryn; HARDACRE, Christopher; JAMES, Stuart L. Application of heterogeneous catalysts prepared by mechanochemical synthesis. Chemical Society Reviews, 2013, 42.18: 7701-7718.

17. BOLDYREV, Vladimir V. Mechanochemistry and mechanical activation of solids. Russian chemical reviews, 2006, 75.3: 177.

18. BALAZ, P. Mechanochemistry in Nanoscience and Minerals Engineering. Springer-Verlag, Berlin Heidelberg. 2008.

19. TAKACS, Laszlo. The historical development of mechanochemistry. Chemical Society Reviews, 2013, 42.18: 7649-7659.

20. IUPAC Compendium of Chemical Terminology, 2nd ed. (the ‘‘Gold Book’’). Compiled by A. D. McNaught and A. Wilkinson. Blackwell Scientific Publications, Oxford (1997). XML on-line corrected version: http://goldbook.iupac.org (2006-) created by M. Nic, J. Jirat, B. Kosata; updates compiled by A. Jenkins. ISBN 0-9678550-9-8. doi:10.1351/goldbook, http://goldbook.iupac.org/ MT07141.html.

21. BEYER, Martin K.; CLAUSEN-SCHAUMANN, Hauke. Mechanochemistry: the mechanical activation of covalent bonds. Chemical Reviews, 2005, 105.8: 2921-2948.

22. BENJAMIN, John S. Dispersion strengthened superalloys by mechanical alloying.Metallurgical transactions, 1970, 1: 2943-2951.

23. PAN, J.; SHAW, W. J. D. Properties of a mechanically processed polymeric material. Journal of applied polymer science, 1994, 52.4: 507-514.

24. BALÁŽ, Matej. Environmental Mechanochemistry. Springer International Publishing, 2021.

25. BOLDYREV, V. V.; TKÁČOVÁ, K. Mechanochemistry of solids: past, present, and prospects. Journal of materials synthesis and processing, 2000, 8: 121-132.

26. FOX, P. G. Mechanically initiated chemical reactions in solids. Journal of Materials Science, 1975, 10: 340-360.

27. Wilkening, M., Düvel, A., Preishuber-Pflügl, F., da Silva, K., Breuer, S., Šepelák, V., Heitjans, P. Structure and ion dynamics of mechanosynthesized oxides and fluorides. Zeitschrift für Kristallographie – Crystalline Materials, 2017, 232(1-3) DOI:10.1515/zkri-2016-1963

28 KRUSENBAUM, Annika, et al. The mechanochemical synthesis of polymers. Chemical Society Reviews, 2022, 51.7: 2873-2905.

29. C. V. Oprea and M. Popa, Mechanochemically Synthesized Polymers with Special Properties, Polym.-Plast. Technol. Eng., 1989, 28, 1025–1058

30. M. Kuzuya, S. Kondo and A. Noguchi, A new development of mechanochemical solid-state polymerization of vinyl monomers: prodrug syntheses and its detailed mechanistic study, Macromolecules, 1991, 24, 4047–4053

31. L. Takacs, Chem. Soc. Rev., 2013, 42, 7649–7659.

32. BOLDYREV, V. V.; TKÁČOVÁ, K. Mechanochemistry of solids: past, present, and prospects. Journal of materials synthesis and processing, 2000, 8: 121-132.

33. E. Boldyreva, in The Future of Dynamic Structural Science SE - 6, ed. J. A. K. Howard, H. A. Sparkes, P. R. Raithby and A. V. Churakov, Springer, Netherlands, 2014, pp. 77–89.

34. P. A. May and J. S. Moore, Chem. Soc. Rev., 2013, 42, 7497–7506.

35. K. S. McKissic, J. T. Caruso, R. G. Blair and J. Mack, Green Chem., 2014, 16, 1628.

36. STOLLE, Achim, et al. Ball milling in organic synthesis: solutions and challenges. Chemical Society Reviews, 2011, 40.5: 2317-2329.

37. OPREA, C.; DAN, Florin; DAN, F. Macromolecular mechanochemistry: Polymer mechanochemistry. Cambridge Int Science Publishing, 2003.

38. Deformation and Fracture Behaviour of Polymers, ed. W. Grellmann and S. Seidler, Springer, Berlin, Heidelberg, 2001.

39 SOFLA, M. Rahimi Kord, et al. A comparison of cellulose nanocrystals and cellulose nanofibres extracted from bagasse using acid and ball milling methods. Advances in Natural Sciences: Nanoscience and Nanotechnology, 2016, 7.3: 035004.

40. I. M. Ward and J. Sweeney, Mechanical properties of solid polymers, John Wiley & Sons, 2012.

41. D. Gross and T. Seelig, Fracture mechanics: with an introduction to micromechanics, Springer, 2011.

42. G. Kaupp, CrystEngComm, 2009,11, 388.

43. PUCCIARIELLO, Rachele, et al. Polymer blends of steam-explosion lignin and poly (ε-caprolactone) by high-energy ball milling. Journal of applied polymer science, 2008, 109.1: 309-313.

44. W. J. D. Shaw, Mater. Sci. Forum, 1998,269–272, 19–30.

45. NAGARAJAN, K. J.; BALAJI, A. N.; RAMANUJAM, N. R. Extraction of cellulose nanofibers from cocos nucifera var aurantiaca peduncle by ball milling combined with chemical treatment. Carbohydrate polymers, 2019, 212: 312-322.

46. HIROTSU, Takahiro; ENDO, Takashi; UMEMURA, Myco. Ball-milling promoted chemical bonding between cellulose and plastics. In: Ball Milling Towards Green Synthesis. 2014. p. 203-240.

47. RASHAD, Alaa M. A comprehensive overview about recycling rubber as fine aggregate replacement in traditional cementitious materials. International Journal of Sustainable Built Environment, 2016, 5.1: 46-82.

48. MAGINI, Mauro; CAVALIERI, F.; PADELLA, F. Mechanochemical treatment of scrap tire rubber. In: Journal of Metastable and Nanocrystalline Materials. Trans Tech Publications Ltd, 2002. p. 263-268.

49. CAVALIERI, F.; PADELLA, F.; CATALDO, F. Mechanochemical surface activation of ground tire rubber by solid-state devulcanization and grafting. Journal of Applied Polymer Science, 2003, 90.6: 1631-1638.

50. KAMEDA, Tomohito, et al. Ball mill-assisted dechlorination of flexible and rigid poly (vinyl chloride) in NaOH/EG solution. Industrial & engineering chemistry research, 2008, 47.22: 8619-8624.

51. Ishida TJ. Mater Sci Lett 1994;13:623.

52. Castricum HL, Yang H, Bakker H, Van Deursen JH. Proc Int Symp Metastable, Mechanically Alloyed and Nanocrystalline Materials, 1997:211, 235–8.

53. ESTERLY, Daniel M.; LOVE, Brian J. Phase transformation to β-poly (vinylidene fluoride) by milling. Journal of Polymer Science Part B: Polymer Physics, 2004, 42.1: 91-97

54 T. Di Nardo and A. Moores, Mechanochemical amorphization of chitin: impact of apparatus material on performance and contamination, Beilstein J. Org. Chem., 2019, 15, 1217–1225

55. Macromolecular Chemistry and Physics, 206 (2005) 2470-2482.

56. Macromolecules 2002, 35, 23, 8672–8675

57. Ganglani M.; Torkelson J. M.; Carr S. H.; Khait K. Trace Levels of Mechanochemical Effects in Pulverized Polyolefins. J. Appl. Polym. Sci. 2001, 80, 671–679.

58. Miu E. V.; Fox A. J.; Jubb S. H.; Wakabayashi K. Morphology and Toughness Enhancements in Recycled High-Density Polyethylene (RHDPE) via Solid-State Shear Pulverization (SSSP) and Solid-State/Melt Extrusion (SSME). J. Appl. Polym. Sci. 2016, 133 (10), 43070.

59. Lebovitz A. H.; Khait K.; Torkelson J. M. In Situ Block Copolymer Formation during Solid-State Shear Pulverization: An Explanation for Blend Compatibilization via Interpolymer Radical Reactions. Macromolecules 2002, 35, 9716–9722.

60. Cavalieri, F.; Padella, F.; Bourbonneux, S. High-energy mechanical alloying of thermoplastic polymers in carbon dioxide. Polymers 2002, 43, 1155–1161.

61. Stone J E, Treiber E, Abrahamson B. Accessibility of regenerated cellulose to solute molecules of a molecular weight of 180 to 2×106, Tappi, 1969, 52(1): p. 108-110

62. D P Delmer, Y Amor, Cellulose biosynthesis. The Plant Cell, 1995, Volume 7, Issue 7, Pages 987–1000

63. KROON-BATENBURG, LM J.; KROON, J.; NORTHOLT, M. G. Chain modulus and intramolecular hydrogen bonding in native and regenerated cellulose fibres. Polymer communications (Guildford), 1986, 27.10: 290-292.

64. AVOLIO, R., et al. A multitechnique approach to assess the effect of ball milling on cellulose.Carbohydrate Polymers, 2012, 87.1: 265-273.

65. HUANG, Lang, et al. Mechanical activation and characterization of micronized cellulose particles from pulp fiber. Industrial Crops and Products, 2019, 141: 111750.

66. MATTONAI, Marco, et al. Effect of ball-milling on crystallinity index, degree of polymerization and thermal stability of cellulose. Bioresource technology, 2018, 270: 270-277.

67. COCCA, M., et al. Amorphized cellulose as filler in biocomposites based on poly (ε-caprolactone). Carbohydrate polymers, 2015, 118: 170-182.

68. AGUIAR, Vinicius O.; DE FATIMA V MARQUES, Maria. Mechanical and morphological evaluation of the reinforcement of polycaprolactone with different cellulose fibers. In: Macromolecular Symposia. 2018. p. 1800122.

69. HE, Xu, et al. Mechanochemically activated waste-derived cellulose as a novel functional additive to enhance melt processability and mechanical properties of poly (vinyl alcohol). Journal of Vinyl and Additive Technology, 2014, 20.3: 177-184.

70. NURUDDIN, Md, et al. A novel approach for extracting cellulose nanofibers from lignocellulosic biomass by ball milling combined with chemical treatment. *Journal of Applied Polymer Science*, 2016, 133.9.

71. DAS, Kunal, et al. Physico-mechanical properties of the jute micro/nanofibril reinforced starch/polyvinyl alcohol biocomposite films. Composites Part B: Engineering, 2011, 42.3: 376-381.

72. FLEMING, Keiran; GRAY, Derek G.; MATTHEWS, Stephen. Cellulose crystallites. Chemistry–A European Journal, 2001, 7.9: 1831-1836.

73. DAHLKE, B., et al. Natural fiber reinforced foams based on renewable resources for automotive interior applications. Journal of cellular plastics, 1998, 34.4: 361-379.

74. AZIZI SAMIR, My Ahmed Said; ALLOIN, Fannie; DUFRESNE, Alain. Review of recent research into cellulosic whiskers, their properties and their application in nanocomposite field. Biomacromolecules, 2005, 6.2: 612-626.

75. ORTS, William J., et al. Application of cellulose microfibrils in polymer nanocomposites. Journal of Polymers and the Environment, 2005, 13: 301-306.

76. NISHINO, Takashi; MATSUDA, Ikuyo; HIRAO, Koichi. All-cellulose composite. *Macromolecules*, 2004, 37.20: 7683-7687.

77. SPAGNUOLO, Laura; D'ORSI, Rosarita; OPERAMOLLA, Alessandra. Nanocellulose for Paper and Textile Coating: The Importance of Surface Chemistry. *ChemPlusChem*, 2022, 87.8: e202200204.

78. MOON, Robert J., et al. Cellulose nanomaterials review: structure, properties and nanocomposites. Chemical Society Reviews, 2011, 40.7: 3941-3994.

79. ANDRESEN, Martin, et al. Properties and characterization of hydrophobized microfibrillated cellulose. *Cellulose*, 2006, 13: 665-677.

80. PIRAS, Carmen C.; FERNÁNDEZ-PRIETO, Susana; DE BORGGRAEVE, Wim M. Ball milling: a green technology for the preparation and functionalisation of nanocellulose derivatives. *Nanoscale Advances*, 2019, 1.3: 937-947.

81. BAHETI, V.; ABBASI, R.; MILITKY, J. Ball milling of jute fibre wastes to prepare nanocellulose. *World Journal of Engineering*, 2012, 9.1: 45-50.

82. HERNÁNDEZ-VARELA, Josué David, et al. Effect of ball milling on cellulose nanoparticles structure obtained from garlic and agave waste. *Carbohydrate Polymers*, 2021, 255: 117347.

83. SOUZA, Alana Gabrieli de, et al. Cellulose nanostructures obtained from waste paper industry: a comparison of acid and mechanical isolation methods. *Materials Research*, 2017, 20: 209-214.

84. NISHIYAMA, Yoshiharu; LANGAN, Paul; CHANZY, Henri. Crystal structure and hydrogen-bonding system in cellulose Iβ from synchrotron X-ray and neutron fiber diffraction. Journal of the American Chemical Society, 2002, 124.31: 9074-9082.

85. NOTLEY, Shannon M.; PETTERSSON, Bert; WÅGBERG, Lars. Direct measurement of attractive van der Waals' forces between regenerated cellulose surfaces in an aqueous environment. Journal of the American Chemical Society, 2004, 126.43: 13930-13931.

86. YAMASHITA, Yuya; SASAKI, Chizuru; NAKAMURA, Yoshitoshi. Development of efficient system for ethanol production from paper sludge pretreated by ball milling and phosphoric acid. Carbohydrate polymers, 2010, 79.2: 250-254.

87. INOUE, Hiroyuki, et al. Combining hot-compressed water and ball milling pretreatments to improve the efficiency of the enzymatic hydrolysis of eucalyptus. Biotechnology for biofuels, 2008, 1.1: 1-9.

88. MILLET, M. A.; EFFLAND, M. J.; CAULFIELD, D. F. Influence of fine grinding on the hydrolysis of cellulosic materials-acid vs enzymic. Adv. Chem. Ser.;(United States), 1979, 181.

89. BOISSOU, Florent, et al. Acid-assisted ball milling of cellulose as an efficient pretreatment process for the production of Butyl Glycosides. ChemSusChem, 2015, 8.19: 3263-3269.

90. SATARI, Behzad; KARIMI, Keikhosro; KUMAR, Rajeev. Cellulose solvent-based pretreatment for enhanced second-generation biofuel production: a review. *Sustainable energy & fuels*, 2019, 3.1: 11-62.

91. MOHAN, Dinesh; PITTMAN JR, Charles U.; STEELE, Philip H. Pyrolysis of wood/biomass for bio-oil: a critical review. Energy & fuels, 2006, 20.3: 848-889.

92. I. Duchesne and G. Daniel, *Nord. Pulp Pap. Res. J.*, 2000, **15**, 54–61.

93. S.-Y. Ding, Y.-S. Liu, Y. Zeng, M. E. Himmel, J. O. Baker and E. A. Bayer, *Science*, 2012, **338**, 1055–1060.

94. S.-Y. Ding, S. Zhao and Y. Zeng, *Cellulose*, 2014, **21**, 863–871.

95. H. V. Scheller and P. Ulvskov, *Annu. Rev. Plant Biol.*, 2010, **61**, 263–289.

96. J. Gu and J. M. Catchmark, *Cellulose*, 2013, **20**, 1613–1627.

97. X. Chen, J. Shekiro, M. A. Franden, W. Wang, M. Zhang, E. Kuhn, D. K. Johnson and M. P. Tucker, *Biotechnol. Biofuels*, 2012, **5**, 8.

98 L. T. Fan, M. M. Gharpuray and Y.-H. Lee, in *Cellulose Hydrolysis*, Springer-Verlag, 1987, ch. 3, pp. 21–120.

99. X. Zhao, L. Zhang and D. Liu, *Biofuels, Bioprod. Biorefin.*, 2012, **6**, 465–482.

100. R. Widyorini, J. Xu, T. Watanabe, S. Kawai, Chemical changes in steampressed kenaf core binderless particleboard, J. Wood Sci. 51 (2005) 26–32. doi: https://doi.org/10.1007/s10086-003-0608-9.

101. VAN SOEST, Peter J. Symposium on nutrition and forage and pastures: new chemical procedures for evaluating forages. Journal of animal science, 1964, 23.3: 838-845.

102. Solo, M. L. Mattalorest. Aikakawsh 1965, 37, 127

105. BYCHKOV, Aleksey, et al. Current achievements in the mechanically pretreated conversion of plant biomass. *Biotechnology and Bioengineering*, 2019, 116.5: 1231-1244.

106. GU, Yang Mo, et al. Effects of water content on ball milling pretreatment and the enzymatic digestibility of corn stover. *Water-Energy Nexus*, 2018, 1.1: 61-65.

107. SINDHU, Raveendran; BINOD, Parameswaran; PANDEY, Ashok. Biological pretreatment of lignocellulosic biomass–An overview. *Bioresource technology*, 2016, 199: 76-82.

108 TABASSO, Silvia, et al. Microwave, ultrasound and ball mill procedures for bio-waste valorisation. *Green Chemistry*, 2015, 17.2: 684-693.

109 LICARI, Anaïs, et al. Comparison of various milling modes combined to the enzymatic hydrolysis of lignocellulosic biomass for bioenergy production: Glucose yield and energy efficiency. *Energy*, 2016, 102: 335-342.

110. LIU, Xuran, et al. Mild alkaline pretreatment for isolation of native-like lignin and lignin-containing cellulose nanofibers (LCNF) from crop waste. ACS Sustainable Chemistry & Engineering, 2019, 7.16: 14135-14142.

111. DA SILVA, Cristina G.; KANO, Fabiany S.; ROSA, Derval S. Lignocellulosic nanofiber from eucalyptus waste by a green process and their influence in bionanocomposites. Waste and biomass valorization, 2020, 11: 3761-3774.

112 BRAGA, Dario, et al. Making crystals from crystals: three solvent-free routes to the hydrogen bonded co-crystal between 1, 1′-di-pyridyl-ferrocene and anthranilic acid. CrystEngComm, 2007, 9.1: 39-45.

113 BEYER, Martin K.; CLAUSEN-SCHAUMANN, Hauke. Mechanochemistry: the mechanical activation of covalent bonds. Chemical Reviews, 2005, 105.8: 2921-2948.

114 Macosko, C. W.; Guegan, P.; Khandpur, A. K.; Nakayama, A.; Marechal, P.; Inoue, T. Macromolecules 1996, 29, 5590-5598.

115 BAKER, Warren E., et al. *Reactive polymer blending*. Munich: Hanser, 2001

116 MANSUROV, Zulkhair A., et al. *Mechanochemical synthesis of composite materials*. CRC Press, 2022.

117 Onwubu S.C.; Mdluli P.S.; Singh S.; Makgobole M.U The application of mechano-chemistry in composite preparation Composites for Environmental EngineeringPages 57 - 6711 October 2019

118 PAVLIDOU, S.; PAPASPYRIDES, C. D. A review on polymer–layered silicate nanocomposites. *Progress in polymer science*, 2008, 33.12: 1119-1198.

119 LIU, Tianbo; BURGER, Christian; CHU, Benjamin. Nanofabrication in polymer matrices. *Progress in Polymer Science*, 2003, 28.1: 5-26.

120 GORRASI, Giuliana; SORRENTINO, Andrea. Mechanical milling as a technology to produce structural and functional bio-nanocomposites. Green Chemistry, 2015, 17.5: 2610-2625.

121 WILBERFORCE, Samuel IJ, et al. The influence of the compounding process and testing conditions on the compressive mechanical properties of poly (D, L-lactide-co-glycolide)/α-tricalcium phosphate nanocomposites. *Journal of the Mechanical Behavior of Biomedical Materials*, 2011, 4.7: 1081-1089.

122 MOREIRA, Francys Kley Vieira; MARCONCINI, José Manoel; MATTOSO, Luiz Henrique Capparelli. Solid state ball milling as a green strategy to improve the dispersion of cellulose nanowhiskers in starch-based thermoplastic matrices. *Cellulose*, 2012, 19.6: 2049-2056.

123 DENG, Jinni, et al. Mechanical and surface properties of polyurethane/fluorinated multi-walled carbon nanotubes composites. *Journal of applied polymer science*, 2008, 108.3: 2023-2028.

124 ISHIDA, T.; TAMARU, S. Mechanical alloying of polymer/metal systems. Journal of Materials science letters, 1993, 12: 1851-1853.

125 ZHU, Y. G., et al. PET/SiO2 nanocomposites prepared by cryomilling. Journal of Polymer Science Part B: Polymer Physics, 2006, 44.8: 1161-1167.

126 ZHANG, Farao, et al. Mechanochemical preparation and properties of a cellulose–polyethylene composite. *Journal of Materials Chemistry*, 2002, 12.1: 24-26.

127 JOSEPH, Jomy, et al. Sustainable conducting polymer composites: study of mechanical and tribological properties of natural fiber reinforced PVA composites with carbon nanofillers. Polymer-Plastics Technology and Materials, 2020, 59.10: 1088-1099.

128 DAS, Oisik, et al. Natural and industrial wastes for sustainable and renewable polymer composites. Renewable and Sustainable Energy Reviews, 2022, 158: 112054.

129 XUE, Beichen, et al. A facile ball milling method to produce sustainable pyrolytic rice husk bio-filler for reinforcement of rubber mechanical property. *Industrial Crops and Products*, 2019, 141: 111791.

130 MIO, Hiroshi; KANO, Junya; SAITO, Fumio. Scale-up method of planetary ball mill. Chemical engineering science, 2004, 59.24: 5909-5916.

131 GUO, Xiuying, et al. A review of mechanochemistry applications in waste management. *Waste management*, 2010, 30.1: 4-10.

132 ZHANG, Farao, et al. Mechanochemical preparation and properties of a cellulose–polyethylene composite. *Journal of Materials Chemistry*, 2002, 12.1: 24-26.

133 SHAO, Weiguo, et al. Preparation and properties of polypropylene/vermiculite nanocomposite through solid-state shear compounding (S3C) method using pan-mill equipment. *Materials and manufacturing processes*, 2006, 21.2: 173-179.

134 LI, Y. B., et al. Transformation of carbon nanotubes to nanoparticles by ball milling process. *Carbon*, 1999, 37.3: 493-497.

Chapter 2

Effects of high energy mechanical treatments on polypropylene

2.1 Introduction

iPP is one of the commodity polymer with the largest share in the plastic market. iPP has many advantageous properties when compared to other thermoplastics, such as polyethylene, in all its forms, and PVC: it has high melting point and low density, it shows excellent chemical resistance, high tensile modulus, it costs less to produce and does not present the issues of PVC when it comes to processing and recycling. Commercial iPP is produced via Ziegler–Natta or metallocene catalysis, and consists of highly linear chains with a relatively narrow molecular weight distribution.[1]

In spite of its excellent features, the modulation of the properties of PP through post-polymerization modification of the chain structure is a topic of broad interest. Much effort in producing branched PP, essentially to improve melt strength for the production of films, has been made in the polymer industry and several commercial grades of high melt strength PP are available. These are mostly produced by grafting long chain branches (LCB) on the PP linear backbone, either by electron beam (EB) irradiation or in the melt by using peroxides with relative low decomposition temperature. These methods produce LCB–PP with broadened molecular weight distribution and complex branch structures. There are also some reports on the direct synthesis of long chain branched PP: using metallocene catalysis and conjugated diene monomers.

Another kind of structural modification widely investigated involves the grafting of specific molecules onto PP chain, typically to impart a higher polarity/hydrophilicity, improving the adhesion of PP to the other components in multilayers and composites. Maleic anhydride (MA) is a common modifier used for such purpose, and the standard grafting process involves melt processing of PP and MA in the presence of peroxide initiators [2].

Finally, the development of PP based copolymers, in particular in combination with polyethylene, is an effective route to produce compatibilizing additives for polyolefin-based blends [3]. Copolymers are generally produced directly from monomers during the polymerization, however, routes for the post processing coupling of polymers through radical reactions have also been investigated [4]. These materials are of general interest for the plastic industry to develop blends with a wide range of properties but, notably, mixed polyolefins also represent the bulk of waste plastics coming from household waste collection and sorting. For this reason, low cost technologies for the production of PP-PE based copolymers can be of large relevance for the recycling of waste plastics.

With these points in mind, the aim of this work was to explore the possibility to induce radical reactions in PP and PP based mixtures through solid state processes (mechanochemical treatments through high energy ball milling), to either promote the formation of chain branching and/or to obtain the grafting of different molecules.

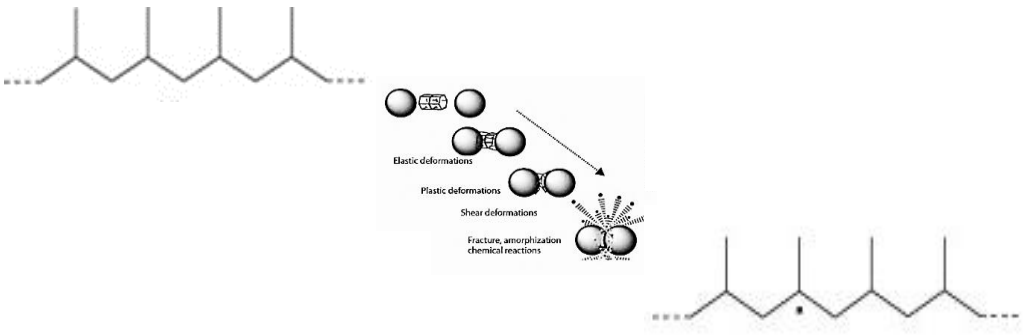

Figure 2.1. *Macroradicals formation on PP chain through mechanochemical treatment*

High energy impacts, through mechanical milling, can extract the labile proton on the tertiary carbon sites of PP; then, the macroradicals may undergo either chain cleavage by β-scission or grafting/crosslinking reactions. Due to the instability of tertiary macroradicals, the chain scission process is extremely fast at high temperature. In iPP, the dominant reactions after formation of free radicals is the β-scission, which induces a molar mass decrease and formation of terminal

double bonds. The subsequent addition of these double bonds to macroradicals can result in the formation of chain branches with a corresponding raise of the molar mass. Disproportionation or recombination reactions of polymer radicals also occur followed by the resultant changes in molar masses [5]. Therefore, the high energy mechanical milling has two potential effects on the molecular structure of polypropylene: changes on the molar mass and formation of chain branching. The scission and recombination processes triggered by mechanical stress are in principle concurrent during the processing of PP, however, their kinetics are highly dependent on temperature: scission dominates at high temperatures, while recombination is favored at lower temperatures (below 60 °C), [6] that is, at the solid state. The fact that this kind of radical reactions have a lower adverse effect on molecular weight at low temperature is the main reason that led to the investigation of solid state modifications of PP. In literature, a method to promote the branching of solid PP has been proposed by Borsig et al. PP long chains have been linked as branches to the original linear iPP chains through a reactions involving peroxides and co-agents.[7]

One of the difficulties in the studies on the addition of branches to linear polymers is the characterization of the resulting structure. This characterization is essential in evaluating the effects of the process experimented. There are three main methods to characterize polymers for LCB: triple-sensor GPC, NMR and rheology. [7] More importantly, it is a challenging task to find an effective mean for detecting whether a polymer contains small amounts of LCB. Rheology provides a good means for detecting even small amounts of LCB, with revealing features being an increase in zero-shear viscosity in comparison to linear chains, the onset of shear thinning behavior at smaller shear rates and also a reduced ratio of the loss modulus over the storage modulus (Yan 1999). [8] A likely reason for this, is because a branched polymer finds additional constrains to flow in the molten state. Extensive work has been done on the rheological behavior of polyolefins: polyethylene has been studied quite extensively in the past few decades as a model polymer. Vega et al. (1998) [9] studied the viscoelastic behavior of 23 non-commercial metallocene-catelyzed PE’s in order to find a correlation between rheological behavior and small amount of long-chain branching. Results point to

the fact that the samples which contain LCB exhibit higher values for zero-shear viscosity, longer relaxation times, higher values of elastic modulus and a higher Arrhenius activation energy all when compared to other PE's of similar MW, polydispersity and amount of short-chain branching (SBC). Wood-Adams and Dealy (2000) [10] investigated the effect of polydispersity, SBC and LCB on the linear viscoelastic behavior of polyethylenes. They found out that for metallocene polyethylene, LCB increased the zero-shear rate viscosity when compared to linear PE's of the same molecular weight. The rheological behavior of LCB polypropylene has also been studied, though significantly less extensively than PE. Kurzbeck et al (1999) [11] investigated two polypropylenes (PP) with different molecular structures, in shear and in elongational flow. He confirmed no strain hardening behavior for linear species, yet for the LCB species he found a more pronounced strain-hardening behavior than any other polyolefin studied up to date. He attributed this behavior to the coexistence of a long chain branched structure and high molecular weight component. Tsenoglou et al (2001)[12] studied the effect of introducing long chain branching on an initially linear PP. They developed a simple rheological method for estimating the degree of long chain branching (the fraction of branched chains or the average number of branches per chain) in a polymer melt undergoing the early stages of cross-linking. Quantitatively, the increase of $\eta_{0,LCB}$ is related to B_n, the average number of branches per molecule, as reported in *Eq.2.1*:

*Eq.2.*1 $$Bn \approx \frac{ln(\eta_{0LCB}/\eta_{0L})}{\alpha\left(\frac{Mw}{Mc}-1\right)-3\ln(\frac{Mw}{Mc})}$$

Where M_c is the molecular weight at the onset of entanglements (=13640 g/mol for PP, Langston et al.) [13] and α is a constant. The method works only for polymers where the branches are the same as the backbone (same chain flexibility), where there is no significant change of the molecular weight upon modification, and for $B_n \ll 1$. It should be noted here that, upon increasing B_n above 1, η_0 may go through a maximum and may start decreasing again. [14] A well known example is LDPE, which usually has a lower zero shear viscosity than HDPE with equivalent M_w.

A more detailed method to estimate LCB by comparing the zero shear viscosity of the linear and the branched polymer has been proposed by Janzen and Colby [14]. This method works even when the molecular weight changes. An average molecular weight between branches, Mb, was introduced to characterize LCB and the zero shear viscosity was related to Mw and Mb. For a branched polymer, $M_b < M_w$, the ratio M_b/M_w should decrease as the degree of branching increases, because more of the molecular weight corresponds then to the parts of chain between the branch points or to the branches themselves. When compared to that of the equivalent linear chain polymer, the shape of the dynamic viscosity curve, $\eta^*(\omega)$, can also give information on the presence of LCB and the polydispersity.

Summarizing, long-chain-branched, moderately cross-linked or highly branched polymers usually show the following rheological properties:

- lower Newtonian viscosity and strong shear thinning with respect to linear polymers of same molecular weight,
- strong melt elasticity expressed by the first normal stress difference and storage modulus,
- enhanced strain hardening under elongational flow. [1]

Apart from rheological measurements, the treated PP samples were also characterized in terms of chemical structure (FTIR, solid state NMR spectroscopy), thermal properties (DSC calorimetry), X-ray diffraction, tensile properties. The formation of radical centers as a consequence of BM was verified by chemiluminescence measurements, while the effects on molecular weight were assessed by gel permeation chromatography. All of these characterizations were directed to the analysis of modifications induced by the mechanical treatments. Preliminary tests on the exploitation of reactive radical centers for the grafting of small molecules to the PP backbone were finally carried out.

2.2 Experimental section

2.2.1 Materials

Moplen HF501N, an unstabilized PP homopolymer powder, was kindly provided by LyondellBasell.

Irganox 1010, Irgafos 168 as stabilizers were proved by Ciba. All other solvents and chemicals were reagent grade products provided by Merck and were used without further purification.

2.2.2 Sample Preparation

Neat PP (PP TQ) was treated in a planetary ball milling (Retsch PM100) apparatus in order to perform the mechanochemical treatments. About 60g of polymer powder were charged in a 500 cm^3 steel grinding jar with 20 mm diameter stainless steel balls, using a 10/1 ball/material weight ratio. The rotation speed used is 400 rpm, with different processing time: 1, 4, 8, 10, 15 hours. These samples were coded PP BM *x*h where *x* represents the ball milling time.

Immediately after treatment, about 45g of PP powders were melt compounded in a Brabender Plastograph EC batch mixer equipped with a 65 cm^3 mixing chamber and two counter rotating blades, at 200°C, 60 rpm, for 8 min. 1 wt% of a mixture of Irganox 1010 (Ciba) (33.3 wt%), and Irgafos 168 (66.6 wt%) was added as stabilizer. After compounding, materials were pelletized and compression molded in a Collin hot plat press at 200°C for 5 min in order to obtain about 200 µm films; all samples were than quenched at room temperature through water circulating cooling plates. Neat PP (PP TQ) was also processed in the batch mixer and molded in the same conditions to be used as a reference.

2.2.3 FT-IR analysis

The IR spectra were obtained on powders and films using a Perkin Elmer Spectrum 100 FTIR spectrometer. Powder spectra were collected in Attenuated Total Reflectance (ATR) mode, scanning between 600 and 4000 cm^{-1}, while

spectra of thin films were collected in transmission mode. 16 scans were accumulated for each sample at a resolution of 4 cm^{-1}.

2.2.4 Chemiluminescence analysis

Chemiluminescence experiments were performed on the photon-counting instrument Lumipol 2, manufactured by the Polymer Institute of Slovak Academy of Sciences, Bratislava, Slovakia. The measurements were done under an air flow (approx.. 3 l/h). Powder specimens (initial mass of about 3 mg), were put into an aluminium pan with a diameter of 9 mm, which was placed in the test chamber and heated from 30 to 230 °C with a heating rate of 10 °C/min.

2.2.5 Gel permeation chromatography (GPC)

GPC analysis was performed with a Freeslate Rapid-GPC, equipped with two mixed-bed Agilent PLgel 10 µm columns and a Polymer Char IR4 infrared detector. Polymer samples were dissolved in 1,2-dichlorobenzene (DCB), with the addition of 4-methyl-2,6-di-tert-butylphenol (BHT) as a stabilizer, and injected at 145°C. Universal calibration was performed using monodisperse polystyrene samples.

2.2.6 Thermal Properties by Differential Scanning Calorimetry (DSC)

The thermal properties of PP samples were measured in terms of peak melting (T_f) and crystallization (T_c) temperatures, and % crystallinity (X_c) using a differential scanning calorimeter TA Q2000 under nitrogen atmosphere. The instrument was calibrated using pure indium. To study the crystallization and melting behaviors, about 4 mg of sample were melted at 200°C for 2 min to erase thermal history, followed by a cooling run at a rate of 10°C/min and a second heating run to 200°C at a rate of 10°C/min. The percentage of crystallinity was determined during the second heating run and the following equation:

Eq.2.2 $$X_c = \frac{\Delta H_f}{\Delta H^{\infty}_f} \times 100\%$$

Where ΔH_f and ΔH^{∞}_f are respectively, the melting enthalpy of the experimental sample and of the perfect (defect-free) i-PP crystal (of infinite lamellar thickness and molar mass), equal to 209 J g^{-1}.

2.2.7 X-Ray Diffraction (WAXS)

WAXS measurements were performed on a subset (neat PP and BM times of 1h, 4h and 10h) of powders and film samples in a Panalytical X'Pert X-ray diffractometer equipped with detector X'Celerator. The diffraction data were collected in continuous at room temperature in a Bragg–Brentano θ−2θ geometry with a Cu Kα radiation (λ=1.54 Å). The equipment was operated at 40 kV and 40 mA with a 2θ scan range between 5° and 40° with a step size of 0.01°.

2.2.8 Tensile tests

Tensile tests were performed on dumb-bell specimens (6mm^2 cross section, 0.2 mm thickness, 50 mm gage length) at a cross-head speed of 50 mm/min by using a 5564 Instron machine. Young's modulus (E), yield stress (σ_Y), stress at break (σ_b) and elongation at break (ε_b) were calculated as average values over at least 10 tested samples.

2.2.9 Rheological measurements

Dynamic Shear measurements were carried out on a RheoStress 6000 rotational rheometer (Haake instruments) using parallel plates with a diameter of 20 mm. The gap height of the plates was about 1 mm for the frequency sweeps. The samples were prepared by compression molding at 200°C, followed by die cutting. The frequency range was 0.01–100 rad/s, and the maximum strain was fixed at 10±1%. We confirmed that these conditions were within the linear viscoelastic region by performing preliminary amplitude sweep measurements.

The temperature was kept constant at 200 °C, and dry nitrogen was used to suppress oxidative degradation of the samples during the experiments.

2.3 Results and Discussion

2.3.1 Chemical analysis

The analysis of possible chemical modifications of the PP samples subjected to BM treatments was carried out through FT-IR spectroscopy, performed on both the treated powders and on melt processed and stabilized films**.**

The ATR-FTIR spectrum of PP powder samples (Figure 2.2 a) shows four large peaks in the wave number range 3000–2800 cm^{-1}: the peaks at 2955 and 2873 cm^{-1} can be attributed to CH_3 asymmetric and symmetric stretching vibrations respectively, while the peaks at 2922 and 2843 cm^{-1} are due to CH_2 asymmetric and symmetric stretching vibrations, respectively [15, 16].The spectrum also shows two intense peaks at 1460 and 1378 cm^{-1}: the peak at 1460 cm^{-1} is caused by CH_3 asymmetric vibrations or CH_2 scissor vibrations, while the peak at 1378 cm^{-1} is due to CH_3 symmetric vibrations. Peaks of minor intensity are observed in the wavenumber range 1200–750 cm^{-1} that can be attributed to C–C stretching, CH_3 rocking and C–H wagging vibrations [16]. The spectra collected on processed films show the same absorptions, with small additional features attributed to the presence of the stabilizers (Figure 2.2 b).

In all samples, no significant differences in FTIR absorptions were evidenced as a function of BM treatments, indicating that no major chemical modification was induced by the treatment. In particular, no strong evidences of newly formed oxidized groups (such as carbonyls), that are the key indicators of thermo-oxidative degradations, were found.

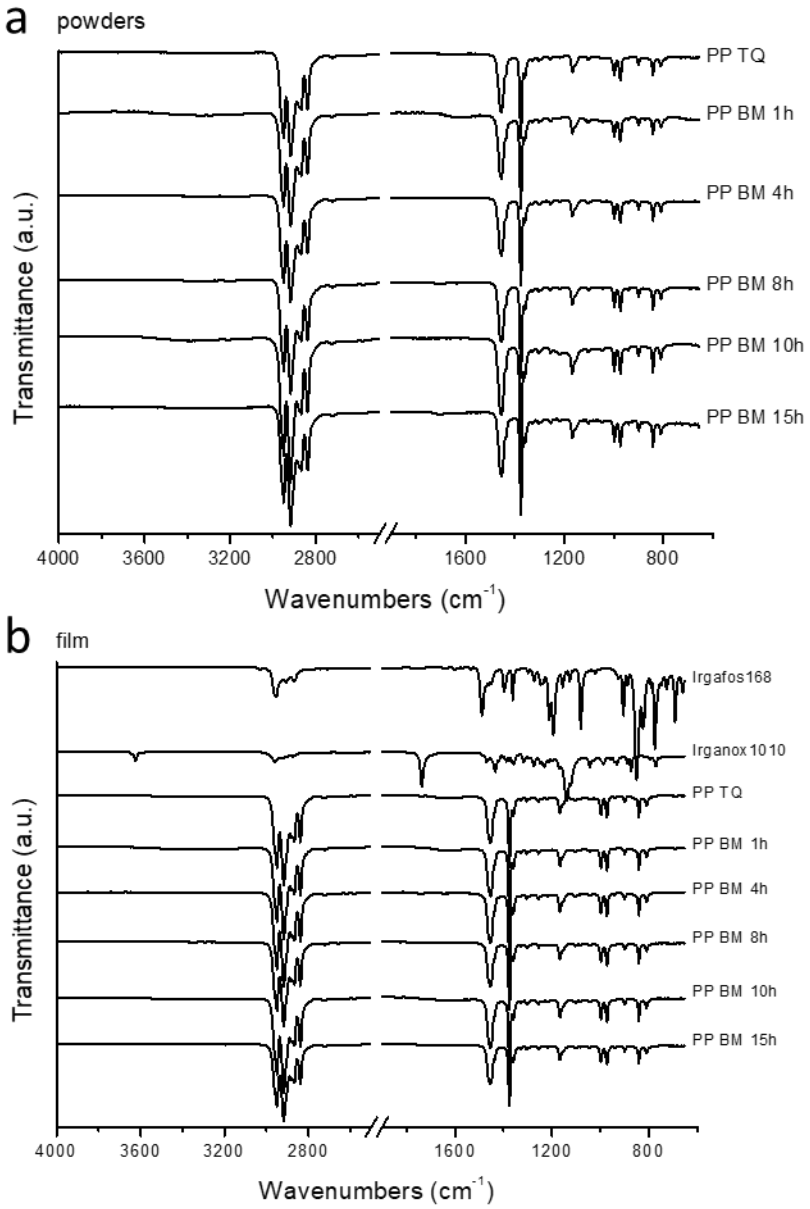

Figure 2.2 *ATR FT-IR spectra of neat and BM treated PP powders (a) and processed films (b) The spectra of stabilizing additives are reported as a reference.*

Non isothermal chemiluminescence (CL) emission of the PP powders samples at selected ball milling times were investigated by means of a Lumipol 2 apparatus. CL is generated in organic materials as a consequence of some specific chemical reactions; it and can be used, then, as a mean to reveal the occurrence of such reactions. In polyolefins, in particular, a weak CL signal is observed during thermo-oxidative degradation and has been related to the decomposition of

hydroperoxides (commonly observed as intermediate species in the decomposition pathway) with the formation of oxidized species, and to chain scissions with the formation of alkyl and carbonyl residues [17,]. Such degradation reactions are expected in polymers subjected to thermo-mechanical stresses and are self-accelerating, that is, the accumulation of reactive hydroperoxides into the material lead to an increase in reaction kinetics [18].

CL curves recorded on PP samples are reported in Figure 2.3.

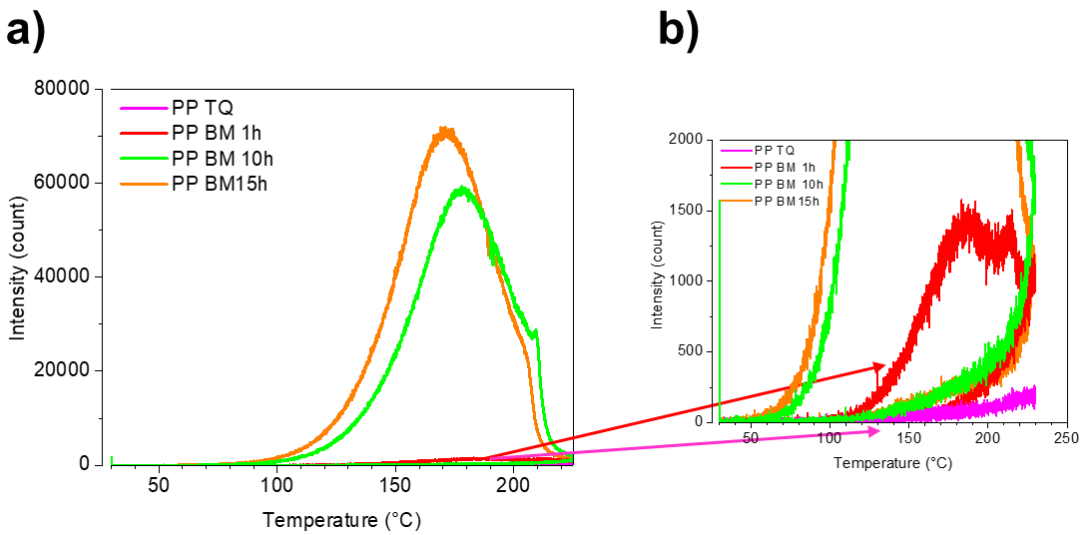

Figure 2.3 *Chemiluminescence of PP powders at different ball milling time a), magnification of the onset area b).*

As can be observed, the intensity of CL recorded increases and the onset is shifted to lower temperatures with increasing ball milling time. In particular, for samples treated for 10 and 15h (orange and green curves) CL is much more intense with respect to samples treated for short times. These results suggest that a relatively large number of species involved in CL generation, such as hydroperoxides and peroxy radicals, is accumulated in PP samples [19] during the BM treatment. Such species are generated from alkyl radicals in the presence of oxygen (air) [18] giving an evidence of the formation of reactive radicals during the BM treatment. We should underline that he presence of oxidized groups, though sufficient to give a clear CL signal thanks to the high sensitivity of the technique,

is not high enough to be clearly evidenced by ATR FTIR analyses, as discussed above.

The evidence of the formation of radicals and reactive species related to degradation is clearly a suggestion of the occurrence of chain scission processes, letting us to suppose a decrease in the molecular weight of PP. Moreover, CL data reveal that further degradation reactions are promoted by heating, starting at temperatures as low as 60 °C. Melt processing of the treated PP powders ad high temperature can, in principle, result in further degradation, if the amount of reactive species is high enough to overcome the action of stabilizing additives. In order to gather quantitative data on the molecular weight of PP samples, gel permeation chromatography (GPC) analyses were carried out on processed film samples, with results reported in Table 2.1.

***Table 2.1**. GPC results of PP processed film samples as a function of ball milling time.*

Sample ID	M_n (kDa)	M_w (kDa)	PDI
PP TQ	61	275	4.5
PP BM 1h	58	270	4.7
PP BM 4h	61	252	4.1
PP BM 10h	42	152	3.6
PP BM 15h	40	135	3.4

GPC data confirmed the occurrence of a degradation in molecular weight as a function of BM time, with a much stronger reduction of both Mn and Mw in samples treated for more than 4 hours. The decrease recorded, however, are not dramatic, demonstrating that the amount of stabilizers is sufficient to allow melt processing without triggering an excessive degradation of polymer chains.

2.3.2 Thermo-mechanical and structural analysis

Thermal properties of the PP samples were measured in terms of melting temperature (T_m), crystallization temperature (T_c) and crystallinity content (X_c),

using a differential scanning calorimeter (DSC). In *Figure 2.4,* DSC thermograms of all PP samples (powders and films) are shown.

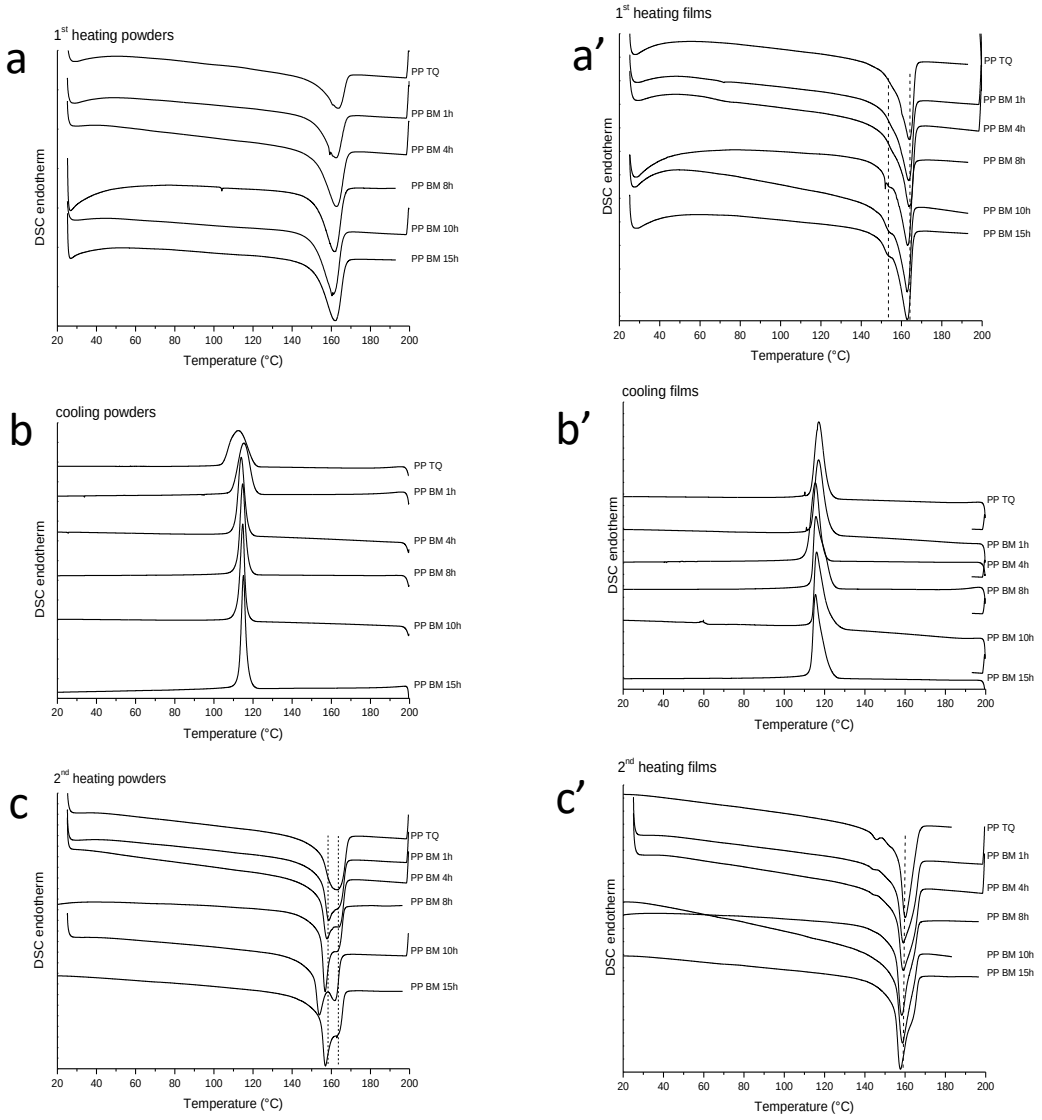

Figure 2.4 *DSC thermograms of PP powders samples (a, b, c) and PP film samples (a', b', c').*

In powder samples, a large effect of BM on the shape of the crystallization peak is evidenced, in particular, the peak become much narrower indicating a faster crystallization. Correspondingly, the second heat melting peak of BM powders exhibit a low temperature component whose intensity increases with increasing BM time. This component can be ascribed to the melting of defective crystals. In

processed samples, a decrease of the crystallization temperature is observed as a consequence of BM, even if the shape of the peak is less affected than in powders; at the same time, the melting temperature (second heat) is reduced and a marked asymmetry of the peak is also observed. These findings point out an increased defectivity, or heterogeneity, induced by the BM treatment, that affect the crystallization and melting behaviour of PP chains. The crystallinity of all the samples was calculated by Eq. (2) and the other calorimetric data were listed in Table 2.2 (PP powders) and Table 2.3 (PP films). As shown in Table 2.2 and Table 2.3, the overall crystallinity of samples is not strongly affected by the ball milling time. Given the absence of strong chemical modifications induced by BM, as discussed in previous section, the defects generated by BM can probably be related to the presence of polymer fractions with a lower molecular weight [20], [21], as evidenced by GPC.

***Table 2.2**. Melting and Crystallization Parameters of neat PP and BM PP powders samples.*

Samples	Neat PP	PP BM 1h	PP BM 4h	PP BM 8h	PP BM 10h	PP BM 15h
T_m(°C)	160	160	159.8	163	164	164
T_m^{II}(°C)	/	/	/	158	158	157
T_c(°C)	112	115	114	114.7	114.7	115
X_c(%)	61	60	61	54	57	52

**Tm(°C) refers to the second heating scans*

***Table 2.3**. Melting and Crystallization Parameters of neat PP and BM PP film samples.*

Samples	Neat PP	PP BM 1h	PP BM 4h	PP BM 8h	PP BM 10h	PP BM 15h
T_m(°C)	160	160.2	160.3	158.3	158.6	157.6
T_m^{II}(°C)	145.5	145.7	/	/	/	/
T_c(°C)	117.1	116.9	116.1	115.7	116.1	115.4
X_c(%)	53	56	56	59	62	57

**Tm(°C) refers to the second heating scans*

As isotactic polypropylene can crystallize into different crystalline structures depending on micro-structural features, crystallization conditions and other factors like the use of specific nucleants [22, 23, 24], wide angle X-ray diffraction analyses were carried out on selected samples to investigate polymorphism of PP samples as a function of BM. Three different polymorphic modifications, α, β

and γ, united by a three-fold conformation, have been reported as well as a mesomorphic phase obtained by fast quenching. Among these, the monoclinic α form, is the typical and the most stable crystalline structure, characterized for first time by Natta and Corradini [25].

Figure 2.5 (a, b) shows the typical wide angle X-ray diffraction patterns of the PP sample. All the samples (powders and films) have similar profiles with strong diffraction peaks located at the scattering angles 2θ= 14°, 17°, 18.5° and 21.7°, which correspond to the planes (110), (040), (130), (111), and (131) of α crystal. As regarding powders, neat PP (PP TQ) has a peak located at the angle 2θ= 19.5° that belongs to the reflection (117) of γ orthorombic cristal phase. However, this reflection disappeared in powders subjected to ball milling, suggesting that the metastable γ form observed can be the result of the conditions experienced during the polymerization of PP and that the mechanical treatment, even at the shortest time explored, was sufficient to remove it. In the case of films, neat PP (PP TQ) has a peak located at the angle 2θ of 16.1° belonging to the reflection of β (300) crystal plane. The evidences of β (300) peak are strongly reduced after 1h of BM and no more visible for longer treatments. The results of X-Ray diffraction, then, further supports a slight effect of BM on the crystallization behavior of PP, without strong consequences on the crystalline form obtained.

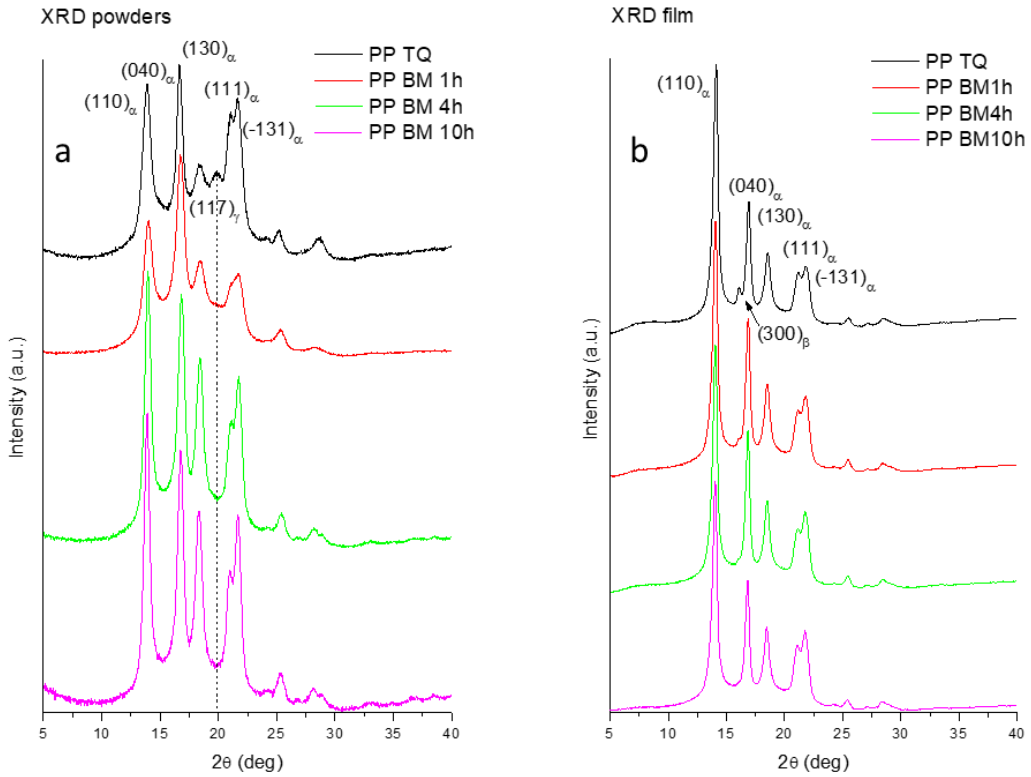

***Figure 2.5**. X-Ray diffraction profile of neat PP and BM PP powders (a) and films (b) samples.*

In order to evaluate the influence of BM treatments on the macroscopic mechanical properties of PP samples, tensile tests (Figure 2.6) were performed on processed film samples. As can be inferred by a qualitative analysis of the stress/strain curves as well as by the analysis of mechanical parameters recorded in Table 2.4, a strong decrease in the elongation at break value (related to ductility) was recorded for samples subjected to BM for more than 4 hours. In these samples, the stress-strain curve does not show any clear yield point and, at the same time, the elastic modulus recorded is higher, thus indicating a transition towards a brittle behavior. Samples treated up to 4 hours showed a mechanical behavior very similar to neat PP. It can be concluded that the decrease in molecular weight evidenced in previous section for samples with BM time ≥ 8h is responsible for the loss of ductility observed in tensile tests.

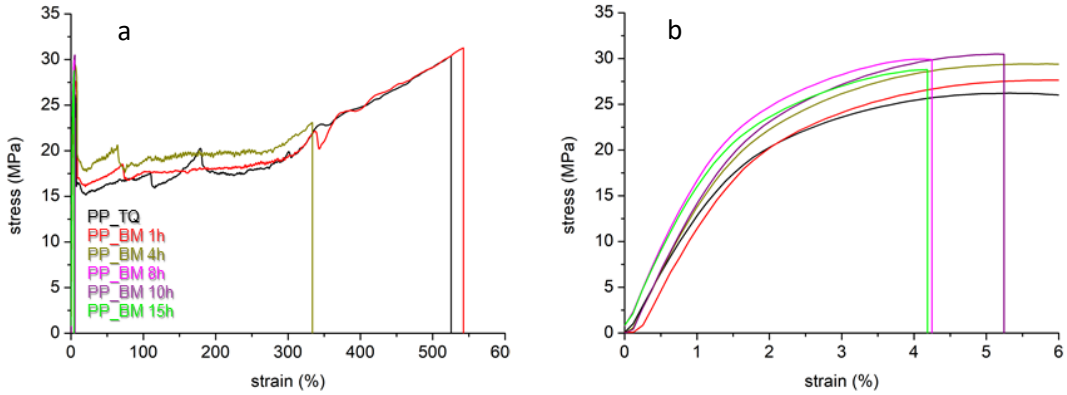

Figure 2.6 *Examples of Stress–strain curves recorded on PP film samples with a magnification of the low strain region*

Table 2.4*. Mechanical parameters as calculated from tensile tests: Elastic modulus (E), maximum stress (σ_{max}), strain at break (εb)*

Sample ID	E (MPa)	σ_{max} (MPa)	ε_b (%)
PP TQ	1200 ± 100	27 ± 1	300 ± 100
PP BM 1h	1200 ± 100	27 ± 1	300 ± 100
PP BM 4h	1200 ± 50	29 ± 1	300 ± 200
PP BM 8h	1610 ± 50	29 ± 2	5 ± 1
PP BM 10h	1480 ± 60	30 ± 1	6 ± 1
PP BM 15h	1590 ± 40	27 ± 1	4 ± 1

2.3.3 Rheological analysis

All the film samples were tested from a rheological point of view. In *Figures 2.7 a, b, c, d, e, f* are shown the storage modulus G' and the loss modulus G" plotted as a function of angular frequencies at a temperature of 200°C. According to the literature[26], the dynamic storage modulus (G') translates the elastic behavior of the material and is related to the amount of the elastically stored energy, while the dynamic loss modulus (G'') represents the amount of dissipated energy. The shear behavior of the samples is in line with literature reports for non-crosslinked polymers: at low frequencies, the viscous flow dominates over the elastic response and G" is larger than G'.

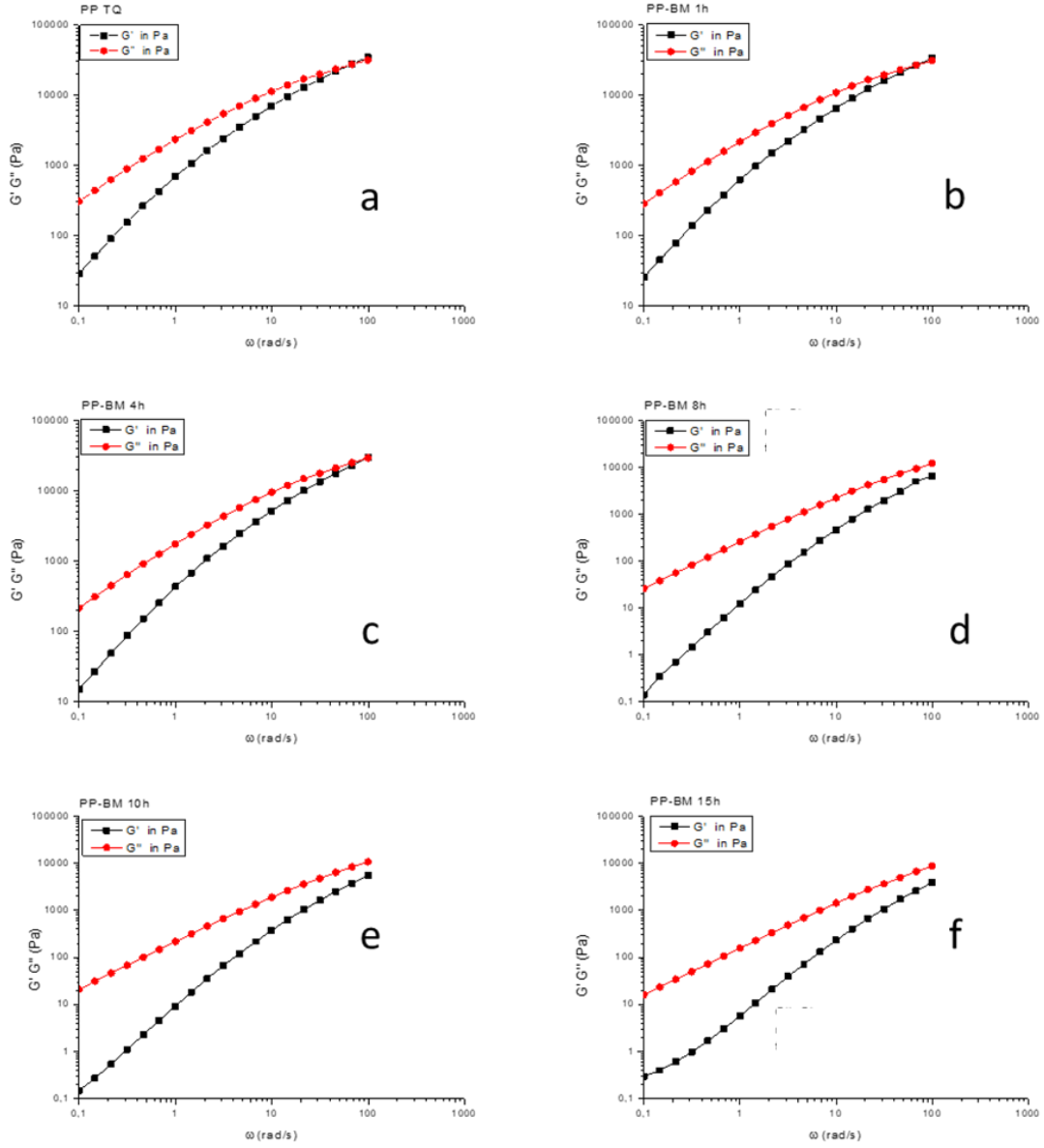

Figure 2.7 *Storage modulus (G'), and loss modulus (G") plotted as a function of angular frequency (ω) of a) PP TQ; b) PP BM 1h; c) PP BM 4h; d) PP BM 8h; e) PP BM 10h; f) PP BM 15h*

Observing *Figures. 2.7 d, e, f* it is worth to note that values of G' and G" of PP samples with BM time > 4 hours are "parallel" to each other over the wide frequency range tested here, that is, no crossover is observed. The crossover modulus, Gc, defined as the point where G'=G'', and the correspondent frequency, ω_c, are reported in *Figure 2.8* and can be used to obtain further information on the structural modifications in PP.

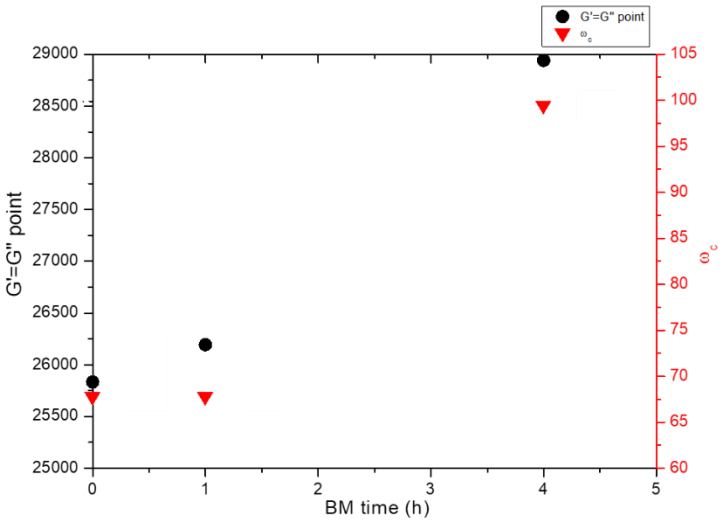

Figure 2.8 *Crossover point vs milling time.*

From a rheological point of view, the frequency value of the crossover point (G'=G'') gives an indication of the relaxation time of the material. In the case of samples treated at ball milling times > 4 hours (PP BM 8h, PP BM 10h and PP BM 15h), the absence of the crossover point in the range of frequency investigated, matches with short relaxation times implying a prevalently liquid-like behavior. The prevalence of a viscous or liquid-like behavior and the shift to higher frequencies of the crossover point with increasing BM time, suggest a decrease in molecular weight of the PP samples as a consequence of the mechanical treatment. In fact, a reduction in the molecular weight of polymer chains will result in a reduction of entanglements in the melt, leading to a lower elastic contribution in the viscoelastic behavior at any given frequency and, at the same time, to a shift of the crossover point to higher frequencies.

Figure 2.9 shows the change of the complex viscosity, η^*, with frequency for neat PP and BM sample. Neat PP (PP TQ) and samples up to 4 h of BM, have high complex viscosity show a clear shear-thinning behavior at higher frequencies. On the other hand, the samples for BM times > 4h have a long Newtonian plateau (viscosity not dependent on shear rate) and low values of zero shear (η_0) viscosity, as we can see in *Figure* 2.*9*, where the complex viscosity is plotted as a function of ball milling time.[27]

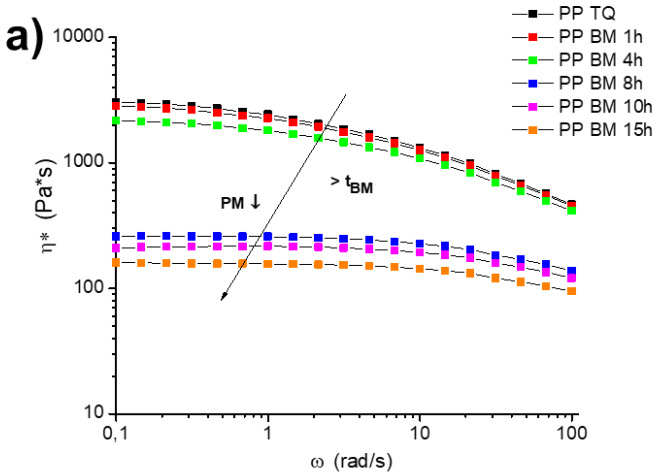

Figure 2.9 *Complex viscosities η*(Pa*s) vs ω(rad/s) of PP*

The viscosity at very low shear rates, known as zero-shear viscosity, has been discovered to grow exponentially with molecular weight. Berry and Fox (1968)[28] performed a study of several nearly monodisperse polymers and found that their viscosity scales linearly with molecular weight up to a certain value of MW they defined as critical (Mc), from which point viscosity scales as a power law $\eta_0 \approx MW^{3.4}$.

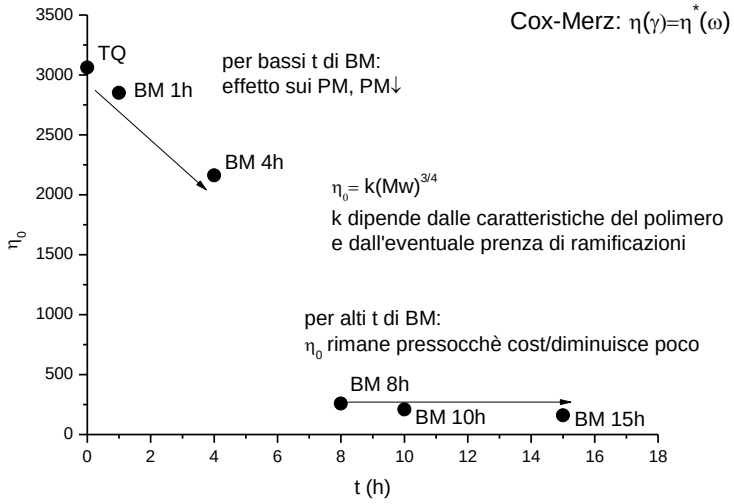

Figure 2.10 *Zero shear viscosity vs ball milling time (a) PP samples, (b) LLDPE samples.*

Figure 2.10 show zero shear viscosity as a function of the ball milling time. Again, a clear distinction can be made between PP samples treated up to 4 hours and samples with longer BM times. Up to 4 hours, the decrease in η_0 observed is limited to about -33%, while for samples treated for 8, 10 and 15 hours η_0 shows a dramatic drop and seems to have reached a plateau, with relatively small differences among samples.

As discussed, rheological features and in particular η_0 are sensitive parameter for the detection of LCB in linear polymers; however, the large prevalence of effects related to molecular weight decrease on the rheological response of PP samples prevents any conclusions on the possible presence of chain branches.

2.4 Grafting trials

Considering the evidence obtained of the formation of reactive radicals during BM treatments, to provide a proof of concept of their exploitability for the obtainment of chemical modifications in PP, BM treatments were performed on PP the presence of chemicals with unsaturated groups, namely low Mw polybutadiene (BR) and glycidyl methacrylate (GMA), Figure 2.11. The double bonds contained in these molecules, in fact, can undergo radical reactions, leading to their possible grafting onto PP chains. Liquid reagents were selected to guarantee a good contact with PP powder during treatments.

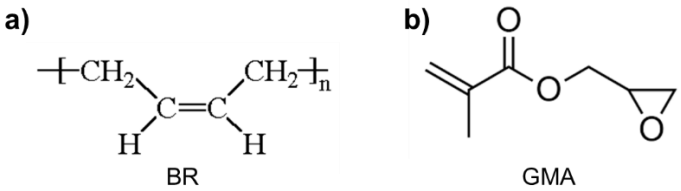

***Figure 2.11**. BR a) and GMA b) structure.*

2.4.1 PP-g-BR trial

40 g of neat PP (PP TQ) were treated in BM for 4 hours (conditions as reported in the Materials and Methods section), to promote radical formation. Then, 40 g of BR were added to the system, in order to obtain a 1:1 ratio. This ratio was selected to obtain a good wetting of the PP powder. An additional ball milling cycle of 4 hours was then carried out to achieve the intimate mixing of the components and to further promote grafting reactions.

In order to determine the result of the grafting reaction, the PP-BR mixture was extracted with hot toluene in a Soxhlet apparatus for 24 h, to remove any unreacted BR. After extraction, the sample was recovered, dried under vacuum and weighed, recording a mass excess of 18% with respect to the neat PP.

ATR FTIR spectra were then collected, in order to confirm grafting, as reported in Figure 2.12.

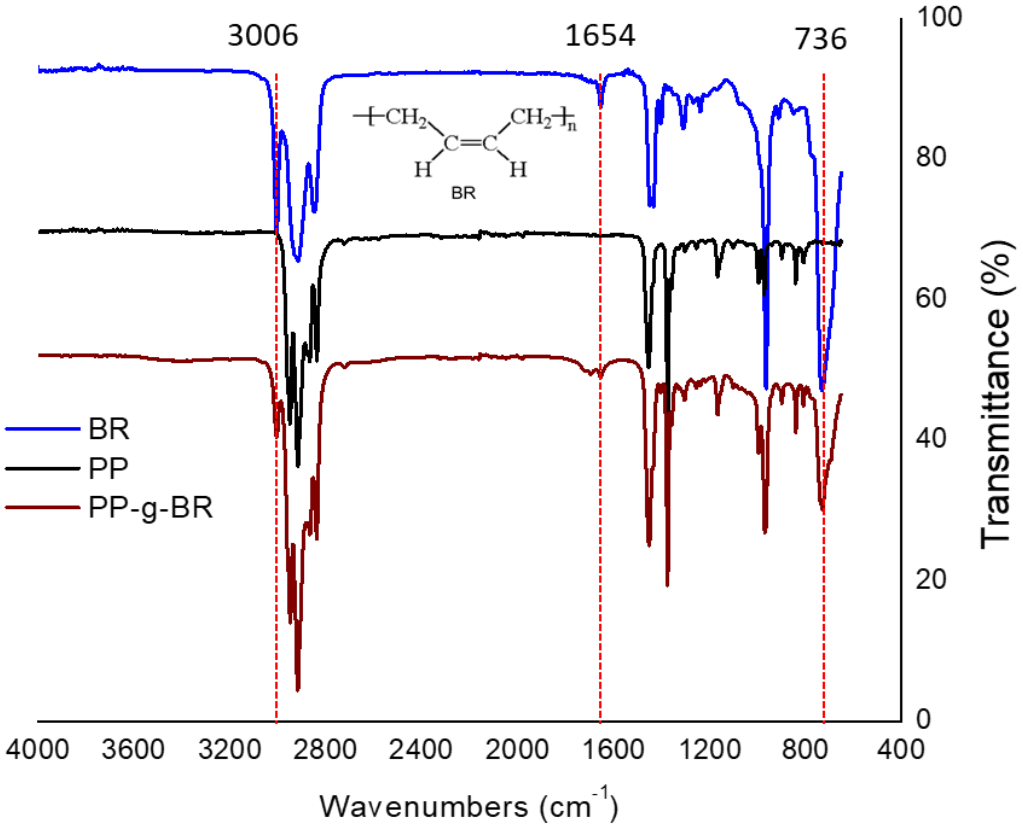

Figure 2.12 *ATR spectra of Neat PP (red), BR (green) and PP-g-BR (blue).*

Comparing the spectra of neat PP and PP-g-BR, new absorption peak, characteristic of BR, are evidenced in the latter sample: at 3006 cm^{-1}, attributed to unsaturated C-H stretching, at 1654 cm^{-1} (C=C stretching peak) and at 736 cm^{-1}, (C-H wagging). FTIR analysis confirmed then that about 18 wt% of BR was grafted into PP chains.

2.4.2 PP-g-GMA trial

60 g of neat PP were treated in BM for 4 hours (conditions as reported in the Materials and Methods section), to promote radical formation. After treatment, 12g of GMA were added to the system, in order to obtain a 4:1 ratio. This ratio was sufficient to ensure a good wetting of PP powder, due to the low viscosity of GMA with respect to BR. An additional ball milling cycle of 4 hours was then carried out to further promote grafting reactions.

After treatment, the mixture was extracted with ethanol, a good solvent for GMA in a Soxhlet apparatus, a reflux temperature for 24 h. After extraction, the sample was recovered, dried under vacuum and weighed; however, the weight recorded was comparable, taking into account experimental errors, to the weight of the PP fraction only.

FTIR analysis was performed on the obtained, purified material. To enhance the intensity of small peaks, spectra were recorded in transmission mode on compression molded films with thickness of about 30 μm, as reported in Figure 2.13.

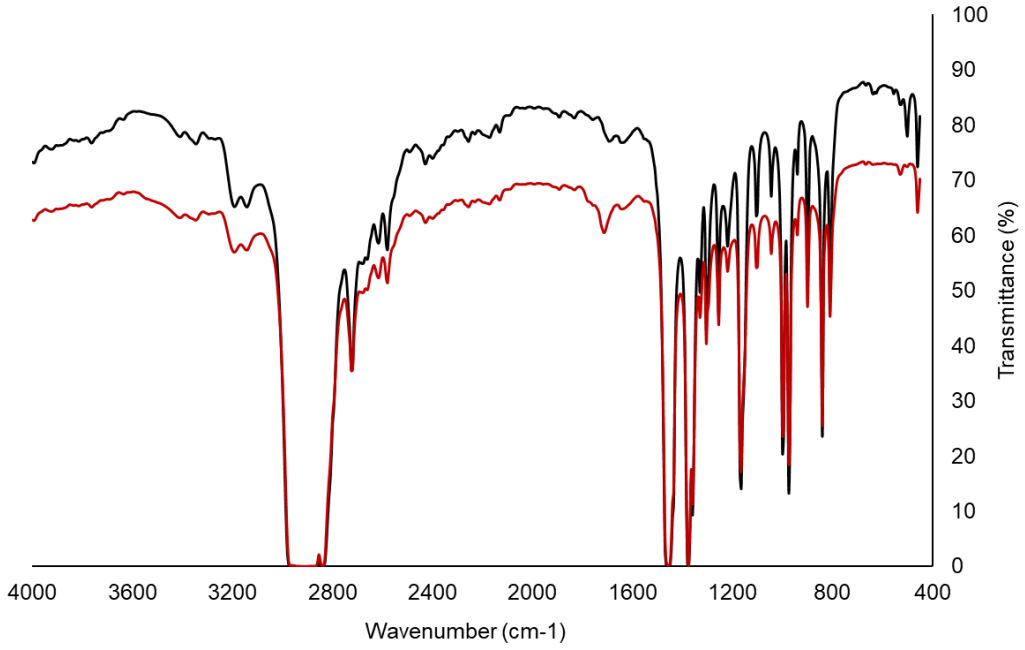

Figure 2.13 *FTIR spectra in transmission mode of neat PP (black), and PP-g-GMA (red).*

Due to the high thickness of the films analysed, the absoption of the main peaks of PP was too large, leading to saturation (e.g. transmittance is nearly zero). Nevertheless, this allowed us to evidence the presence of a small, yet recognizable, carbonyl peak centred at about 1710 cm^{-1}, providing evidence of the grafting of a small amount of GMA onto PP.

2.5 Conclusions

An detailed study of the effects of ball milling mechanochemical tratments on polypropylene (PP), has been carried out, with the aim to verify the occurrence of radical reactions in the solid state and to either promote the formation of chain branching and/or to obtain the grafting of different molecules.

Physico-chemical modifications induced in treated PP samples were analyzed through various characterization techniques. Chemiluminescence analysis revealed a relatively large number of reactive species formed by radical pathways, especially in samples milled for long times. Thermo-mechanical and rheological analyses highlighted that molecular weight is decreased, in particular,

a strong reduction is observed in samples treated for more than 4 hours. As a consequence molecular weight effects dominated the rheological behaviour of PP samples and no clear evidence of long chain branching could be observed.

To provide a proof of concept of the reactivity of mechanically generated radicals towards other molecules, and of their exploitability to induce chemical modifications in PP, BM treatments were performed on PP in the presence of chemicals susceptible to radical reactions, low MW polybutadiene and glycidyl methacrylate. On treated materials, the mechanochemical grafting of a small amount of both molecules onto PP was demonstrated.

BIBLIOGRAPHY

1. SUGIMOTO, Masataka, et al. Melt rheology of long-chain-branched polypropylenes. Rheologica acta, 2006, 46.1: 33-44.

2. Cha, J., White, J.L. Maleic anhydride modification of polyolefin in an internal mixer and a twin-screw extruder: Experiment and kinetic model. Polymer Engineering and Science, 41, 7, 1227-1237. https://doi.org/10.1002/pen.10824

3. Vervoort, S.; den Doelder, J.; Tocha, E.; Genoyer, J.; Walton, K. L.; Hu, Y.; Munro, J.; Jeltsch, K. Compatibilization of Polypropylene-Polyethylene Blends. Polym. Eng. Sci., 2018, 58 (4), 460–465. https://doi.org/10.1002/pen.24661.

4. Graebling, D.; Lambla, M.; Wautier, H. PP/PE Blends by Reactive Extrusion: PP Rheological Behavior Changes. J. Appl. Polym. Sci., 1997, 66 (5), 809–819. https://doi.org/10.1002/(SICI)1097-4628(19971031)66:5<809::AID-APP1>3.0.CO;2-Z

5. VALENZA, A.; PICCAROLO, S.; SPADARO, G. Influence of morphology and chemical structure on the inverse response of polypropylene to gamma radiation under vacuum. Polymer, 1999, 40.4: 835-841.

6. Rätzsch, M.; Arnold, M.; Borsig, E.; Bucka, H.; Reichelt, N. Radical Reactions on Polypropylene in the Solid State. Prog. Polym. Sci., 2002, 27 (7), 1195–1282. https://doi.org/10.1016/S0079-6700(02)00006-0

7. BORSIG, E., et al. Long chain branching on linear polypropylene by solid state reactions. European Polymer Journal, 2008, 44.1: 200-212.

8. YAN, D.; WANG, W.-J.; ZHU, S. Effect of long chain branching on rheological properties of metallocene polyethylene. Polymer, 1999, 40.7: 1737-1744.

9. VEGA, J. F., et al. Small-amplitude oscillatory shear flow measurements as a tool to detect very low amounts of long chain branching in polyethylenes. Macromolecules, 1998, 31.11: 3639-3647.

10. WOOD-ADAMS, Paula M.; DEALY, John M. Using rheological data to determine the branching level in metallocene polyethylenes. Macromolecules, 2000, 33.20: 7481-7488.

11. KURZBECK, S., et al. Rheological properties of two polypropylenes with different molecular structure. Journal of Rheology, 1999, 43.2: 359-374.

12. TSENOGLOU, Christos J.; GOTSIS, Alexandros D. Rheological characterization of long chain branching in a melt of evolving molecular architecture. Macromolecules, 2001, 34.14: 4685-4687.

13. LANGSTON, Justin A., et al. Synthesis and characterization of long chain branched isotactic polypropylene via metallocene catalyst and T-reagent. Macromolecules, 2007, 40.8: 2712-2720.

14. JANZEN, J.; COLBY, R. H. Diagnosing long-chain branching in polyethylenes. Journal of Molecular Structure, 1999, 485: 569-583.

15. Sciarratta V, Vohrer U, Hegemann D, Muller M, Oehr C. Surf. Coat.Technol. 2003; 174: 805

16. Socrates G. Infrared and Raman Characteristic GroupFrequencies – Tables and Charts (3rd edn). John Wiley & Sons: WestSussex, 2001

17. N.C. Billingham, E.T.H. Then, P. Gijsman. Chemiluminescence from peroxides in polypropylene. Part I: relation of luminescence to peroxide content. Polym Degrad Stab, 34 (1991), p. 263

18. J. Rychlý, L. Matisová-Rychlá, K. Csomorová, I. Janigová, M. Schilling, T. Learner. Non-isothermal thermogravimetry, differential scanning calorimetry and chemiluminescence in degradation of polyethylene, polypropylene, polystyrene and poly(methyl methacrylate). Polymer Degradation and Stability, 2011, 96: 1573-1581.

19. OSAWA, Z.; WU, S.; KONOMA, F. Properties and chemiluminescence of polypropylene stored for a long period. Polymer degradation and stability, 1988, 22.2: 97-107.

20. Paukkeri, R.; Lehtinen, A. Thermal Behaviour of Polypropylene Fractions: 1. Influence of Tacticity and Molecular Weight on Crystallization and Melting Behaviour. Polymer (Guildf)., 1993, 34 (19), 4075–4082. https://doi.org/10.1016/0032-3861(93)90669-2

21. Elmoumni, A.; Gonzalez-Ruiz, R. A.; Coughlin, E. B.; Winter, H. H. Isotactic Poly(Propylene) Crystallization: Role of Small Fractions of High or Low Molecular Weight Polymer. Macromol. Chem. Phys., 2005, 206 (1), 125–134. https://doi.org/10.1002/macp.200400130

22. Brückner S, Meille SV, Petraccone V, Pirozzi B. Prog Polym Sci 1991;16:361.

23. Lotz B, Wittmann JC, Lovinger AJ. Polymer 1996;37:4979.

24. Varga JJ. Mater Sci 1992;27:2557

25. Natta G, Corradini P. Nuovo Cimento 1960;15(Suppl):40

26. UTRACKI, Leszek A.; FAVIS, B. D. Polymer alloys and blends. Handbook of polymer science and technology, 1989, 4: 121-185.

27. NAM, G. J.; YOO, J. H.; LEE, J. W. Effect of long-chain branches of polypropylene on rheological properties and foam-extrusion performances. Journal of Applied Polymer Science, 2005, 96.5: 1793-1800.

28. BERRY, Guy C.; FOX, Thomas G. The viscosity of polymers and their concentrated solutions. In: Fortschritte der Hochpolymeren-Forschung. Springer, Berlin, Heidelberg, 1968. p. 261-357

Chapter 3

Valorization and mechanical recycling of heterogeneous post-consumer polymer waste through a mechano-chemical process

The results of this chapter have been published as Capuano, R.; Bonadies, I.; Castaldo, R.; Cocca, M.; Gentile, G.; Protopapa, A.; Avolio, R.; Errico, M.E. Valorization and Mechanical Recycling of Heterogeneous Post-Consumer Polymer Waste through a Mechano-Chemical Process. Polymers 2021, 13, 2783. https://doi.org/10.3390/polym13162783

3.1. Introduction

The versatility and performances of plastics have led to their use in virtually all of the major product categories, with applications spanning from household to aerospace. About 40% of the world consumption of plastics is in the packaging sector [1], which refers to food and beverages, pharmaceuticals, personal and household products. It has been estimated that the value of the global plastic packaging market amounted to USD 348.08 billion in 2020 and it is expected to grow at a compound annual growth rate (CAGR) of 4.2% from 2021 to 2028 [2].

Plastic packaging is characterized by a quite short service life resulting in a) a high rate of waste generation (the package is disposed of in a short time), and b) high intrinsic value of the discarded materials (high quality raw materials are used for food contact, low service life produces relatively low degradation issues) [3, 4]. Despite this, only a small part of post-consumer plastic packaging is actually recycled [5]. It is estimated that 95% of the material value of used plastic packaging, accounting to around 120 billion dollars, is lost annually [6]. Then, in spite of important society benefits deriving from the widespread use of plastics, the

management of plastics at the end-of-life causes serious environmental and economic problems.

In the frame of a circular economy, a radical change of the waste concept is necessary: what was once considered as a waste must become a valuable resource. This means addressing technological, economical and legislative challenges to move towards the maximization of secondary raw material recovery and recycling [5].

To develop efficient recycling strategies for polymer waste, some important issues must be addressed, concerning: the compositional and structural complexity of most plastic products; the contamination and the thermo-mechanical degradation affecting plastic during its life cycle; the limited efficiency of collection and sorting systems unable to accurately separate pure materials; the high compositional heterogeneity of the plastic waste stream, which depends on the geographical area as well as on the season [7,8]. Finally, it has to be considered that the low price of some virgin commodities does not encourage to invest large resources to improve recycling efficiency.

The compositional heterogeneity, caused by complex item composition (filler, additives, multilayered structures) and/or contamination by organic and inorganic substances during the life cycle and/or incomplete separation during the sorting procedure, represents a major technological challenge for the recycling, in terms of the obtainable quality or properties of recycled materials [7].

It is well known that the realization of polymer based multicomponent materials requires an effective strategy able to induce an intimate mixing between different polymer fractions, thus controlling morphology and properties of the blend. To this aim, several approaches are reported in literature, mainly involving the addition of compatibilizing agents and/or reactive additive such as anhydrides or peroxides during the processing [9,10].

Polymeric compatibilizers are generally very effective, but their chemical structure needs to be carefully designed for a specific blend composition [11], making them unsuitable for the intrinsically heterogeneous and highly variable waste plastic mixtures. On the other hand, the addition of reactive substances during the processing ensures greater flexibility and lower cost but, at the same

time, it could cause material degradation as well as the formation of extensive crosslinks, which makes final properties very sensitive to processing conditions [12]. Therefore, summarizing, in order to maximize the recovery of secondary raw material from plastic waste it is very important to define versatile, eco-friendly and cost effective recycling approaches.

In this paper, a strategy based on high energy mechanical treatment to valorize and recycle polyolefin rich heterogeneous plastic waste is proposed. In particular, this mechano-chemical treatment was performed on a small-sized film fraction rich in polyolefins, named FIL/S, deriving from household collection and provided by Corepla, by means of a planetary ball mill (BM).

This technology is traditionally used in the field of ceramics and metals to obtain a fine grinding and to produce new alloys and metastable compounds. Recently it has been extended to polymeric systems as a solid state strategy able to induce morphological and structural modifications [13, 14], to enhance the dispersion of various nanofillers in composites [15] and as a tool to realize recycled polymeric materials with improved properties [16, 17, 18].

On this basis, FIL/S was processed in a BM to investigate the effects induced by the intense mechanical stresses on morphology and properties. It is important to underline that the mechano-chemical treatment has been performed at room temperature and in absence of solvents, thus responding to the requirements of eco-friendly processes. Moreover, the possibility to promote the compatibilization between different fractions by adding a small amount of an organic peroxide during the ball milling treatment has been explored.

Before processing, FIL/S was characterized performing spectroscopic (solid state NMR and FTIR) analyses, to evaluate its composition [19] and define treatment conditions. Processed materials were analyzed through morphological and mechanical analyses, assessing processing-structure-properties relationships.

3.2. Materials and Methods

3.2.1. Materials

FIL/S, post-consumer plastic films of small size, was kindly supplied by COREPLA (Italian Consortium for the Collection and Recycling of Plastic

packages). This material is one of the fractions derived from the sorting process of household plastic waste; it contains films smaller than an A3 sheet (approximately 30 x 40 cm), recovered by air aspiration during the waste sorting process and shredded to few cm fragments.
Di-benzoyl peroxide (BPO), Fluka, reagent-grade, was used without further purification.
Low density polyethylene (Lupolen 2426 H, density 0.925 g/cm^3, MFR 1.9 g/10 min) was kindly supplied by COREPLA and used as a reference material.

3.2.2. Processing of FIL/S

FIL/S material was ground in a SM100 rotary knife mill (Retsch GmbH, Haan, Germany), using a bottom sieve with 4 mm openings.

Ground FIL/S was processed in a PM100 planetary ball mill (Retsch GmbH, Haan, Germany), using either 125 or 500 mL steel grinding bowl and 10 or 20 mm steel balls. The ball/sample weight ratio was set at 10/1. Different bowl rotation speed and grinding time were tested, as specified in the discussion section, ranging from 4 to 10 hour and from 400 to 600 rpm.
Moreover, ground FIL/S was processed in combination with 0.5 and 1 wt% of BPO: pristine ground FIL/S was ball milled for 2 hours to obtain a fine powder with high surface area, then the peroxide was added and the BM process continued for further 2 hours.
Ball–milled materials were processed in a benchtop twin screw extruder (Haake Minilab, Haake, Germany) operated in continuous mode, at a screw rotation speed of 60 rpm and a barrel temperature of 180 °C. Then, materials were pelletized and successively compression-molded in a heated press at 190 °C and 50 bar obtaining 1.5 mm thick sheets to be used for subsequent analysis.

3.2.3. Techniques

Infrared spectra were recorded by means of a Spectrum 100 FTIR spectrometer (PerkinElmer, Waltham, MA, USA), equipped with an attenuated total reflectance accessory (ATR). The scanned wavenumber range was 4000–400 cm^{-1}. All

spectra were recorded with a resolution of 4 cm^{-1}, and 16 scans were averaged for each sample.

Solid state ^{13}C Magic Angle Spinning (MAS) Nuclear Magnetic Resonance (NMR) spectra were collected on a Bruker Avance II 400 spectrometer (Bruker Biospin, Billerica, MA, USA) operating at a static field of 9.4 T, equipped with a 4 mm MAS probe. Ground LRP samples were packed into 4 mm zirconia rotors sealed with Kel-F caps and spun at 5 kHz. Cross-polarization (CP) spectra were recorded with a relaxation delay of 5 s and a contact time of 2 ms under high-power proton decoupling. Spectra were referenced to external adamantane (CH_2 signal at 38.48 ppm downfield of tetramethylsilane (TMS), set at 0.0 ppm).

Tensile tests were performed on dumb-bell specimens (6 mm^2 cross section, 1.5 mm thickness, 26 mm gauge length) at a cross-head speed of 10 mm/min by using an Instron 5564 testing machine (ITW Inc. Glenview, IL, USA). Young's modulus (E), peak stress (σ), and elongation at break (ε) were calculated as average values over at least 6 tested samples.

Scanning electron microscopy (SEM) was carried out on a Quanta 200 FEG microscope (FEI, Hillsboro, OR, USA) working in high vacuum mode with an acceleration voltage ranging from 10 to 30 kV and using a secondary electron detector. Before SEM observations, cryofractured surfaces were sputter-coated with an Au/Pd alloy by means of an Emitech K575X sputtering device.

Image analysis was carried out on SEM micrographs to obtain quantitative geometrical information on the dispersed phase, by means of the ImageJ software package. Dispersed phase inclusions were manually identified and fitted to ellipses (Figure S1 in section 5).

3.3. Results

3.3.1. Analysis of FIL/S

Spectroscopic analyses were performed on the FIL/S to better clarify its composition as well as any degradation phenomena affecting the FIL/S polymer fractions as a result of the life cycle.

Considering the high heterogeneity of the provided material, ATR-FTIR spectroscopy was performed on several different film fragments, with some examples reported in Figure 3.1.

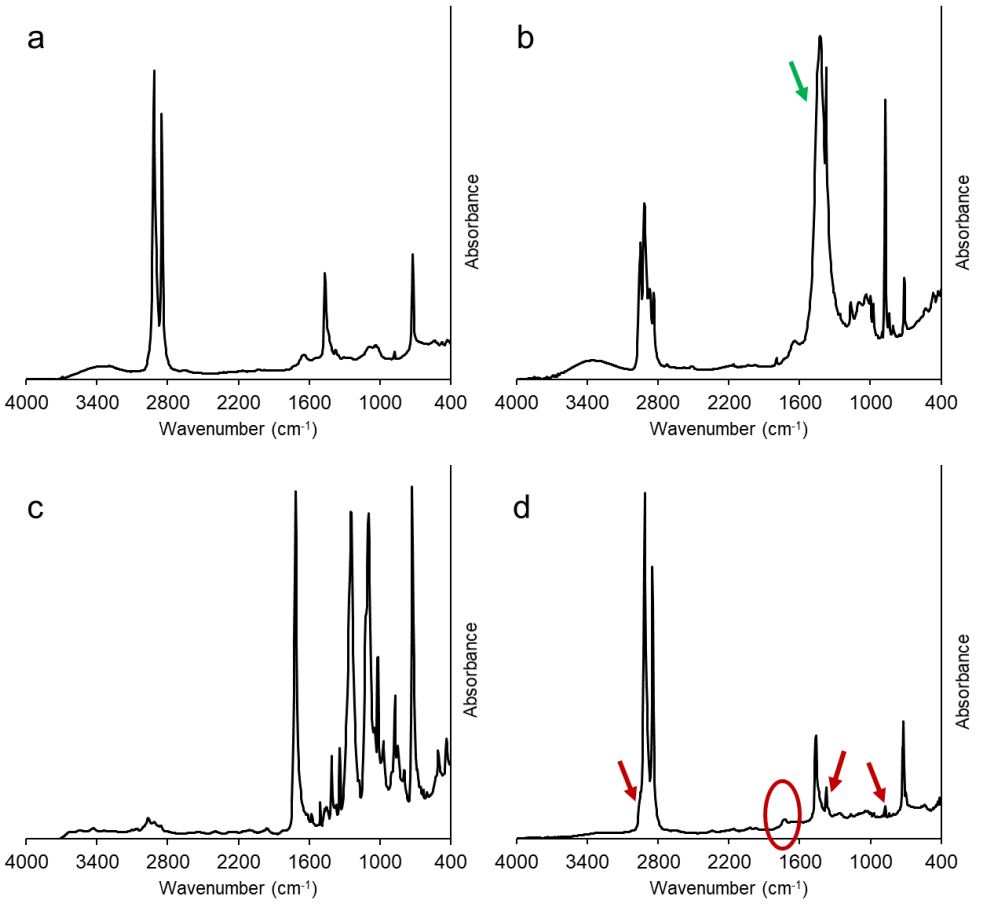

Figure 3.1. *ATR-FTIR spectra of selected FIL/S film fragments (a, b, c) and of a film obtained after melt mixing and molding (d).*

The majority of films analyzed showed the typical absorption of polyethylene (PE), as reported in Figure 3.1a, with strong peaks at 2916, 2850, 1470, and 720 cm^{-1} due to CH_2 asymmetric and symmetric stretching, bending and rocking deformations respectively. The presence of some weaker bands in the spectrum can be related to additives (stabilizers, pigments) and surface contamination. The spectra of a minor family of film fragments, as in Figure 3.1b, reveal the presence of polypropylene (PP) with the typical, composite absorption bands in the range 2980 – 2830 cm^{-1}, in some case filled with inorganic additives as calcium carbonate whose adsorption is indicated by the green arrow [20]. The presence of

polyethylene terephthalate (PET) films, with main absorptions of the ester group (carbonyl at 1715 cm^{-1}, C-O at 1240 and 1095 cm^{-1}), phenyl ring (1408 and 1340 cm^{-1}) [21], often laminated with PE or PP, was evidenced in some samples (Figure 3.1c). An "averaged" composition can be observed in the spectrum 3.1d, recorded after melt processing and molding: the main features of PE can be easily identified, with much less intense peaks attributed to PP (875, 1375 cm^{-1} and the shoulder at 2950 cm^{-1}, indicated by red arrows). A weak absorption in the carbonyl region (1720 cm^{-1}) can also be observed, which could be attributed to organic contaminants (e.g. PET, as observed in Figure 3.1c) and to a possible limited oxidative degradation of the polyolefin fractions [22].

^{13}C solid state NMR was also performed on finely ground FIL/S samples, as reported in Figure 3.2, to elucidate and quantitatively define the composition of the FIL/S mixture.

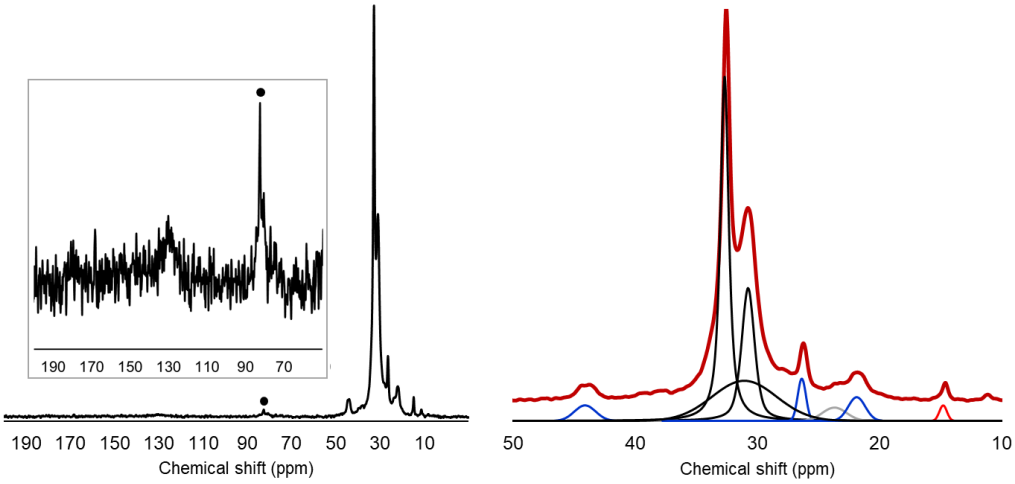

Figure 3.2. *^{13}C solid state NMR spectrum of FIL/S, left, with insert showing a magnification of the aromatic/carbonyl region. On the right, spectral deconvolution of the region containing the main signals of PE and PP. Spinning sidebands are marked by a dot.*

Analyzing the ^{13}C spectrum, the main resonances are found in the region 10 – 50 ppm and are assigned to PE (intense peaks centered at 30.8 and 32.6 ppm) and PP (signals at about 22, 26 and 44 ppm) moieties. The peak observed at 15 ppm was assigned to methyl groups of LDPE/LLDPE chain branches [23]. In the low-field section of the spectrum, reported in the insert at high magnification, some residual signals of unsaturated carbons and carbonyls (about 130 and 175 ppm)

can be observed, while a signal around 70 ppm is partially masked by the intense spinning sideband centered at about 75 ppm (marked by a dot in Figure 3.2). These signals are compatible with the presence of PET [24], in agreement with FTIR analysis.

Through a spectral deconvolution procedure, the peaks relative to the different components were isolated and the respective areas were calculated. The result of deconvolution is reported graphically in the right panel of Figure 3.2: peaks assigned to PE, PP and methyl terminals of PE branches are black, blue and red, respectively. It is to be noted that PE main chain at the solid state shows multiple resonances, due to the coexistence of crystalline and amorphous domains. Comparing the areas calculated, the content of PP was estimated at 12 wt%. Moreover, assuming that the number of chain branches (NB) is 20 for every 1000 CH_2 groups in the main chain, a reasonable estimation for LLDPE [25], from the area of the peak at 15 ppm it was evaluated that about 65% of PE in the FIL/S mixture is branched.

Summarizing, spectroscopic analyses clarified that FIL/S mixture was mainly composed by polyethylene, of which at least 65 wt% is branched, in addition to a moderate (12 wt%) amount of PP, traces of inorganic fillers and polymeric contaminations (essentially PET fragments).

3.3.2. BM treatment, processing and testing

The findings reported confirm the compositional complexity of the FIL/S mixture, as PE families with different chain structures are not easily processed together, and are generally not miscible with PP. To set up a versatile processing strategy, able to avoid phase separation and to allow the valorization and the recycling of the FIL/S, our approach was based on a high energy mechanical treatment [17]. The material, previously grounded as reported in the experimental part, was processed in a planetary ball mill, consisting in a steel milling jar containing steel balls and subjected to a planetary-like rotation-revolution motion. The balls accelerated by the fast rotation of the jar, generates strong local shear and compressive stresses on the processed materials.

Processing conditions were optimized changing jar and ball size, ball to material weight ratio, rotation rate and processing time. As described in the experimental section, two general BM conditions were selected: a “high energy” setup, obtained using 20 mm steel balls and a 500 mL jar, and a “low energy” setup based on 125 mL jars and 10 mm balls. Larger balls in fact result in higher impact energy, and larger jars due to their larger diameter increase the acceleration of balls. For the high energy conditions, rotation speed was limited to 400 rpm as any further increase led to overheating with a partial melting of the materials, while using 125 mL jars allowed rotation speed up to 600 rpm. Ball milled samples, reduced to a fine powder, were then melt processed and compression molded to 1.5 mm thick sheets and characterized, performing tensile tests and morphological analyses. For comparison, untreated FIL/S and a commercial neat LDPE were also characterized. In Table 3.1 the processing conditions, the relative code of the processed sample and the main mechanical parameters are resumed. The ball milled samples have been identified with AxB type codes where A represents the duration in hours of the treatment and B represents the rotation rate of the ball mill.

Table 3.1. *Codes, BM conditions and mechanical parameters of the recycled materials.*

BM geometry (jar vol. ball φ)	**BM conditions (time, speed)**	**Code**	**E (MPa)**	**σ (MPa)**	**ε (%)**
-	-	LDPE	300 ± 30	12.9 ± 0.5	450 ± 8
	-	FIL/S	348 ± 6	11.0 ± 0.7	20 ± 8
125 mL jar	4h, 600 rpm	4x600	330 ± 10	11.1 ± 0.3	20 ± 10
10 mm balls	8h, 600 rpm	8x600	317 ± 5	10.5 ± 0.1	60 ± 10
(Low Energy)	10 h, 600 rpm	10x600	340 ± 20	11.2 ± 0.1	30 ± 10
500 mL jar	4 h, 400 rpm	4x400	320 ± 10	10.9 ± 0.1	54 ± 3
20 mm balls	8h, 400 rpm	8x400	321 ± 6	11.1 ± 0.2	47 ± 8
(High Energy)					

The untreated FIL/S shows a low elastic modulus and low strength, comparable to those of a low density polyethylene (LDPE) and in line with compositional

analysis that identified branched PE as the main component of the mixture. However, a significantly lower value of the elongation at break than that of commercial LDPE was also recorded. The low evidence of signals relative to oxidized groups in the spectroscopic analyses allows to exclude thermo-oxidative degradation of the polymers as the cause of the low elongation observed. Then, this behavior could be attributed to the heterogeneity of the mixture. The presence of different immiscible polymers in a bulk mainly composed by LDPE causes an embrittlement of the material because these fractions act as defects generating a premature failure of the sample [26]. Observing data of treated materials, the ball milling does not affect the tensile modulus and the stress at break values, which are comparable to those of untreated FIL/S. On the contrary the mechano-chemical treatment induces an improvement as concerning the deformability of the samples, in particular the elongation at break value recorded on the of 8x600 and 4x400 samples is two and half times higher than the neat FIL/S.

Morphological analysis was performed on cryogenically fractured surface of the untreated and BM treated samples, to further investigate the effects of BM treatments: SEM micrographs of untreated FIL/S and of samples 8x600 and 4x400 are shown in Figure 3.3.

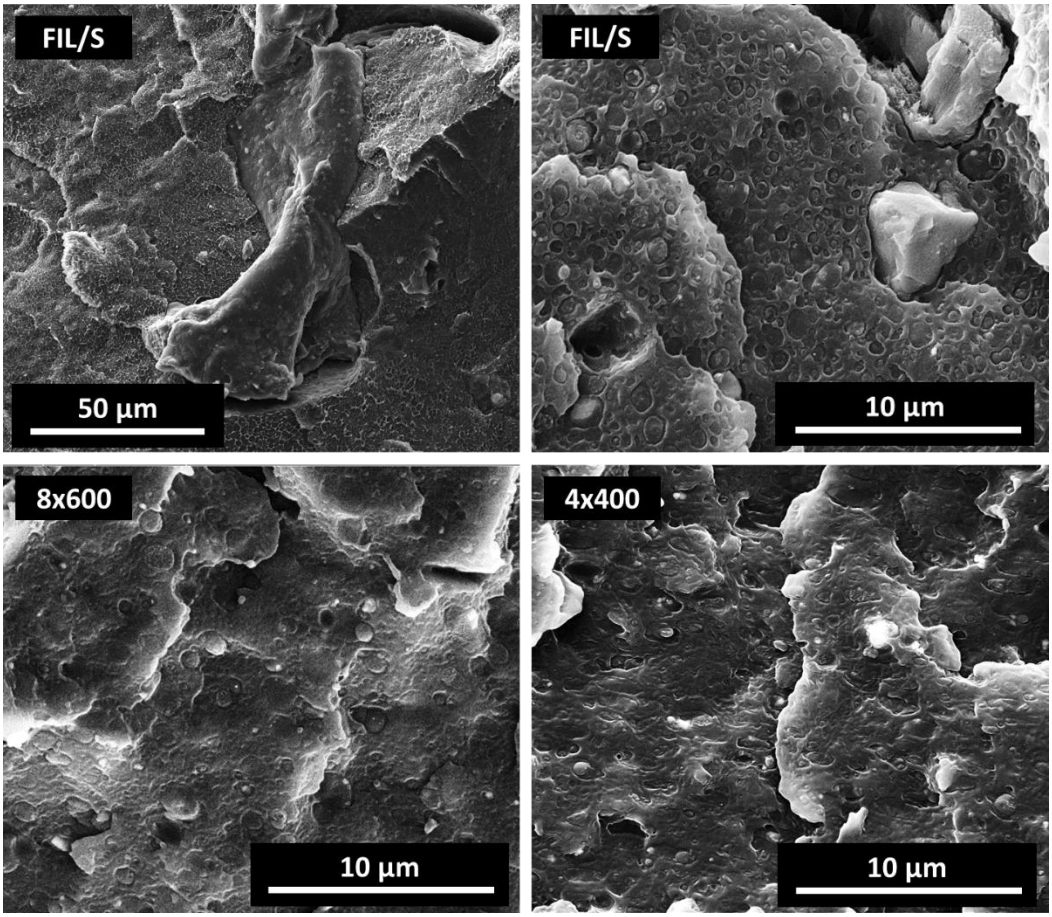

Figure 3.3. *SEM micrographs of cryo-fractured surfaces of FIL/S, 8x600 and 4x400 samples*

Comparing the morphology of the different materials, ball milling revealed a double effect on the structure of treated samples. First of all, large (few µm to tens of µm) inclusions with irregular shape, frequently observed in neat FIL/S, are practically absent in BM treated materials, evidencing a very effective homogenization induced by the milling. Such inclusions appear completely debonded from the FIL/S matrix and are the main responsible for the low elongation shown by FIL/S, representing defects and failure-starting points [27]. Large, film-like inclusions such as the one observed in the first panel of Figure 3.3 may be attributed to polymeric contaminants like PET, not melted during the processing. As a second finding, globular inclusions of micrometric and submicrometric size, observed in large numbers in FIL/S (affected, again, by evident debonding and pull-out due to low interfacial adhesion), are less evident in BM treated samples where they appear homogeneously dispersed and partially covered/anchored to the polymer bulk. Image analysis carried out on

SEM micrographs showed that the area occupied by the dispersed phase (approximated by 2D elliptical shapes, see section 5) is much larger in FIL/S, than in the BM treated samples. As shown in Table 3.2, the dispersed phase represents almost 20% of the fracture surface in FIL/S and is reduced to 7.4 and 4.6% in 8x600 and 4x400 samples, respectively. These observations underline a strong beneficial effect of the intimate mixing of the different polymeric phases induced by BM also at a micrometric level [17].

Table 3.2. *Surface fraction attributed to the dispersed phase obtained by image analysis of SEM micrographs.*

Sample	Dispersed phase area (%)
FIL/S	9.8
8x600	7.4
4x400	4.6

Summarizing, SEM analysis confirms the effects of the BM pretreatment on the morphology of the prepared materials, which is specifically the substantial size reduction of dispersed inclusions, thus resulting in the intimate mixing of different components and consequently in the improved homogeneity of the mixture. These effects justify lower occurrence of debonding phenomena and determine the enhancement of the elongation at break observed in mechanical tests for samples 8x600 and 4x400.

Moreover, in addition to the size reduction of inclusions, the BM processing could also promote, through mechanical stresses and local temperature increase produced by high energy impacts, the formation of reactive radical species, with the in-situ generation of graft copolymers able to actively compatibilize polymer blends [28]. This kind of reactions could be very useful to achieve a versatile, non-specific compatibilization of mixed polymer mixtures, by a simple and solvent-free process.

3.3.3. BM treatment coupled to the presence of peroxide

To explore the possible role of radical species formation and their reactions at the solid state, moderate amounts (0.5 and 1 wt%) of benzoyl peroxide (BPO) were added during the ball milling process. The BM treatment parameters granting the best properties/BM time balance (4x400) were selected for such test. BPO was added after 2 hours of milling, to ensure a sufficient grinding and thus a high available surface area; the treatment was then continued for 2 further hours.

After processing and compression molding, tensile tests were performed. Results of mechanical analysis are reported in Table 3.3 and compared with values of the unprocessed FIL/S and 4x400 materials.

Table 3.3. *Codes and mechanical parameters of the materials treated with BPO, as compared to neat FIL/S and 4x400 samples.*

Additive	**Code**	**E (MPa)**	**σ (MPa)**	**ε (%)**
-	FIL/S	348 ± 6	11.0 ± 0.7	20 ± 8
-	4x400	320 ± 10	10.9 ± 0.1	54 ± 3
0.5 wt% BPO	0.5 BPO (2+2)x400	444 ± 6	10.5 ± 0.3	40 ± 10
1 wt% BPO	1 BPO (2+2)x400	520 ± 20	11.5 ± 0.2	60 ± 10

In the presence of BPO, a significant increase of elastic modulus was recorded, correlated to the amount of peroxide. These data suggest that BPO is likely to induce some level of crosslinking in the polyethylene matrix, responsible for the increased stiffness. A very light degree of crosslinking can be hypothesized, as the materials were processed in the extruder and compression molded without any evidence of gels or obstructions to viscous flow. Notwithstanding the increased stiffness, BPO containing materials showed a higher ultimate elongation with respect to FIL/S and, at 1 wt% of BPO, even higher than the 4x400 sample. The effect of peroxides on single polyolefins and on their blends has been widely investigated, reporting beneficial effects on the compatibility of PE-PP blends [29] but also a crosslinking effect on the PE fraction [30]. The

deformability of materials is strongly dependent on composition, generally decreasing with increasing peroxide content [31, 32].

Interestingly, it has been reported that the use of peroxides at low temperature, in solution [30] or at the solid state [33], can largely prevent crosslink/degradation of polyolefins. We can thus conclude that the addition of BPO during the BM process, at moderate temperatures (maximum T recorded is 80 °C), followed by the extrusion process of the blend, has a lower adverse effect on the polymer structure in comparison to the direct addition of BPO during melt processing (temperatures above 180 °C). The higher elongation showed at higher BPO content suggests a synergistic effect of BM treatment and peroxide action on the structure of the final materials, which will require further studies to be fully elucidated. SEM analysis of the best performing material, 1 BPO (2+2)x400, is shown in Figure 3.4 in comparison with 4x400.

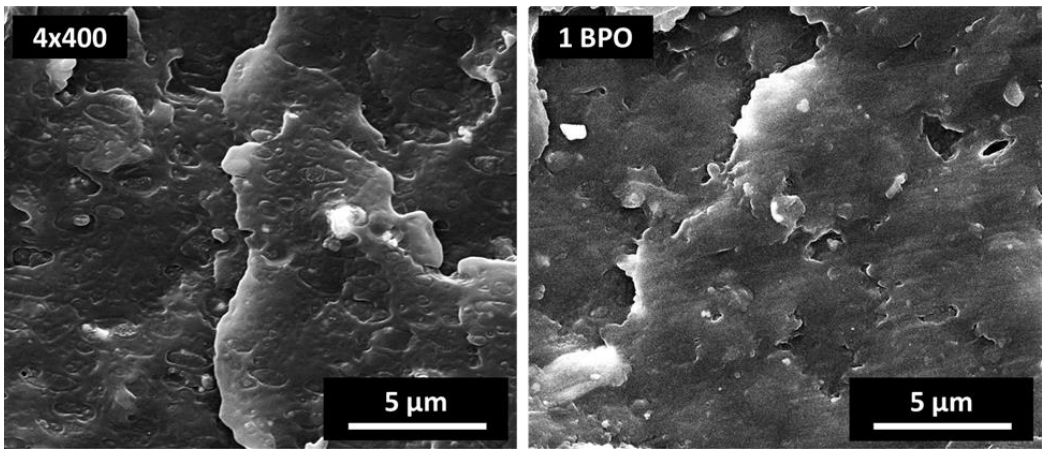

Figure 3.4. *SEM micrographs of cryo-fractured surfaces of 4x400 and 1 BPO (2+2)x400 samples*.

Spherical, immiscible inclusions are much less evident in the sample processed with BPO, thus suggesting the achievement of an effective compatibilization through the reactive BM treatment. Although a mixing of the heterogeneous polymer mixture at molecular level is unlikely, the better dispersion and stronger interfacial adhesion induced by the processing reduce interface failure during cryo-fracturation, resulting in smoother surfaces.

3.4. Conclusions

A strategy based on high energy mechanical treatments was investigated to valorize and recycle polyethylene rich heterogeneous post-consumer mixture. This strategy allows to induce a fine grinding of different polymeric fractions and contaminants thus promoting an intimate mixing between different components. As a result, an improvement of mixture morphology and a higher deformability were obtained. Then, the addition of small amounts of benzoyl peroxide during the ball milling was also explored to promote radical formation. The low temperature of the process reduced the adverse effects of the peroxide on polymers, granting higher stiffness while retaining a significant ductility, phenomena ascribable to the effective compatibilization and to the formation of very light crosslinking.

This technology can be considered an advancement towards sustainability, considering that the treatments were carried out in absence of solvent and at room temperature and no further purification/refinement steps were needed.

3.5. Appendix

Image analysis

Image analysis was carried out on SEM micrographs of cryo-fractured surfaces, to obtain quantitative geometrical information on the dispersed phase.

The ImageJ software package was used for the analysis. Contrast and brightness of the micrographs were adjusted to evidence any discontinuity in the surface, then the dispersed phase was identified and inclusions were manually fitted to ellipses. For neat FIL/S, the area of the micrograph containing large (> 5 μm) inclusions of irregular shape was excluded from the analysis.

In Figures S1 and S2, the analyzed areas and the results of dispersed phase identification are shown, respectively.

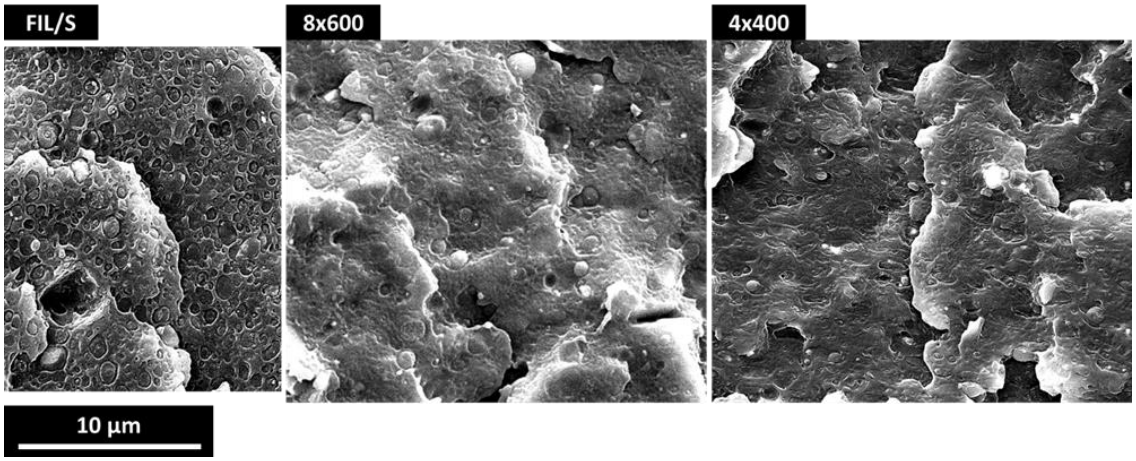

Figure S1. Areas selected for image analysis with contrast enhancement

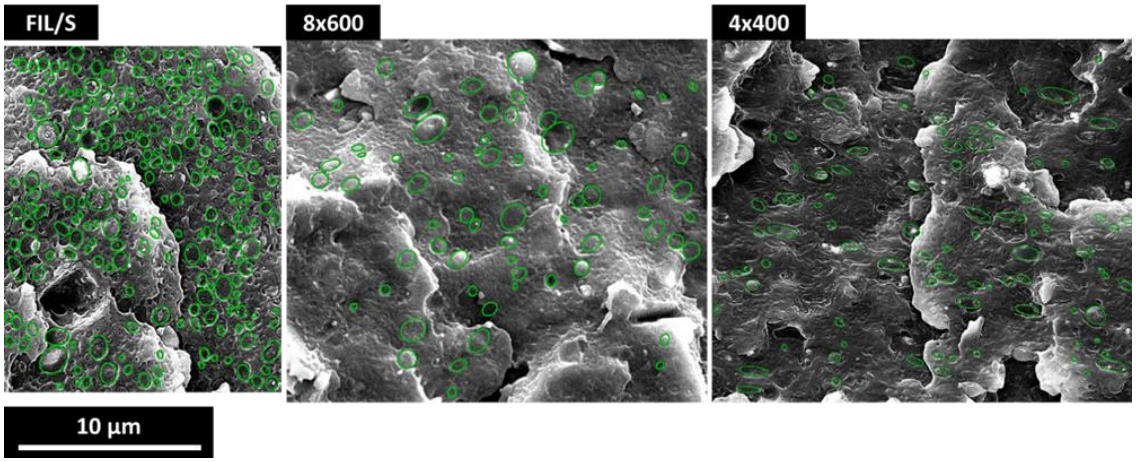

***Figure S2**. Dispersed phase inclusions identified and fitted to ellipses*

BIBLIOGRAPHY

1. Plastics Europe. Plastics – the facts 2020. An analysis of European plastics production, demand and waste data. https://www.plasticseurope.org/download_file/force/4829/419 (Accessed on 20/07/2021).

2. Grand View Research, Inc. Plastic Packaging Market Trends & Growth Report, 2021-2028. https://www.grandviewresearch.com/industry-analysis/plastic-packaging-market (Accessed 21/07/2021).

3. Luijsterburg, B.; Goossens, H. Assessment of plastic packaging waste: Material origin, methods, properties. Resour. Conserv. Recy. 2014, 85, 88-97. DOI: 10.1016/j.resconrec.2013.10.010

4. Lebreton, L.; Andrady, A. Future scenarios of global plastic waste generation and disposal. Palgrave Commun 2019, 5, Art. n. 6. DOI: 10.1057/s41599-018-0212-7

5. The European Commission. A European Strategy for Plastics in a Circular Economy, 2018. https://eur-lex.europa.eu/legal-content/EN/TXT/?uri=COM:2018:28:FIN (Accessed on 07/08/2021).

6. Ellen MacArthur Foundation. The New Plastics Economy, Rethinking the Future of Plastics and Catalysing Action, 2017. https://www.ellenmacarthurfoundation.org/assets/downloads/publications/NPECHybrid_English_22-11-17_Digital.pdf (Accessed on 20/07/2021).

7. Martijn Roosen, M.; Mys, N.; Kusenberg, M.; Billen, P.; Dumoulin, A.; Dewulf, J.; Van Geem, K.M.; Ragaert, K.; De Meester, S. Detailed Analysis of the Composition of Selected Plastic Packaging Waste Products and Its Implications for Mechanical and Thermochemical Recycling. Environ. Sci. Tech. 2020, 54, 13282−13293. DOI: 10.1021/acs.est.0c03371.

8. Kaiser, K.; Schmid, M.; Schlummer, M. Recycling of Polymer-Based Multilayer Packaging: A Review. Recycling 2018, 3, Art. n. 1. DOI: 10.3390/recycling3010001.

9. Utracki, L.A. Role of Polymer Blends' Technology in Polymer Recycling. In Polymer Blends Handbook; Utracki, L.A., Eds.. Kluwer Academic Publishers, Dordrecht, The Netherlands, 2003; 1117-1165. DOI: 10.1007/0-306-48244-4_16.

10. Maris, J.; Bourdon, S.; Brossard, J-M.; Cauret, L.; Fontaine, L.; Montembault, V. Mechanical recycling: Compatibilization of mixed thermoplastic wastes. Polym. Degrad. Stabil. 2018, 147, 245-266. DOI: 10.1016/j.polymdegradstab.2017.11.001.

11. Covas, J.A.; Pessan, L.A.; Machado, A.V.; Larocca, N.M. Polymer Blend Compatibilization by Copolymers and Functional Polymers. In Encyclopedia of Polymer Blends; Isayev, A.I., Ed. Wiley-VCH Verlag & Co. KGaA, Weinheim, Germany, 2011; 315-356. DOI: 10.1002/9783527805242.ch7.

12. Brown, S.B. Reactive Compatibilization of Polymer Blends. In: Polymer Blends Handbook; Utracki, L.A., Eds., Kluwer Academic Publishers, Dordrecht, The Netherlands, 2003; 339-415. DOI: 10.1007/0-306-48244-4_5.

13. Bonadies, I.; Avella, M.; Avolio, R.; Carfagna, C.; Gentile, G.; Immirzi, B.; Errico, M.E. Probing the effect of high energy ball milling on PVC through a multitechnique approach. Polym. Test. 2012, 31, 176–181. DOI: 10.1016/j.polymertesting.2011.10.010.

14. Castaldo, R.; Avolio, R.; Cocca, M.; Gentile, G.; Errico, M.E.; Avella, M.; Carfagna, C.; Ambrogi, V. A Versatile Synthetic Approach toward Hyper-Cross-Linked Styrene-Based Polymers and Nanocomposites. Macromolecules 2017, 50, 4132-4143. DOI: 10.1021/acs.macromol.7b00812.

15. Delogu, F.; Gorrasi, G.; Sorrentino, A. Fabrication of polymer nanocomposites via ball milling: Present status and future perspectives. Progr. Mater. Sci. 2017, 86, 75–126. DOI: 10.1016/j.pmatsci.2017.01.003.

16. Yin, S.; Tuladhar, R.; Shi, F.; Shanks, R.A.; Combe, M.; Collister, T. Mechanical reprocessing of polyolefin waste: A review. Polym. Eng. Sci. 2015, 55, 2899-2909. DOI: 10.1002/pen.24182.

17. Avolio, R.; Spina, F.; Gentile, G.; Mariacristina Cocca, M.; Avella, M.; Carfagna, C.; Tealdo, G.; Errico, M.E. Recycling Polyethylene-Rich Plastic Waste from Landfill Reclamation: Toward an Enhanced Landfill-Mining Approach. Polymers 2019, 11, 208; DOI: 10.3390/polym11020208.

18. Cappucci, G.M.; Avolio, R.; Carfagna, C.; Cocca, M.; Gentile, G.; Scarpellini, S.; Spina, F.; Tealdo, G.; Errico, M.E.; Ferrari A.M. Environmental life cycle assessment of the recycling processes of waste plastics recovered by landfill mining. Waste Manage. 2020, 118, 68-78. DOI: 10.1016/j.wasman.2020.07.048.

19. Castaldo, R.; De Falco, F.; Avolio, R.; Bossanne, E.; Cicaroni Fernandes, F.; Cocca, M.; Di Pace, E.; Errico, M.E.; Gentile, G.; Jasiński, D.; Spinelli, D.; Albein Urios, S.; Vilkki, M.; Avella, M. Critical Factors for the Recycling of Different End-of-Life Materials: Wood Wastes, Automotive Shredded Residues, and Dismantled Wind Turbine Blades. Polymers 2019, 11, 1604; DOI: 10.3390/polym11101604

20. Lin, J-H.; Pan, Y-J.; Liu, C-F.; Huang, C-L.; Hsieh, C-T.; Chen, C-K.; Lin, Z-I.; Lou, C-W. Preparation and Compatibility Evaluation of Polypropylene/High Density Polyethylene Polyblends. Materials 2015, 8, 8850-8859. DOI: 10.3390/ma8125496.

21. Bach, C; Dauchy, X.; Etienne, S. Characterization of poly(ethylene terephthalate) used in commercial bottled water. IOP Conf. Ser.: Mater. Sci. Eng. 2009, 5, 012005. DOI: 10.1088/1757-899X/5/1/012005.

22. Almond, J.; Sugumaar, P.; Wenzel, M.N.; Hill, G.; Wallis, C. Determination of the carbonyl index of polyethylene and polypropylene using specified area under band methodology with ATR-FTIR spectroscopy. e-Polymers 2020, 20, 369-381. DOI: 10.1515/epoly-2020-0041.

23. Klimke, K.; Parkinson, M.; Piel, C.; Kaminsky, W.; Spiess, H.W.; Wilhelm, M. Optimisation and Application of Polyolefin Branch Quantification by Melt-State 13C NMR Spectroscopy. Macromol. Chem. Phys. 2006, 207, 382-395. DOI: 10.1002/macp.200500422.

24. Avolio, R.; Gentile, G.; Avella, M.; Carfagna, C.; Errico, M.E. Polymer-filler interactions in PET/CaCO3 nanocomposites: Chain ordering at the interface and physical properties. Eur. Polym. J. 2013, 49, 419-427. DOI: 10.1016/j.eurpolymj.2012.10.008

25. Salakhov, I.I.; Shaidullin, N.M.; Chalykh, A.E.; Matsko, M.A.; Shapagin A.V.; Batyrshin, A.Z.; Shandryuk, G.A.; Nifant'ev, I.E. Low-Temperature Mechanical Properties of High-Density and Low-Density Polyethylene and Their Blends. Polymers 2021, 13, 1821. DOI: 10.3390/polym13111821.

26. Dorigato, A. Recycling of polymer blends. Adv. Ind. Eng. Polym. Res. 2021, 4, 53-69. DOI: 10.1016/j.aiepr.2021.02.005.

27. Avella, M.; Avolio, R.; Bonadies, I.; Carfagna, C.; Errico, M.E.; Gentile, G. Recycled multilayer cartons as cellulose source in HDPE-based composites: Compatibilization and structure-properties relationships. J. Appl. Polym. Sci. 2009, 114, 2978-29851. DOI: 10.1002/app.30913.

28. Cavalieri, F.; Padella, F.; Bourbonneux, S. High-energy mechanical alloying of thermoplastic polymers in carbon dioxide. Polymer 2002, 43, 1155-1161. DOI: 10.1016/S0032-3861(01)00721-2.

29. Vivier, T.; Xanthos, M. Peroxide modification of a multicomponent polymer blend with potential applications in recycling. J. Appl. Polym. Sci. 1994, 54, 569-575. DOI: 10.1002/app.1994.070540507.

30. Braun, D. Richter, S.; Hellmann, G.P.; Rätzsch, M. Peroxy-initiated chain degradation, crosslinking, and grafting in PP–PE blends. J. Appl. Polym. Sci. 1998, 68, 2019-2028. DOI: 10.1002/(SICI)1097-4628(19980620)68:12<2019::AID-APP16>3.0.CO;2-W.

31. Gu, J.; Xu, H.; Wu, C. The Effect of PP and Peroxide on the Properties and Morphology of HDPE and HDPE/PP Blends. Adv. Polym. Tech. 2013, 32, art. n. 21326. DOI: doi.org/10.1002/adv.21326.

32. González-Sánchez, C.; Martínez-Aguirre, A.; Pérez-García, B.; Acosta, J.; Fonseca-Valero, C.; de la Orden, M.U. Sánchez, C.; Martínez Urreaga, J. Enhancement of mechanical properties of waste-sourced biocomposites through peroxide induced crosslinking. Composites Part A: App. Sci. Manufacturing 2016, 80, 285-291. DOI: 10.1016/j.compositesa.2015.10.032.

33. Diop, M.F.; Torkelson, J.M. Novel synthesis of branched polypropylene via solid-state shear pulverization. Polymer 2015, 60, 77-87. DOI: 10.1016/j.polymer.2015.01.016.

Chapter 4

Ball mill treated cellulose as reinforcement in plasticized PLA based composites

The results of this chapter are under preparation for submission to a journal in the field of polymer composites

4.1. Introduction

Polymeric materials produced from renewable resources and/or capable of being completely biodegraded at the end of their useful life are increasingly used to replace fossil-derived polymers. In fact, they ideally guarantee environmental sustainability both in the production phase, which is essentially independent of petrochemical derivatives, and in the management of their end-of-life. In order to compete with traditional polymers, bio-based materials must show adequate physical and thermo-mechanical properties, good processability but also reasonably low costs. Often, to obtain the desired properties, it is necessary to include in the formulation of bio-based plastics some specific additive or different polymeric species, thus creating polymeric blends or composite materials.

Among biodegradable thermoplastics, poly(lactic) acid (PLA), an aliphatic polyester, is characterized by chemo-physical and mechanical properties comparable to those of many polymers of fossil origin, with the advantage of being produced from renewable sources through a low environmental impact and low cost. PLA can be used in numerous applications, ranging from automotive to food packaging [1,2]; however, some intrinsic characteristics of PLA, including in particular its poor ductility and brittle behavior, limit a wider diffusion. Therefore, the research on new solutions to produce PLA based materials with improved ductility, by mixing it with suitable additives, has experienced strong development in recent years [3].

Plasticizers are additives with low glass transition temperature and low modulus of elasticity that can be used to tune the thermo-mechanical properties of glassy

polymeric matrices. The final properties of a given polymer/plasticizer blend depend on the miscibility between the components, the concentration of the additive, the processing conditions: usually the increase in ductility and toughness, induced by the plasticizer, is coupled with a strong decrease in the elastic modulus and tensile strength. Furthermore, low molecular weight plasticizers are often prone to develop phase separation and/or migration to the surface of the materials [4]. These phenomena result in a change in thermo-mechanical behavior, with a progressive stiffening of the system, and can lead to contamination of products (e.g. foods) put in contact with the plasticized polymer.

The realization of composites and nanocomposites can be an effective strategy to improve and modulate the response of polymeric materials, thus exploiting a synergistic effect between the properties of the polymeric matrix and the organic/inorganic fillers [5]. In ternary systems, where a plasticizer additive is introduced in combination with the polymeric matrix and solid particles, the interaction between the three components can have strong effects on the mechanical response and on the evolution of properties over time [6].

Cellulose, which is the most abundant natural polymer, has many fields of application and is widely used in the sector of polymer based composites. Cellulosic fibers have a high stiffness and can exert a mechanical reinforcement action, improving the response to loads of polymeric materials [7,8]. Furthermore, in the case of plasticized composite systems, a strong interaction is expected between the surface of the cellulose, rich in hydroxyl groups, and the plasticizer molecules (for example through hydrogen bonds), envisaging a positive effect on the evolution of properties over time.

To induce morphological and/or structural changes in cellulose, it is possible to exploit mechano-chemical processes through treatments in a planetary ball mill (ball mill, BM). Mechanochemistry, which consists in the use of intense mechanical stimuli to induce chemical reactions or structural modifications in different types of materials [9, 10] has recently found application in the field of green chemistry, as it allows to carry out treatments in relatively mild conditions and, in many cases, in the absence of solvents. Ball mills represent one of the most

widespread technologies for this type of treatment. Studies on BM treatments on cellulose reveal that in 'dry' conditions (absence of solvent) the treatment leads to an amorphization of the cellulose itself, with a progressive evolution from a fiber-like to a particle-like morphology [11]. In the case of treatments carried out in the presence of a liquid phase ('wet' BM), on the other hand, a deconstruction of the cellulosic fibers can be obtained without strong effects on crystallinity, leading to the liberation of fibrils [12] with a high aspect ratio. BM therefore represents a flexible process technique that allows to modify the structure and morphology of the cellulose in different ways, by modulating the process conditions.

In this research, PLA-based composites were realized, containing cellulosic materials as an organic filler and an oligomeric ester of lactic acid as a plasticizing agent. The cellulosic fraction was subjected to different BM treatment, resulting in a range of different morphologies, with the aim to modulate the properties of the composites. The thermo-mechanical properties of the ternary systems produced were measured as a function of the aging time under controlled conditions; the influence of composition on vapor permeability and on the biodegradability under soil burial conditions were also evaluated.

4.2. Materials and methods

4.2.1 Materials

The polylactic acid used for the present work (Ingeo 4032D, Natureworks) is characterized by an L isomer content > 98%. As plasticizing agent, an oligomeric ester of lactic acid was selected, characterized by hydroxyl chain end groups (OLA), whose efficacy and high chemical compatibility with the matrix were previously demonstrated [13] REF. As reinforcement, pure cellulose fibers were used, with an average length of about 200 microns and an average diameter of 20 microns (Arbocel BWW40). In order to modify the structure and morphology of the fibers, mechanochemical treatments were experimented as detailed in the next section. Before the various treatments and mixing, the cellulose was dried under vacuum at 90°C for 24h, while PLA and OLA_OH were dried under vacuum at 60°C for 24h.

4.2.2 Preparation methods

As mentioned, the BM treatment can lead, depending on the conditions used, to the obtainment of cellulosic materials with different properties. Binary systems, that is, PLA composites containing cellulose, were produced as follows. Neat cellulose was subjected to a dry BM process in a planetary ball mill (Retsch PM 100) using a 125 ml stainless steel jar, 10 g of cellulose and 25 10 mm steel spheres, milling at 600 rpm for 1 hour. Dry treated cellulose was coded BMCEL. Composites with increasing content of BMCEL (10, 20 and 30 wt%) and a reference system with 20 wt% of unmodified fibrous cellulose (BWW40) were then prepared by melt mixing. The mixing was carried out at 170°C, using a twin blades internal mixer (Brabender Plastograph EC), with a rotation speed of 60 rpm and a total mixing time of 8 minutes. The materials obtained were pelletized and compression molded at 170 °C, 50 bar, obtaining films with a thickness of about 200 µm. For the realization of ternary systems containing both the cellulose and the plasticizer, different BM conditions were explored, with the dual purpose of favoring the mixing and homogenization of the cellulose/OLA system or to defibrillate, at least partially, the cellulose itself. In the first approach, the previously obtained BMCEL was mixed with OLA and subjected to a short (30 min) homogenization treatment in BM, using a 125 mL steel jar, 25 10 mm spheres and a speed of 400rpm. In the second approach, a wet BM process was implemented, treating neat BWW40 cellulose in BM in the presence of OLA, under the same conditions reported above, for times of 2 hours and 4 hours. The cellulose/OLA ratio was fixed in order to obtain, once mixed with PLA, composites with a PLA/OLA weight ratio equal to 80/20 and a cellulose content equal to 20 wt%. The mixing of cellulose/OLA mixtures with molten PLA and the subsequent compression molding were carried out as described above.

The compositions and codes of materials prepared are reported in Table 4.1

Table 4.1. *Composition and codes of all materials prepared*

Sample	PLA/OLA ratio	Cellulose (wt%)
PLA	-	-
PLA+10BMCEL	-	10
PLA+20BMCEL	-	20
PLA+30BMCEL	-	30
PLA+20BWW40	-	20
PLA+(PLA/BMCEL) BM30'	80/20	20
PLA+(PLA/BWW40) BM2h	80/20	20
PLA+(PLA/BWW40) BM4h	80/20	20

4.2.3 Aging

To study the effect of aging time on the main properties of plasticized composites, molded films were aged in a climatic chamber maintained at 25 ± 0.1 °C and 50 ± 1% RH and tested at regular intervals.

4.2.4 Techniques

Tensile tests were carried out using an Instron 5564 apparatus, using dumb-dell shaped specimens with a section of about 0.8 mm^2, a gage length of 28 mm and a deformation rate of 10 mm/min. The test temperature was set at 27 ± 1 °C using an Instron 3119 thermal chamber. From the recorded stress/strain curves, the parameters of elastic modulus, stress at break and elongation at break were calculated.

Calorimetric analyses were carried out using a TA-Q2000 DSC, equipped with an RCS-90 cooling unit. For the measurements, samples weighing about 5 mg were placed in an aluminum pan and heated/cooled at a rate of 20°C/min. The temperature range explored goes from -70 to 190 °C for plasticized materials, and from -20 to 190 °C for plasticizer-free composites. The parameters obtained from the DSC measurements are the glass transition temperature, the temperatures corresponding to the cold crystallization and melting peaks. The crystallization/melting enthalpy values and the degree of crystallinity were

calculated considering the PLA fraction contained in the systems. The enthalpy of fusion for fully crystalline PLA used to evaluate the degree of crystallinity is 93.6 J/g [14].

Analysis of the morphology of cellulosic materials subjected to ball milling under different conditions was performed using a FEI Quanta 200 FEG SEM scanning electron microscope (FEI, Eindhoven, The Netherlands) in high vacuum mode. The cellulose subjected to the different ball milling processes was analyzed after extracting the plasticizer through repeated washings in acetone.

Water vapor permeability tests were performed by recording the weight loss of cups containing water, sealed with films of the prepared composite materials and kept in controlled humidity and temperature conditions, according to the ASTM E96 standard.

The soil burial tests were performed by burying circular samples (3 replicates for each material) at a depth of about 5 cm in a mixed cultivation soil (characteristics declared: C org. % SS 40; electrical conductivity dS/m 1.0; dry bulk density kg/m^2 950; total porosity %v/v 85.0; pH 7), kept at room temperature and maintaining a high humidity level by regular water addition. The weight of each sample was recorded at regular intervals, recovering the samples and delicately cleaning them with filter paper. The weight was stabilized by storing the samples at room temperature under vacuum for at least 5 hours.

4.3. Results and discussion

4.3.1 Unaged samples

To evaluate the effects of the BM treatments on the cellulose/plasticizer systems, the morphologies of cellulose fractions were analyzed by SEM microscopy. From the analysis of the micrographs, shown in Figure 4.1, it can be observed that the cellulose, initially showing a fibrous morphology (Figure 4.1a), when subjected to a dry BM treatment undergoes a strong fragmentation of the fibers, resulting in a particle-like appearance (Figure 4.1b). On the contrary, the treatment in wet conditions in the presence of the liquid plasticizer (Figures 4.1c and 4.1d), favors

a partial defibrillation of the pristine cellulose fibers with the formation of fibrils with a high aspect ratio, observable at high magnification. The different morphologies observed underline the flexibility of the BM treatments in order to obtain cellulosic materials with different characteristics.

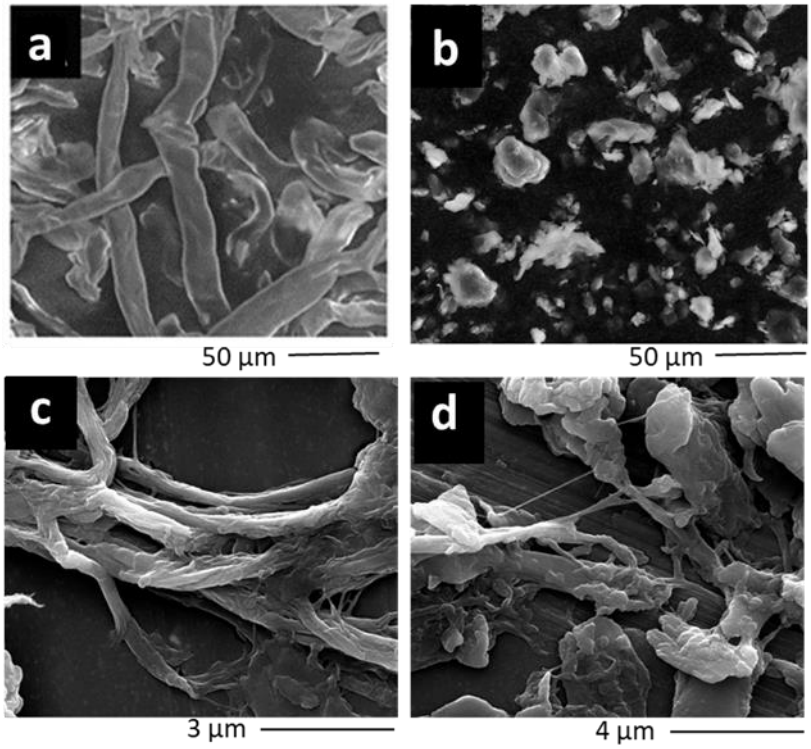

Figure 4.1. *SEM images of the commercial BWW40 cellulose used to make the composites a); BWW40 cellulose after ball-milling treatment in dry conditions (BMCEL) b); cellulose system BWW40-plasticizer treated for 2h in ball-milling c); cellulose system BWW40-plasticizer treated for 4h in ball-milling d)*

The initial (unaged) values of the thermal and mechanical parameters of the various composites produced were measured after a conditioning time in a climatic chamber, at controlled humidity and temperature values, equal to 24h. The results of the DSC calorimetric tests (Table 4.2) and mechanical tensile tests (Table 4.3) relating to PLA, PLA/cellulose composites and plasticised ternary systems are reported below.

Table 4.2. *Calorimetric parameters recorded during the first heating run: glass transition temperature Tg(°C), cold crystallization temperature TIcc (°C), cold crystallization enthalpy ΔHcc (J g-1), melting temperature TIf (°C), enthalpy of fusion ΔHf (J g-1), degree of crystallinity Xc of PLA and composites.*

Sample	Tg (°C)	Tcc (°C)	Tm (°C)	Xc (%)
PLA	55	106	167	5
PLA+10BMCEL	55	106	168	7
PLA+20BMCEL	53	107	168	10
PLA+30BMCEL	55	104	169	8
PLA+20BWW40	55	108	169	5
PLA+(PLA/BMCEL) BM30’	31	80	159	17
PLA+(PLA/BWW40) BM2h	31	79	160	18
PLA+(PLA/BWW40) BM4h	31	79	160	17

Table 4.3. *Young's modulus E (MPa), ultimate elongation εb (%) and maximum stress (σb) of PLA and composites.*

Sample	E (MPa)	εb (%)	σb (%)
PLA	2750 ± 90	4.0 ± 0.1	56 ± 1
PLA+10BMCEL	3000 ± 100	2.1 ± 0.3	48 ± 4
PLA+20BMCEL	3100 ± 100	1.5 ± 0.3	39 ± 4
PLA+30BMCEL	3100 ± 100	1.2 ± 0.1	28 ± 5
PLA+20BWW40	3200 ± 70	1.2 ± 0.3	38 ± 5
PLA+(PLA/BMCEL) BM30’	1900 ± 200	110 ± 30	13 ± 1
PLA+(PLA/BWW40) BM2h	1800 ± 200	60 ± 10	12 ± 1
PLA+(PLA/BWW40) BM4h	2200 ± 200	70 ± 20	12 ± 1

From the analysis of the thermal properties measured by differential scanning calorimetry (DSC), a decrease of the glass transition temperature (Tg) and of the cold crystallization temperature (Tcc) is highlighted in all the plasticized materials, if compared to PLA and PLA/cellulose composites. These features are coupled to a higher crystallinity degree. These phenomena are expected and related to the action of the plasticizer that, increasing chain mobility, induces both a

lowering in glass transition and accelerates crystallization [15]. However, the melting temperature in plasticized materials is lower than in PLA, suggesting an effect of the plasticizer also on the structure of the crystalline phase [16]. No low-temperature transitions were observed, confirming the good mixing of the plasticizer with the polymer matrix. In non-plasticized composites, the presence of cellulose did not show any significant effect on the main thermal transitions observed.

As far as the mechanical properties are concerned, the presence of cellulose fibers induces an increase in the elastic moduli in the composites with respect to neat PLA, which however is accompanied by a lowering of ultimate elongation and ultimate strength. This behavior is indicative of an imperfect adhesion at the interface between the polymer matrix and the cellulose reinforcement, which leads to a separation between the components following mechanical stresses and, consequently, to a premature failure of the composites. The mechanical parameters of composites containing fibrous cellulose is comparable to that observed in BMCEL composites, although fibrous, high aspect ratio reinforcements are expected to show a stronger effect on the mechanical response. The low reinforcing efficiency observed in the PLA+20 BWW40 system is probably related to the lack of fiber orientation and to a non optimal dispersion of cellulose fibers, that are prone to the formation of bundles and agglomerates, thus reducing the actual aspect ratio of the cellulosic filler.

In ternary systems, the scenario changes as the action of the plasticizer dominates the mechanical properties. In this case, in fact, the high ductility of the polymeric matrix results in materials with high ultimate elongations (up to 100%). The presence of cellulose has an important effect on the elastic modulus of plasticized composites, that is higher than observed in the PLA/OLA systems reported in literature [13]. The morphology of the cellulosic phase, in these systems, essentially influences the deformability of the composites: particle-like cellulose (BMCEL) induces a higher ductility resulting in higher ultimate deformation of the sample PLA+(OLA/BMCEL)30’ with respect to samples containing fibrillated cellulose. The different elongation, however, is not coupled to significant differences in strength and stiffness: again, the higher aspect ratio of partly

fibrillated cellulose is counterbalanced by the imperfect distribution of fibers and by the low adhesion at the interface.

Transport properties, of interest for possible applications of our composites in the packaging sector, were evaluated in terms of water vapor transmission rate (WVTR), measured using the cup method (ASTM E96). Tests were carried out with a temperature of 25°C and a relative humidity (RH) difference of 50% across the polymer film under test. The results of the water vapor transmission rate obtained (WVTR) are shown in Table 4.4. For all the composites tested, the transmission of water vapor is increased compared to PLA, following the high hydrophilicity of the cellulosic fibers. The WVTR recorded in binary formulation is, in fact, roughly proportional to the cellulose content. Interestingly, in plasticized materials, the increase in WVTR is greater than in composites containing the same amount (20%) of cellulose, highlighting an effect of the plasticizer. Oligomeric esters are expected to be more hydrophilic than PLA, and this factor can contribute to a higher water absorption and transport across the composite. Moreover, the increase in free volume caused by plasticization can also be responsible for a higher solubility of gases and vapors into the polymeric matrix, further increasing permeation.

It should be also underlined that the fibrillated cellulose (present in PLA/OLA/CEL BM 2h and 4h materials) caused a strong increase in WVTR, pointing out a higher available surface (that is, a higher hydrophilicity). The water permeation properties of our composites are relevant also in view of their soil burial degradation behavior, as discussed in Section *4.3.3* will be capable of forming a network of highly hydrophilic fibers within the composite, gives the materials greater permeability to water vapor.

Table 4.4. *WVTR recorded on PLA and on all the prepared composites.*

Sample	WVTR (g mm/(24h m^2))
PLA	2.7
PLA+10BMCEL	3.9
PLA+20BMCEL	4.8
PLA+30BMCEL	7.4
PLA+20BWW40	4.7
PLA+(PLA/BMCEL) BM30’	5.6
PLA+(PLA/BWW40) BM2h	7.0
PLA+(PLA/BWW40) BM4h	7.4

4.3.2 Aging and stability of properties

The evolution of the properties of ternary systems with aging time was monitored through the analysis of the mechanical response of materials stored under controlled conditions. The study was limited to plasticized composites only, as only in these systems a fast change in properties can be expected, due to the evolution of plasticizer phase distribution.

The main mechanical parameters recorded as a function of the aging time are shown in Figure 4.2. The values of the elastic modulus recorded in all systems show a slight increase in the first 2 weeks of aging and then remains almost constant, although with small fluctuations. Likewise, the tensile strength of the different materials does not show significant variations, showing a good stability up to 16 weeks. Elongations at break, on the other hand, show more marked variations, in particular for the PLA+(OLA/BMCEL)30' material. In this sample, in fact, the high elongation recorded in the non-aged material (110%) progressively decreases, up to about 40% after 16 weeks. In materials plasticized with fibrous cellulose, on the other hand, the decrease observed is much less marked, from about 60% to about 40%. This result highlights a variation in the properties of the material due, as mentioned, to a variation in the distribution of the plasticizer

within the polymeric matrix, and mediated by the presence of cellulose. Previous investigations on ternary systems [6] highlighted that fillers can interact with plasticizer molecules and adsorb them at their surface, affecting their tendency to develop a macroscopic phase separation from the PLA matrix, that is ultimately responsible for the deterioration of mechanical properties. The different morphology of the cellulosic fillers tested resulted in a different effect on OLA phase separation, with fibrillated cellulose, exhibiting a high surface available to interactions with OLA, imparting a higher stability.

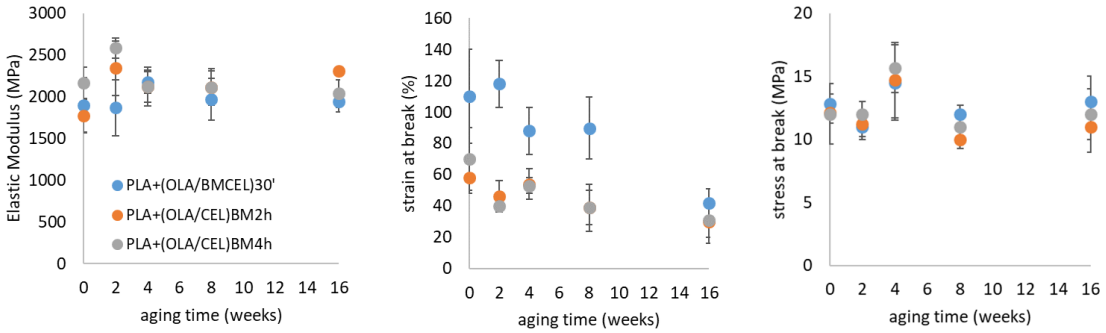

Figure 4.2. *Mechanical parameters recorded on ternary systems as a function of aging time*

4.3.3 Soil burial degradation test

In order to evaluate the rate of degradation of the prepared materials in contact with the soil, that is, in a condition reproducing an accidental dispersion into the environment, all the samples were buried in standard soil and their weight was measured as a function of the burial time. In Figure 4.3, the weight loss recorded on all samples is reported.

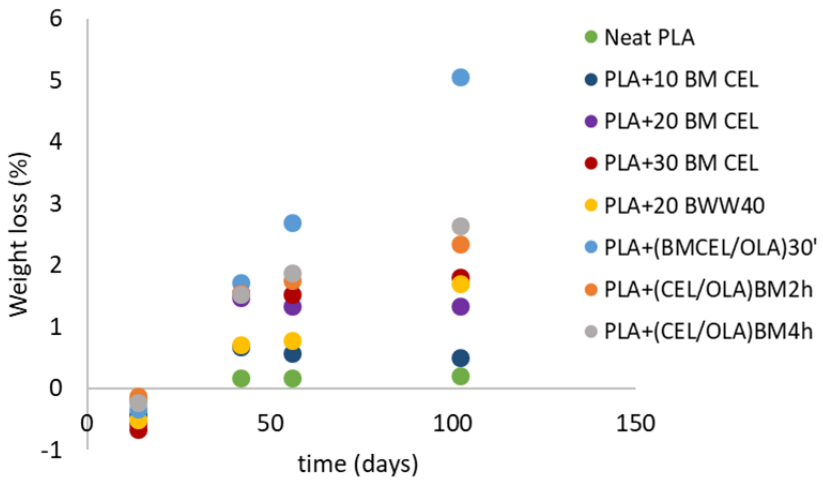

Figure 4.3. *Results (weight loss vs. time) of soil burial tests carried out on the prepared materials*

It can be noted that the first experimental point shows a negative weight loss, that is, a slight gain in sample weight. This is expected at the first stages of soil burial tests, as some water is absorbed into the samples that cannot be removed by the mild vacuum treatment used to stabilize weight. This small weight gain, however, is largely superseded by the weight loss recorded for longer burial time and indicative of an ongoing degradation of the composites. For longer time, indeed, a general trend can be observed, with all cellulose-containing materials showing a larger weight loss than PLA, and plasticized materials showing larger weight loss than non-plasticized composites. This trend can be rationalized considering that on one side, materials containing cellulose have a higher hydrophilicity in general agreement with WVTR data, on the other side by considering that the increased molecular mobility induced by the plasticizer can also accelerate reactions occurring in the solid state, as the hydrolysis of PLA chains. Moreover, the highest weight loss rate has been shown by the sample PLA+(BMCEL/OLA) 30', suggesting that at least a part of the weight loss can be attributed to the degradation of the cellulose fraction. BMCEL particles are in fact highly amorphous, and thus, more prone to be degraded with respect to crystalline fibres/fibrils [17].

4.4 Conclusions

In this work, the realization of PLA-based plasticized composites, containing an oligomeric plasticizer (OLA) and cellulose as reinforcement, has been investigated. The morphology of the cellulose phase has been modified by means of different ball milling treatments, to explore the effect of this morphology on thermo-mechanical properties, as a function of aging time, water vapor permeability and soil burial degradation.

Cellulose proved effective in increasing the stiffness of composites, in particular in plasticized materials where the increased ductility is coupled to a decrease in elastic modulus. In particular, partlally fibrillated cellulose led to slightly higher elastic modulus and to lower ultimate elongation, with respect to particle-like BMCEL. The stability of plasticized composites was also affected by the presence of cellulose, and this stability was correlated to the morphological features of the filler as induced by BM.

An increase in water vapor transport was observed in all composites, related to the high hydrophilicity of cellulose. This finding was correlated to a faster degradation in soil burial conditions, that is further accelerated by the plasticizer.

The realization of PLA based ternary systems containing both cellulose, as a reinforcement, and plasticizers, can then be considered as an effective strategy to modulate mechanical response, time stability, transport properties and degradation rate of polymeric materials.

BIBLIOGRAPHY

1 Mohan, S.; Panneerselvam, K. A short review on mechanical and barrier properties of polylactic acid-based films. Mater. Today Proc. 2022, 56, 3241–3246. https://doi.org/10.1016/j.matpr.2021.09.375.

2 Nagarajan, V.; Mohanty, A.K.; Misra, M. Perspective on Polylactic Acid (PLA) based Sustainable Materials for Durable Applications: Focus on Toughness and Heat Resistance. ACS Sustain. Chem. Eng. 2016, 4, 2899–2916. https://doi.org/10.1021/acssuschemeng.6b00321.

3 Zengwen, C.; Pan, H.; Chen, Y.; Bian, J.; Han, L.; Zhang, H.; Dong, L.; Yang, Y. Transform poly (lactic acid) packaging film from brittleness to toughness using traditional industrial equipments. Polymer 2019, 180, 121728. https://doi.org/10.1016/j.polymer.2019.121728

4 Ye Yuan, Zeyu Hu, Xiaowei Fu, Liang Jiang, Yao Xiao, Kai Hu, Peiyao Yan, Jinxin Lei. Poly(lactic acid) plasticized by biodegradable glyceryl lactate. Journal of Applied Polymer Science 2016, 43460. DOI: 10.1002/app.43460

5 Zaferani, S.H. Introduction of polymer-based nanocomposites. In Polymer-Based Nanocomposites for Energy and Environmental Applications; Elsevier: Amsterdam, The Netherlands, 2018; pp. 1–25. https://doi.org/10.1016/B978-0-08-102262-7.00001-5.

6 Avolio, R.; Castaldo, R.; Avella, M.; Cocca, M.; Gentile, G.; Fiori, S.; Errico, M.E. PLA-based plasticized nanocomposites: Effect of polymer/plasticizer/filler interactions on the time evolution of properties. Compos. Part B Eng. 2018, 152, 267–274. https://doi.org/10.1016/j.compositesb.2018.07.011

7 Miao, C., Hamad, W.Y. Cellulose reinforced polymer composites and nanocomposites: a critical review. Cellulose 2013, 20, 2221–2262. https://doi.org/10.1007/s10570-013-0007-3

8 Paul, U.C.; Fragouli, D.; Bayer, I.S.; Zych, A.; Athanassiou, A. Effect of Green Plasticizer on the Performance of Microcrystalline Cellulose/Polylactic Acid Biocomposites. ACS Appl. Polym. Mater. 2021, 3, 3071–3081. https://doi.org/10.1021/acsapm.1c00281.

9 Delogu, F.; Gorrasi, G.; Sorrentino, A. Fabrication of polymer nanocomposites via ball milling: Present status and future perspectives. Progr. Mater. Sci. 2017, 86, 75–126. DOI: 10.1016/j.pmatsci.2017.01.003.

10 Avolio, R.; Spina, F.; Gentile, G.; Mariacristina Cocca, M.; Avella, M.; Carfagna, C.; Tealdo, G.; Errico, M.E. Recycling Poly-ethylene-Rich Plastic Waste from Landfill Reclamation: Toward an Enhanced Landfill-Mining Approach. Polymers 2019, 11, 208; DOI: 10.3390/polym11020208.

11 Avolio, R., Bonadies, I., Capitani, D., Errico, M.E., Gentile, G., Avella, M. A multitechnique approach to assess the effect of ball milling on cellulose. Carbohydrate Polymers 2012, 87.1: 265-273. https://doi.org/10.1016/j.carbpol.2011.07.047

12 Piras C.C., Fernández-Prieto S., De Borggraeve W.M. Ball milling: a green technology for the preparation and functionalisation of nanocellulose derivatives. Nanoscale Adv. 2019, 1(3), 937-947. doi: 10.1039/c8na00238j.

13 Avolio, R.; Castaldo, R.; Gentile, G.; Ambrogi, V.; Fiori, S.; Avella, M.; Cocca, M.; Errico, M.E. Plasticization of poly(lactic acid) through blending with oligomers of lactic acid: Effect of the physical aging on properties. Eur. Polym. J. 2015, 66, 533–542. https://doi.org/10.1016/j.eurpolymj.2015.02.040

14 Fischer, E.W.; Sterzel, H.J.; Wegner, G. Investigation of the structure of solution grown crystals of lactide copolymers by means of chemical reactions. Kolloid-Zeitschrift und Zeitschrift für Polym. 1973, 251, 980–990. https://doi.org/10.1007/BF01498927.

15 Martin, O.; Avérous, L. Poly(lactic acid): Plasticization and properties of biodegradable multiphase systems. Polymer 2001, 42, 6209–6219. https://doi.org/10.1016/S0032-3861(01)00086-6.

16 Gracia-Fernández, C.A.; Gómez-Barreiro, S.; López-Beceiro, J.; Naya, S.; Artiaga, R. New approach to the double melting peak of poly(l-lactic acid) observed by DSC. J. Mater. Res. 2012, 27, 1379–1382. https://doi.org/10.1557/jmr.2012.57

17 Erdal, N.b.,Hakkarainen, M. Degradation of Cellulose Derivatives in Laboratory, Man-Made, and Natural Environments. Biomacromolecules 2022, 23, 7, 2713–2729. https://doi.org/10.1021/acs.biomac.2c00336

Chapter 5

Up-cycling coffee silverskin into biobased functional coatings

The results of this chapter have been submitted for publication to Journal of Cleaner Production

5.1. Introduction

Coffee silverskin (CS) is a strongly adherent layer that directly envelops the green coffee bean. Its detachment occurs during roasting due to the physical expansion of the beans, resulting in a major by-product of coffee production [1]. It has been estimated that about 400 thousand tonnes of CS is generated each year by the coffee roasting industry. Recently, different approaches to the valorization of coffee industry byproducts and, in particular, of CS have been suggested, attempting to address sustainability issues implementing a circular economy approach. Indeed, the valorization of by-products deriving from the food industry, aiming at reducing waste production and maximizing the efficiency of food value chains, is an important challenge and a key objective to move towards the circularization of economy.

Many research groups have been focusing on the utilization of coffee wastes as source of sugars, minerals and fibers, alternative renewable energy sources (bio-diesel oil and bio-ethanol), electrode materials, soil fertilization, and cosmetic application [2–5]. On the other hand, studies on the utilization of coffee by-products as filler/reinforcement in composite materials, based on both traditional fossil polymers and bio-based polymers were carried out [6–9]. These efforts represent a first step towards the development of fully bio-based and biodegradable formulations able to provide the same functionalities as petroleum-based materials [10].

In the frame of circular economy, the attention to so-called bioplastics has recently boosted, attracting large investments from both academic actors, plastic

industries and policy makers. An increased use of bio-based polymers in the plastic markets, in substitution for oil-based polymers, is indeed seen as a key step to reduce the consumption of fossil carbon sources and to mitigate the environmental impact of plastics, in particular concerning their end of life [11, 12]. At the European level, the European Green Deal and new circular economy action plan has been developed, in which the European Commission announced a policy framework for the regulation of the sourcing, labelling and use of bio-based, biodegradable and compostable plastics [13]. Polylactic acid (PLA) is one of the most commonly used bioplastic [14]. However, PLA has low thermal stability and poor water vapor and gas barrier properties [15] if compared, for instance, to other benchmark packaging polymers such as polyolefins and polyethylene terephthalate (PET). These facts are limiting its application in the packaging sector, where gas/vapour barrier properties are a fundamental objective in order to guarantee high quality and safety, considering that oxygen is the involved in most food degradation processes. Most commercial solutions to improve the barrier properties of polymer films rely on the realization of multilayer structures containing metal layers (vacuum deposited aluminium or laminated aluminium foil) or high barrier synthetic polymers, such as poly(vinyl alcohol). These kind of solutions, while offering a high protective function, are obviously an issue for the recycling or the biodegradation/composting of the materials, so that their application to bioplastic packaging solutions is no longer sustainable. To ensure circularity and sustainability of plastics and plastic packaging, their end of life must be taken into account in the all design steps [16], significantly reducing the complexity of packaging products, as well as decreasing the amount of non-recyclable fractions, including barrier layers and coatings. In this respect, in recent years, a number of environmentally-friendly, high barrier solutions have been proposed, aiming at the realization of films and coatings based on natural, biodegradable or even edible materials. Coatings based on lipids, polysaccharides and proteins, alone or in combination, can provide both moisture and gas barrier properties [17–20]. In particular, highly polar polymers, such as many proteins and polysaccharides, are largely exploited since they exhibit large

amount of hydrogen bonding, resulting in extremely low gas permeability values, especially at low relative humidity (RH) [18, 21].

Here, a fully bio-based coating has been developed by mechano-chemical treatment of coffee silverskin and deposited onto PLA substrates, demonstrating its beneficial effects on the barrier properties of PLA, thus realizing a renewable and sustainable material for packaging. The coating has been produced exploiting all components of CS, without implementing any separation step, taking advantage of the high protein and cellulose content of the biomass [22, 23] and of the structural modification obtained by the mechano-chemical treatment. CS was treated by means of a planetary ball milling apparatus, in mild conditions and using only water as solvent/dispersing medium. Ball milling treatment (BM) has been proposed, among other uses, as a green, effective physical method for the deconstruction of the complex, hierarchical structure of lignocellulosic biomasses [24], to allow an easy recovery and exploitation of the different constituents. Treatment conditions, in particular the presence of water, have a profound influence on the morphological and structural modification produced by BM [25]. After BM, the destructured CS suspension were deposited onto PLA substrates by rod coating. Electron microscopy and spectroscopic analyses were employed to gather information on the effects of the BM treatment on the structure and chemical composition of CS. CS coatings were characterized in terms of morphology, optical and oxygen barrier properties. The stability of the gas barrier properties of CS coatings exposed to high relative humidity was also assessed.

5.2. Materials and Methods

5.2.1. Materials

Coffee silverskin was kindly supplied by local coffee roasting plants, as a byproduct of their process.

Poly (lactic acid) film, thickness 40 μm, corona treated with a surface tension > 38 dyne/cm, was kindly supplied by Flex Packaging AL S.p.A. (Cava de' Tirreni, Italy).

5.2.2. Ball Milling Treatment

Coffee silverskin samples were processed in a Retsch PM100 planetary ball milling system (Haan, Germany) in wet conditions, using a 125 mL zirconia milling cup and 10 mm zirconia spheres. The BM treatment was carried out for 6 hours at 300 rpm, with a spheres/dry CS weight ratio of 25:1. Three different CS/water compositions were prepared and tested: 3 g of CS were added in the milling cup with 30 mL, 40 mL or 60 mL of distilled water and the mixture was ball-milled. The processed CS suspensions were coded as CS_BM_X, where X indicates the amount of water employed.

For further analyses, CS_BM_X samples were centrifuged for 15 minutes, at 10°C and 13000 rpm, in order to separate the supernatant and the precipitate fraction, coded as CS_BM_X_S and CS_BM_X_P, respectively.

5.2.3. Coatings Realization

CS_BM_X suspensions were deposited onto PLA films by rod coating ("K hand coater", Royston, United Kingdom), using different rods to adjust the amount of material deposited. Dry CS based coatings of nominal thickness ranging from 1.5 μm to 5.8 μm were obtained after water evaporation at room temperature (25°C and 50% RH). Coated PLA films were coded as CS_BM_X_Y where Y indicates the nominal thickness in μm of the coating.

5.2.4. Characterization

Fourier transform infrared spectra were collected on untreated CS, on dried BM samples (CS_BM_X) and the respective supernatant and precipitate fractions CS_BM_X_S and CS_BM_X_P, by means of a Perkin Elmer Spectrum One FTIR

spectrometer (Perkin Elmer Inc., USA), equipped with an attenuated total reflectance accessory (ATR). Spectra were recorded using a resolution of 4 cm−1 and 32 scans, in the 4000-650 cm-1 range.

1H NMR spectra were recorded on CS_BM_X_S samples (water soluble fractions) by means of a 600 MHz Bruker Avance III 600 spectrometer, equipped with a a 5-mm CPTCI CryoProbe. An excitation sculpting pulse sequence was used to strongly reduce the intensity of water resonance.

Scanning electron microscopy (SEM) analysis was carried out with a FEI Quanta 200 FEG SEM (Thermo Fisher Scientific Inc., USA) using a secondary electron detector and an acceleration voltage of 10–30 kV. The morphological characterization was performed on the coated PLA films (CS_BM_X_Y) surfaces and on the BM suspensions (CS_BM_X) pre-diluted with distilled water and deposited on aluminium SEM stubs. Before the analysis, samples were sputter coated with gold/palladium by means of an Emitech K575X sputter coater.

Bright field transmission electron microscopy (TEM) analysis of CS_BM_X and CS_BM_X_S was performed by using a FEI Tecnai G12 Spirit Twin (LaB6 source) apparatus (Thermo Fisher Scientific Inc., USA) operating at 120 kV acceleration voltage. TEM images were collected on a FEI Eagle 4k CCD camera. Before the analysis, CS_BM_X and CS_BM_X_S were properly diluted with distilled water; samples were collected by immersing TEM copper grids in the aqueous dispersions.

UV–visible spectra were recorded on PLA coated films (CS_BM_X_Y) and neat PLA film by means of a V570 UV spectrophotometer (Jasco, Easton, PA, USA) in the range 200–800 nm. The transmittance was measured by placing the specimens vertically in sample holders placed at 5 cm distance from the light source.

Oxygen transmission rate measurements were performed on PLA coated films (CS_BM_X_Y) and neat PLA film using a PermO2 Extrasolution Permeabilimeter (PermTech, Pieve Fosciana, Italy) at 25 °C and 50% RH. A further investigation at variable relative humidity, increasing RH of 10% from 10% to 90% was

performed on CS_BM_40_Y films. The film were tested progressively from the lowest (10%) to the highest (90%) humidity conditions and after completing the 9 measurements, all samples were tested a second time at 50% RH, in order to assess the stability of the CS coatings barrier properties upon exposure to high RH.

5.3. Results and Discussion

5.3.1. Ball-Milled Coffee Silverskin

The effects of the mechano-chemical treatment on the chemical composition, structure and morphology of the coffee silverskins were investigated. In Figure 5.1, ATR FT-IR spectra of ball-milled materials (CS_BM_30, CS_BM_40, CS_BM_60) and untreated CS are shown. As widely reported in literature, from a compositional point of view CS is a complex mixture in which carbohydrates (essentially cellulose and hemicellulose), and proteins are the main components [23] besides lignin, fatty acids, polyphenols, minerals and minor organic/inorganic substances [26, 27]. The main peaks observed in the FTIR spectra appear rather broad, due to the overlapping of the absorbance of the same functional groups present in different components of CS, thus reflecting its heterogeneous composition.

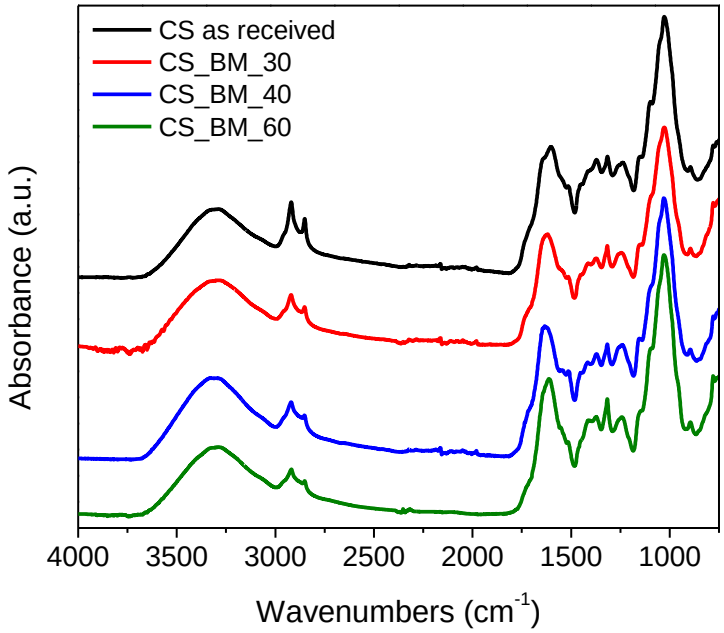

Figure 5.1. *FTIR-ATR spectra of CS and ball-milled CS.*

The main absorptions bands can be assigned as [8, 28, 29]:

- a very broad band centred at 3300 cm-1, assigned to the stretching of OH and NH;

- the asymmetric and symmetric CH stretching signals in the 2920 cm-1 − 2850 cm-1 range;

- a complex peak in the carbonyl region, with a main band centred at 1640 cm-1 assigned to amide (peptide) carbonyls and a shoulder at higher wavenumbers, indicating other carbonyl-containing compounds;

- multiple peaks in the 1500 − 1200 cm-1 range, that can be correlated to C−N and C−O stretch, C−N−H and C−O−H bend;

- an intense complex band centred at 1030 cm-1, typical of polysaccharides, and related to the C–O stretching and the CH rocking vibrations.

Comparing the spectra of ball-milled and untreated CS, no relevant changes can be observed suggesting that the ball milling process does not induce any relevant chemical modification, at least in the most abundant components of CS.

In Figure 5.2, SEM micrographs of untreated and ball-milled CS materials are shown. The morphology of CS is mainly characterized by fibrous, irregular particles, with lateral dimension up to 1 mm and a wide range of thicknesses (Figure 5.2 a). At higher magnification, these fibrous structures appear composed by a complex aggregation of fiber-like formations, with smaller globular particles appearing at the surface (Figure 5.2 b-c). As a result of the ball milling treatment, a profound destructuration of CS was obtained. The biomass fibrous structure results intensely fragmented in CS_BM_40. The ball-milled material exhibits irregularly shaped clusters ranging in size from few microns to less than 1 μm (Figure 5.2 d-e). At higher magnification, also the largest clusters appear composed of submicrometric fibers/particles (Figure 5.2 f). This morphology is not strongly influenced by the water content employed in the BM process, as all materials show analogous morphological features.

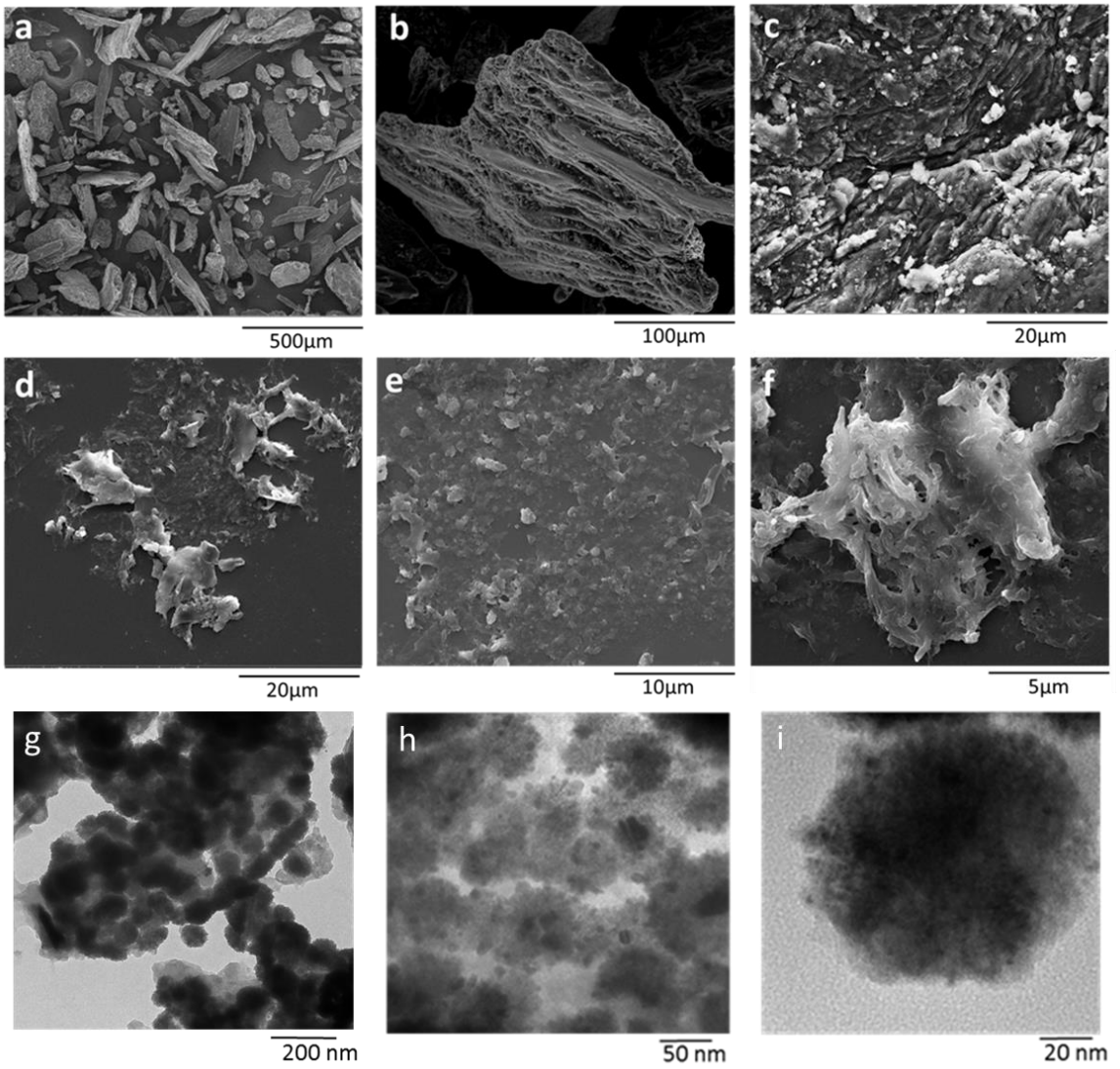

Figure 5.2. *SEM micrographs of untreated CS (a, b, c) and ball-milled samples CS_BM_40 (d, e, f); TEM micrographs of CS_BM_40 (g, h, i).*

TEM analysis (Figure 5.2 g, h, i) further confirmed that the micrometric clusters deriving from the mechanical destructuration of CS are aggregates of primary spherical particles, allowing to define more precisely the size of these particles ranging from 10 to 100 nm. These findings describe a kind of hierarchical structure of the ball milled CS and no relevant differences in shape and dimension of aggregates were observed as a function of wet BM experimental conditions.

5.3.2. Coffee Silverskin Coatings: Morphology and Structure

The ball-milled CS suspensions were deposited onto commercial PLA flexible packaging films to explore the possibility to realize fully bio-based gas barrier coatings. Coatings with thickness ranging from 1.5 µm to 5.8 µm, as a function of the concentration of the suspension and of the rod coater selected for the deposition, were obtained from BM_CS_X samples. These coatings show an excellent adhesion on the PLA substrate, withstanding mechanical stress such as the bending of the films, without damage (Figure 5.3 a). Coated films are translucent and, as the thickness increases, the light-brown coloration of the film increases, due to the native colour of the CS material (Figure 5.3 b-i).

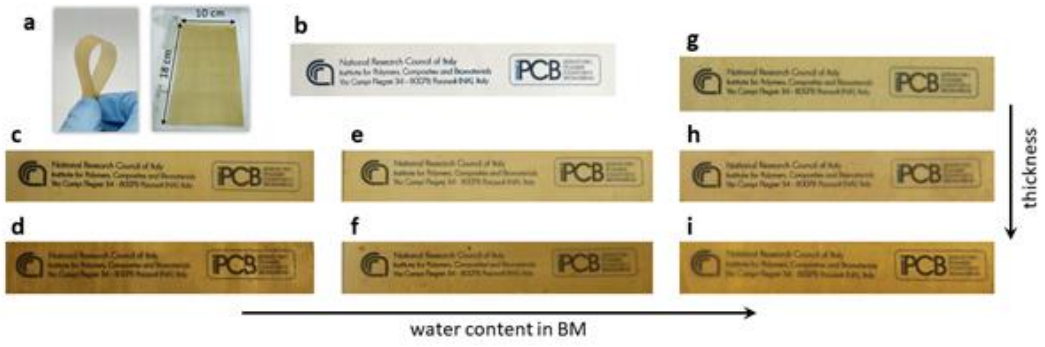

Figure 5.3. *Images of CS coated PLA films showing the flexibility of the coating and the large area (10x18 cm) covered by the coating CS_BM_40_2.1 (a), image of text printed on white paper (b) and covered with CS coated PLA films: CS_BM_30_2.8 (c), CS_BM_30_5.6 (d), CS_BM_40_2.1 (e), CS_BM_40_4.3 (f), CS_BM_60_1.5 (g), CS_BM_60_2.9 (h), CS_BM_60_5.8 (i).*

From a morphological point of view, all CS coatings appear as homogeneous, continuous and compact layers composed by a stacking of micrometric and sub-micrometric globular particles, as evidenced by SEM micrographs of surfaces and cross-sections reported in Figure 5.4. At the lowest water content (sample CS_BM_30, Figure 5.4 a-d), the coating surface appears smoother than the other samples, that is, less particles are shown at the surface, probably due to an influence of water content on the drying process (further discussed in Section 3.3). Nevertheless, for all samples, at higher SEM magnification, the main features observed are spherical particles sized in the range 50 ÷ 300 nm,

apparently embedded in a continuous phase (Figure 5.4 b, f, l), confirming the hierarchical structure of CS_BM materials. These features are common for all films realized, regardless of their thickness, therefore, for the sake of simplicity, SEM images of only one film for each formulation were reported.

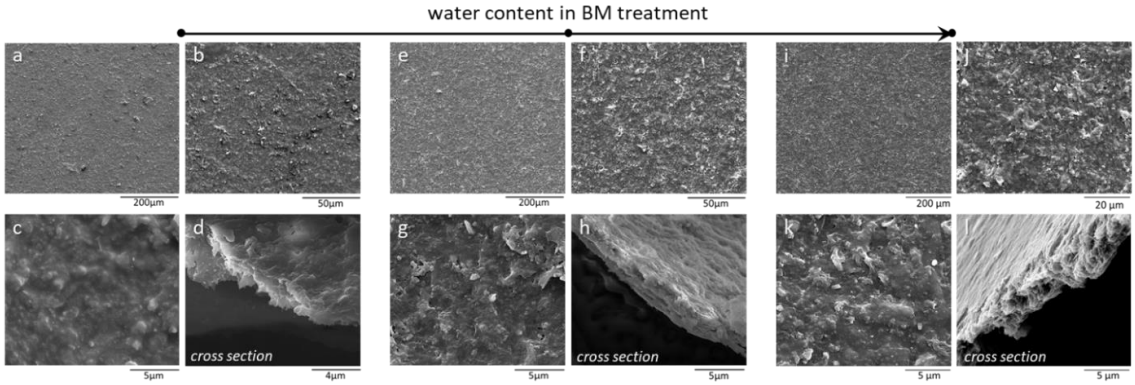

Figure 5.4. *SEM images of coatings CS_BM_30 (a- d); CS_BM_40 (e-h) and CS_BM_60 (i-l).*

Trying to clarify the film forming ability of the coffee silverskin, in relation to its composition and to the BM treatment, water soluble and insoluble fractions of ball-milled CS were separated and recovered as detailed in the experimental section. TEM analysis performed on the soluble fraction evidenced its film forming ability. In fact, after water evaporation, a homogeneous and continuous film was formed in which no particle-like structures can be observed, as shown in the Appendix, Figure S1. On the contrary, large clusters of particles define the morphology of the unsoluble fraction. On the basis of these evidences, the film forming ability of ball-milled CS can be ascribed to the soluble fraction components which act as binder phase incorporating the heterogeneous particle-like structures of CS.

To gather more detailed information on the composition of this soluble fraction, ATR FT-IR spectra were recorded on the soluble fractions CS_BM_X_S and reported in Figure 5.5 in comparison with the spectra of CS_BM_X. As above discussed, the CS composition complexity does not allow a detailed chemical characterization; however, an increased relative intensity of the band at about 1500 cm-1, coupled to the intense signal centred at about 1600 cm-1, can be evidenced in the spectrum of the soluble fraction with respect to that of the neat

CS. Moreover, a further broadening of the large peak centred at 3300 cm-1 can be also observed. These signals can be ascribable to the absorption of amide and -NH moieties, thus suggesting an important presence of peptides/proteins into the soluble fraction recovered from ball-milled CS.

In literature, several papers report the film forming properties of biopolymers like proteins, that are increasingly seen as bio-derivate materials for the realization of sustainable films and coatings. The film forming ability of proteins is linked to their denaturation process, which, from a molecular point of view, corresponds to an increase in disorder, free volume and mobility of the polymer molecules. This process essentially induces a partial or total loss of the secondary and tertiary structure of proteins, without modifying the composition and the sequence of the amino acids, in other words without altering their chemical nature. Generally speaking, different factors could induce proteins denaturation, such as heat, mechanical stress and/or plasticizers (including water), favouring their film forming ability. CS is detached from coffee beans and recovered during the roasting process, carried out at temperatures above 200°C [30]. Then, heat exposure during the roasting process can be considered as the main responsible for denaturation of the protein content of CS, coupled to the stress exerted by the mechano-chemical process in wet condition. This hypothesis is supported by the analysis of 1H NMR spectra (Figure S2 in the Appendix); without entering into qualitative details, the scarce presence of resonances below 0.5 ppm and the low number of resolved peaks in the amide region (6.5 – 9.5 ppm) indicates that essentially unfolded proteins are present [31].

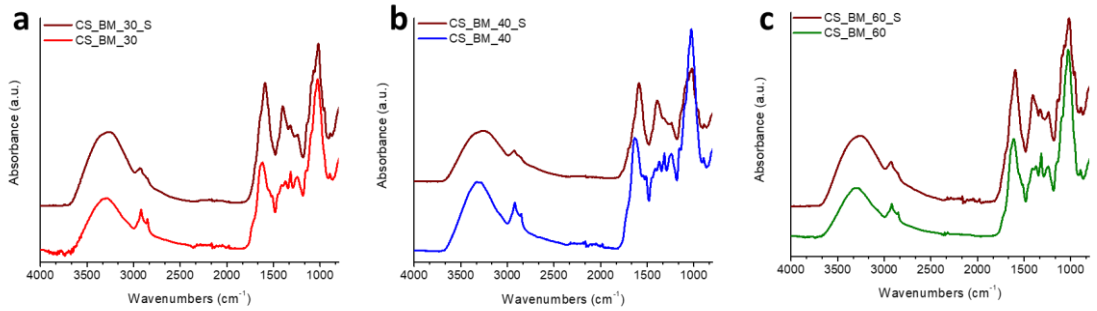

Figure 5.5. *FTIR-ATR spectra of ball-milled samples (CS_BM_X) and of their soluble fractions (CS_BM_X_S)*

5.3.3. Coffee Silverskin Coatings: Functional Properties

CS-coated PLA films were characterized in terms of light and gas barrier, chosen as the most representative parameters for applications in the food packaging field [32].

UV-visible transmission spectra were collected on CS-coated PLA and neat PLA. All coated films show a drastic lowering of light transmittance with respect to uncoated PLA in the investigated 200–800 nm range. In particular, a transmittance reduction ranging from 97 to 99% at 400nm of the CS coatings compared to neat PLA film was recorded, indicating high UV blocking capacity also for the thinner CS coatings (Table 5.1), to be ascribed to the aromatic ring structures of lignin, of which CS is rich [23, 33]. As expected, transmittance values decrease by increasing the coatings thickness but, for comparable thickness values, they are generally lower for CS ball-milled in presence of a larger volume of water (see for example CS_BM_30_5.6 and CS_BM_30_5.8).

Table 5.1. *UV-Vis transmittance and transmittance reduction at 400 nm of PLA and CS_BM coatings*

Sample	Transmittance (%) at 400 nm	Transmittance reduction (%) relative to PLA at 400 nm
PLA	80	-
CS_BM_30_2.8	2.67	96
CS_BM_30_5.6	0.96	99
CS_BM_40_2.1	1.46	98
CS_BM_40_4.3	1.26	98
CS_BM_40_8.6	0.44	99
CS_BM_60_1.5	1.90	97
CS_BM_60_2.9	1.30	98
CS_BM_60_5.8	0.34	99

Oxygen permeability of CS-coated PLA films were tested at 25 °C and 50% RH, in comparison to PLA. As shown in Figure 5.6 a, CS coatings have a significant effect on the gas barrier properties of PLA: all coated samples show remarkable reductions of the OTR of PLA, ranging from 30 % up to 91%. As expected, the coating thickness is an important factor governing the barrier properties of the samples. For each BM condition, by increasing the coatings thickness, the barrier effect increases.

Then, analyzing samples with comparable thickness but different CS/water ratio, a strong effect of water content on the gas barrier of coatings is observed. CS_BM_60_Y based samples exhibit, indeed, the lowest OTR reduction values, while the best barrier properties were obtained with the CS_BM_40 coatings, with remarkable 91% and 84% OTR reductions with coating of thickness of only 4.3 µm and 2.1 µm, respectively. These results can be ascribed to a different self-assembly behaviour of the ball-milled coffee silverskin suspensions and their drying in presence of different amounts of water. In general, the assembly of suspensions is guided by particle-particle interactions and is dependent on the distance between the particles and the environment surrounding the particles [34]. Coatings deposited from suspensions with a lower content of water are characterized by particles that are, on average, closer to each other during the drying process, ensuring a more compact structure and surface once water evaporates. This evidence is clearly true up to a limiting water content (40 mL per 3 g of CS, in this case), as too low amount of water would not allow the uniform deposition of the suspension. Therefore, if the water amount seems to have no significant influence on the effect induced by BM on the morphological features of CS, instead it plays a crucial role in the suspension deposition and film forming mechanism.

a

Sample	OTR [cm³/(m2*24h)] at RH 50%	OTR reduction (%) at 50% RH
PLA	438	-
CS_BM_30_2.8	89	80
CS_BM_30_5.6	52	88
CS_BM_40_2.1	69	84
CS_BM_40_4.3	41	91
CS_BM_60_1.5	308	30
CS_BM_60_2.9	208	52
CS_BM_60_5.8	124	72

b

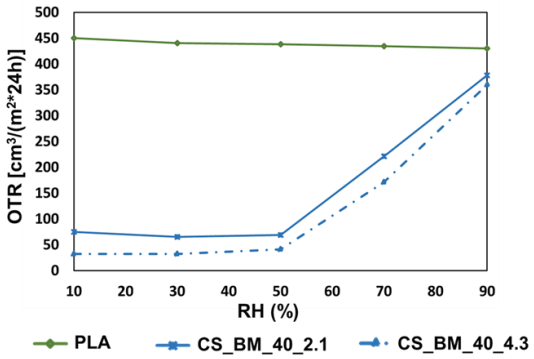

Figure 5.6. *OTR of CS coatings at 25 °C and 50% RH (a); OTR of CS_BM_40_Y coatings and PLA at 25 °C and variable RH (b).*

CS_BM_40_Y samples were tested also at variable RH conditions to investigate the dependence of OTR on the relative humidity. Results are shown in Figure 5.7 b. CS_BM_40_Y coatings exhibit a significant and stable O2 barrier effect in the RH range from 10% to 50 %, with an OTR reduction of about 85-90% respect to neat PLA. Above 50% RH, the barrier properties of the coatings decreased, showing a 49-60% OTR reduction at 70% RH and 12-16% OTR reduction at 90% RH. This behaviour is a consequence of the absorption of water by the hydrophilic CS coatings. In fact, in materials containing polar groups with high H-bond capacity water can be easily absorbed from the humid environment. Water acts in most cases as a plasticizer, increasing the free volume, therefore resulting in an increased permeation rate of gases and vapours through the material [35]. Thus, the plasticizing and swelling effect of moisture uptake on CS coatings results in increased permeability to O2. This water sorption, however, did not produce a disruptive modification of the coatings, since lowering relative humidity led to a recovery of barrier properties. Indeed, further permeability measurements at 50% RH were carried out on the same areas exposed to 70% and 90% RH, showing OTR values of 86 cm3/(m2*24h) and 73 cm3/(m2*24h) for the 4.3 µm and the 2.1 µm coatings, respectively. These results are particularly interesting considering the reduced thickness of the tested coatings, the high hydrophilicity of CS and the very long exposure time to high RH value (about 5 hours).

5.4. Conclusions

In this work, a valorization strategy aiming at the recovery and recycling of coffee silverskin (CS) has been proposed. In particular, CS has been processed in a planetary ball milling in wet conditions. The effect of the mechano-chemical treatments on the morphology and properties as a function of water content was deeply investigated. Ball milling treatments induced a drastic destructuration of CS and ball milled samples display a hierarchical particle structure characterized by the primary particle size of less than 100 nm. Then, the processed suspensions were deposited by rod coating on commercial PLA films obtaining homogeneous, well adhered and flexible coatings. The film-forming ability has been ascribed to the denaturation of the protein fraction composing the CS material induced by both the roasting process and the mechano-chemical treatment. The coatings showed an interesting barrier to UV radiation and oxygen permeation. Finally, the oxygen permeability as a function of relative humidity was also investigated, highlighting the stability of the coating structure also upon exposure to highly humid environment. The results demonstrate the effectiveness of the proposed strategy directed at the realization of bio-based coatings with potential applications in the food-packaging sector.

5.5. Appendix

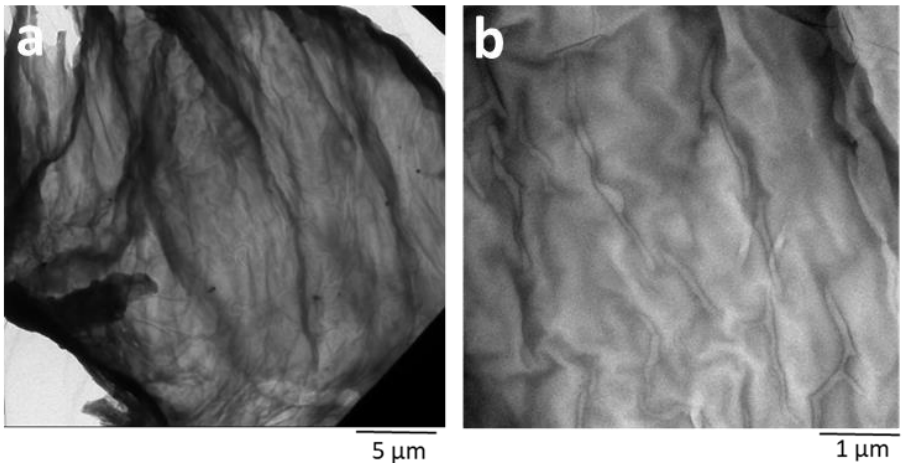

Figure S1. *TEM images at lower (a) and higher (b) magnification of CS_BM_40_S, the soluble fraction isolated by centrifugation.*

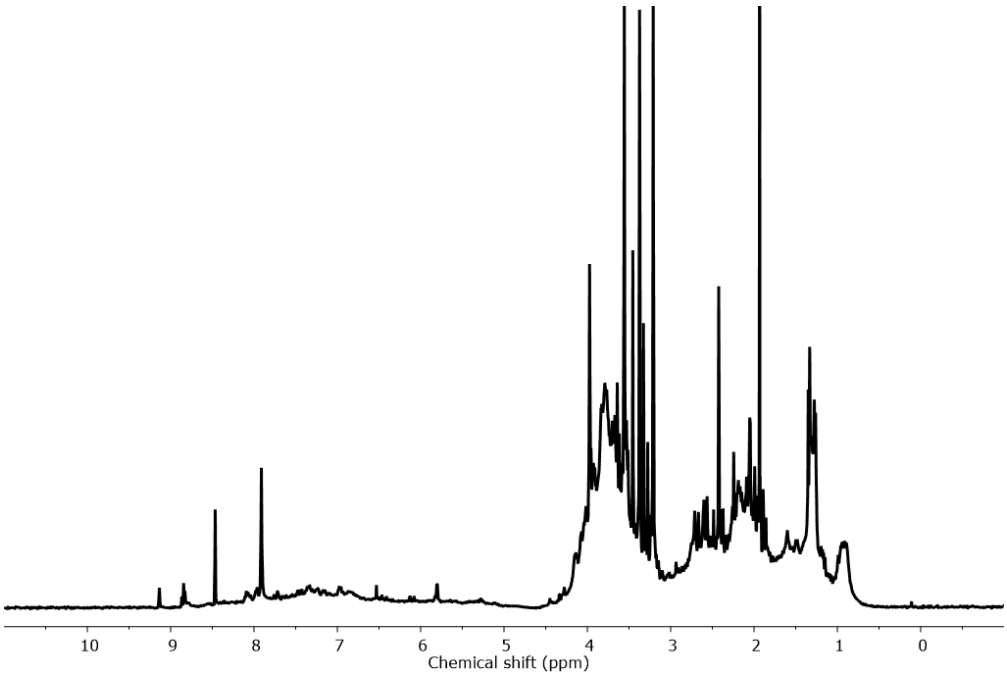

Figure S2. *^{1}H NMR spectrum recorded in H_2O on the CS_BM_40_S sample. A sculpting pulse sequence was applied to reduce the intensity of water resonance.*

BIBLIOGRAPHY

1. Gottstein, V.; Bernhardt, M.; Dilger, E.; Keller, J.; Breitling-Utzmann, C. M.; Schwarz, S.; Kuballa, T.; Lachenmeier, D. W.; Bunzel, M. Coffee Silver Skin: Chemical Characterization with Special Consideration of Dietary Fiber and Heat-Induced Contaminants. Foods, 2021, 10 (8), 1705. https://doi.org/10.3390/foods10081705.

2. Al-Hamamre, Z.; Foerster, S.; Hartmann, F.; Kröger, M.; Kaltschmitt, M. Oil Extracted from Spent Coffee Grounds as a Renewable Source for Fatty Acid Methyl Ester Manufacturing. Fuel, 2012, 96, 70–76. https://doi.org/10.1016/j.fuel.2012.01.023.

3. Kondamudi, N.; Mohapatra, S. K.; Misra, M. Spent Coffee Grounds as a Versatile Source of Green Energy. J. Agric. Food Chem., 2008, 56 (24), 11757–11760. https://doi.org/10.1021/jf802487s.

4. Mussatto, S. I.; Carneiro, L. M.; Silva, J. P. A.; Roberto, I. C.; Teixeira, J. A. A Study on Chemical Constituents and Sugars Extraction from Spent Coffee Grounds. Carbohydr. Polym., 2011, 83 (2), 368–374. https://doi.org/10.1016/j.carbpol.2010.07.063.

5. Bessada, S. Coffee Silverskin: A Review on Potential Cosmetic Applications. Cosmetics, 2018, 5 (1), 5. https://doi.org/10.3390/cosmetics5010005.

6. Ghazvini, A. K. A.; Ormondroyd, G.; Curling, S.; Saccani, A.; Sisti, L. An Investigation on the Possible Use of Coffee Silverskin in <scp>PLA</Scp> / <scp>PBS</Scp> Composites. J. Appl. Polym. Sci., 2022, 139 (22), 52264. https://doi.org/10.1002/app.52264.

7. Sarasini, F.; Tirillò, J.; Zuorro, A.; Maffei, G.; Lavecchia, R.; Puglia, D.; Dominici, F.; Luzi, F.; Valente, T.; Torre, L. Recycling Coffee Silverskin in Sustainable Composites Based on a Poly(Butylene Adipate-Co-Terephthalate)/Poly(3-Hydroxybutyrate-Co-3-Hydroxyvalerate) Matrix. Ind. Crops Prod., 2018, 118, 311–320. https://doi.org/10.1016/j.indcrop.2018.03.070.

8. Zarrinbakhsh, N.; Wang, T.; Rodriguez-Uribe, A.; Misra, M.; Mohanty, A. K. Characterization of Wastes and Coproducts from the Coffee Industry for Composite Material Production. BioResources, 2016, 11 (3). https://doi.org/10.15376/biores.11.3.7637-7653.

.9. Dominici, F.; García García, D.; Fombuena, V.; Luzi, F.; Puglia, D.; Torre, L.; Balart, R. Bio-Polyethylene-Based Composites Reinforced with Alkali and Palmitoyl Chloride-Treated Coffee Silverskin. Molecules, 2019, 24 (17), 3113. https://doi.org/10.3390/molecules24173113.

10. Oliveira, G.; Passos, C. P.; Ferreira, P.; Coimbra, M. A.; Gonçalves, I. Coffee By-Products and Their Suitability for Developing Active Food Packaging Materials. Foods, 2021, 10 (3), 683. https://doi.org/10.3390/foods10030683.

11. European Bioplastics e.V. Bioplastics facts & figures https://docs.european-bioplastics.org/publications/EUBP_Facts_and_figures.pdf (accessed May 16, 2023).

12. Suarez, A.; Ford, E.; Venditti, R.; Kelley, S.; Saloni, D.; Gonzalez, R. Rethinking the Use of Bio-Based Plastics to Accelerate the Decarbonization of Our Society. Resour. Conserv. Recycl., 2022, 186, 106593. https://doi.org/10.1016/j.resconrec.2022.106593.

13. Biobased, biodegradable and compostable plastics https://environment.ec.europa.eu/topics/plastics/biobased-biodegradable-and-compostable-plastics_en (accessed May 16, 2023).

14. Avella, M.; Buzarovska, A.; Errico, M.; Gentile, G.; Grozdanov, A. Eco-Challenges of Bio-Based Polymer Composites. Materials (Basel)., 2009, 2 (3), 911–925. https://doi.org/10.3390/ma2030911.

15. Sanchez-Garcia, M. D.; Lagaron, J. M. On the Use of Plant Cellulose Nanowhiskers to Enhance the Barrier Properties of Polylactic Acid. Cellulose, 2010, 17 (5), 987–1004. https://doi.org/10.1007/s10570-010-9430-x.

16. Guerritore, M.; Olivieri, F.; Castaldo, R.; Avolio, R.; Cocca, M.; Errico, M. E.; Galdi, M. R.; Carfagna, C.; Gentile, G. Recyclable-by-Design Mono-Material Flexible Packaging with High Barrier Properties Realized through Graphene Hybrid Coatings. Resour. Conserv. Recycl., 2022, 179, 106126. https://doi.org/10.1016/j.resconrec.2021.106126.

17. Lin, D.; Zhao, Y. Innovations in the Development and Application of Edible Coatings for Fresh and Minimally Processed Fruits and Vegetables. Compr. Rev. Food Sci. Food Saf., 2007, 6 (3), 60–75. https://doi.org/10.1111/j.1541-4337.2007.00018.x.

18. Chen, H.; Wang, J.; Cheng, Y.; Wang, C.; Liu, H.; Bian, H.; Pan, Y.; Sun, J.; Han, W. Application of Protein-Based Films and Coatings for Food Packaging: A Review. Polymers (Basel)., 2019, 11 (12), 2039. https://doi.org/10.3390/polym11122039.

19. Cazón, P.; Velazquez, G.; Ramírez, J. A.; Vázquez, M. Polysaccharide-Based Films and Coatings for Food Packaging: A Review. Food Hydrocoll., 2017, 68, 136–148. https://doi.org/10.1016/j.foodhyd.2016.09.009.

20. Benbettaïeb, N.; Gay, J.-P.; Karbowiak, T.; Debeaufort, F. Tuning the Functional Properties of Polysaccharide-Protein Bio-Based Edible Films by Chemical, Enzymatic, and Physical

Cross-Linking. Compr. Rev. Food Sci. Food Saf., 2016, 15 (4), 739–752. https://doi.org/10.1111/1541-4337.12210.

21. Edible Coatings and Films to Improve Food Quality; Baldwin, E. A., Hagenmaier, R., Bai, J., Eds.; CRC Press, 2011. https://doi.org/10.1201/b11082.

22. Martuscelli, M.; Esposito, L.; Di Mattia, C.; Ricci, A.; Mastrocola, D. Characterization of Coffee Silver Skin as Potential Food-Safe Ingredient. Foods, 2021, 10 (6), 1367. https://doi.org/10.3390/foods10061367.

23. Nolasco, A.; Squillante, J.; Velotto, S.; D'Auria, G.; Ferranti, P.; Mamone, G.; Errico, M. E.; Avolio, R.; Castaldo, R.; Cirillo, T.; et al. Valorization of Coffee Industry Wastes: Comprehensive Physicochemical Characterization of Coffee Silverskin and Multipurpose Recycling Applications. J. Clean. Prod., 2022, 370, 133520. https://doi.org/10.1016/j.jclepro.2022.133520.

24. Pang, J.; Zheng, M.; Li, X.; Sebastian, J.; Jiang, Y.; Zhao, Y.; Wang, A.; Zhang, T. Unlock the Compact Structure of Lignocellulosic Biomass by Mild Ball Milling for Ethylene Glycol Production. ACS Sustain. Chem. Eng., 2019, 7 (1), 679–687. https://doi.org/10.1021/acssuschemeng.8b04262.

25. Avolio, R.; Bonadies, I.; Capitani, D.; Errico, M. E.; Gentile, G.; Avella, M. A Multitechnique Approach to Assess the Effect of Ball Milling on Cellulose. Carbohydr. Polym., 2012, 87 (1). https://doi.org/10.1016/j.carbpol.2011.07.047.

26. Iriondo-DeHond, A.; Aparicio García, N.; Fernandez-Gomez, B.; Guisantes-Batan, E.; Velázquez Escobar, F.; Blanch, G. P.; San Andres, M. I.; Sanchez-Fortun, S.; del Castillo, M. D. Validation of Coffee By-Products as Novel Food Ingredients. Innov. Food Sci. Emerg. Technol., 2019, 51, 194–204. https://doi.org/10.1016/j.ifset.2018.06.010.

27. Ballesteros, L. F.; Teixeira, J. A.; Mussatto, S. I. Chemical, Functional, and Structural Properties of Spent Coffee Grounds and Coffee Silverskin. Food Bioprocess Technol., 2014, 7 (12), 3493–3503. https://doi.org/10.1007/s11947-014-1349-z.

28. Pancholi, M. J.; Khristi, A.; M., A. K.; Bagchi, D. Comparative Analysis of Lignocellulose Agricultural Waste and Pre-Treatment Conditions with FTIR and Machine Learning Modeling. BioEnergy Res., 2023, 16 (1), 123–137. https://doi.org/10.1007/s12155-022-10444-y.

29. Agudelo-Cuartas, C.; Granda-Restrepo, D.; Sobral, P. J. A.; Castro, W. Determination of Mechanical Properties of Whey Protein Films during Accelerated Aging: Application of FTIR

Profiles and Chemometric Tools. J. Food Process Eng., 2021, 44 (5). https://doi.org/10.1111/jfpe.13477.

30. Münchow, M.; Alstrup, J.; Steen, I.; Giacalone, D. Roasting Conditions and Coffee Flavor: A Multi-Study Empirical Investigation. Beverages, 2020, 6 (2), 29. https://doi.org/10.3390/beverages6020029.

31. Page, R.; Peti, W.; Wilson, I. A.; Stevens, R. C.; Wüthrich, K. NMR Screening and Crystal Quality of Bacterially Expressed Prokaryotic and Eukaryotic Proteins in a Structural Genomics Pipeline. Proc. Natl. Acad. Sci., 2005, 102 (6), 1901–1905. https://doi.org/10.1073/pnas.0408490102.

32. Mullan, M.; McDowell, D. Modified Atmosphere Packaging. In Food and Beverage Packaging Technology; Wiley-Blackwell: Oxford, UK, 2011; pp 263–294. https://doi.org/10.1002/9781444392180.ch10.

33. Li, B.; Xu, C.; Liu, L.; Yu, J.; Fan, Y. Facile and Sustainable Etherification of Ethyl Cellulose towards Excellent UV Blocking and Fluorescence Properties. Green Chem., 2021, 23 (1), 479–489. https://doi.org/10.1039/D0GC02919J.

34. Jiang, S.; Van Dyk, A.; Maurice, A.; Bohling, J.; Fasano, D.; Brownell, S. Design Colloidal Particle Morphology and Self-Assembly for Coating Applications. Chem. Soc. Rev., 2017, 46 (12), 3792–3807. https://doi.org/10.1039/C6CS00807K.

35. [HONG, S.-I.; KROCHTA, J. M. Oxygen barrier properties of whey protein isolate coatings on polypropylene films. Journal of Food Science, 2003, 68.1: 224-228]

Chapter 6

Conclusions

In this doctoral thesis, processing methodologies based on high energy mechanical treatments have been developed and applied to different systems, including polymers and polymer blends, cellulose and ligno-cellulosic biomasses. The treatments developed involve the application of intense shear and compressive forces to solid materials through the action of a planetary ball mills apparatus, in order to induce morphological, structural and chemical modifications in the systems investigated.

An detailed study of the effects of ball milling mechanochemical tratments on polypropylene (PP), has been carried out, with the aim to verify the occurrence of radical reactions in the solid state and to either promote the formation of chain branching and/or to obtain the grafting of different molecules. Chemiluminescence analysis revealed a relatively large number of reactive species formed by radical pathways, especially in samples milled for long times. Thermo-mechanical and rheological analyses highlighted that molecular weight is decreased, in particular, a strong reduction is observed in samples treated for more than 4 hours. As a consequence, molecular weight effects dominated the rheological behaviour of PP samples and no clear evidence of long chain branching could be observed. Moreover, a proof of concept of the reactivity of mechanically generated radicals towards other molecules was obtained carrying out milling trials in the presence of chemicals susceptible to radical reactions, low MW polybutadiene and glycidyl methacrylate.

In a second approach, a strategy based on high energy mechanical treatments was investigated to valorize and recycle polyethylene rich heterogeneous post-consumer mixtures. The treatments induced a fine grinding of the different polymeric fractions and contaminants, thus promoting an intimate mixing. As a result, an improvement of mixture morphology and a higher deformability were obtained. Then, the addition of small amounts of benzoyl peroxide during the ball milling was explored to promote radical formation. The low temperature, solid

state process reduced the adverse effects of the peroxide on polymers, granting higher stiffness while retaining a significant ductility, phenomena ascribable to an effective compatibilization and to the formation of very light crosslinking.

The third system investigated concerned the realization of PLA-based plasticized composites, containing an oligomeric plasticizer (OLA) and cellulose as reinforcement. The morphology of the cellulose phase has been modified by means of different ball milling treatments,in both wet and dry conditions. Cellulose proved effective in increasing the stiffness of composites, in particular in plasticized materials where the increased ductility is coupled to a decrease in elastic modulus. In particular, partlally fibrillated cellulose (from wet BM) led to slightly higher elastic modulus and to lower ultimate elongation, with respect to particle-like cellulose (dry BM). The stability of plasticized composites towards phase separation was also affected by the presence of cellulose, and correlated to the morphological features of the filler as induced by BM. An increase in water vapor transport was observed in all composites, related to the high hydrophilicity of cellulose. This finding was correlated to a faster degradation in soil burial conditions, that is further accelerated by the plasticizer.

The last system studied was a food industry byproduct, namely coffee silverskin (CS). CS has been processed in a planetary ball milling in wet conditions, and the effect of the mechanochemical treatments on the morphology and properties was deeply investigated. A drastic destructuration of CS was evidenced, as BM samples display a hierarchical particle structure with primary particle size of less than 100 nm. The processed suspensions were deposited by rod coating on commercial PLA films obtaining homogeneous, well adhered coatings, with good film-forming ability ascribed to the presence of a denaturated protein fraction. The coatings showed an interesting barrier to UV radiation and oxygen permeation and a remarkable structural stability upon exposure to high humidity levels.